

See discussions, stats, and author profiles for this publication at: <https://www.researchgate.net/publication/329075645>

# Investing the influence of tides, inflows, and exports on sub-daily flows in the Sacramento-San Joaquin Delta

Preprint · November 2018

DOI: 10.13140/RG.2.2.20374.80967

---

CITATIONS

0

READS

87

3 authors, including:



Bradley Cavallo

Cramer Fish Sciences

18 PUBLICATIONS 134 CITATIONS

[SEE PROFILE](#)



Jenny Melgo

Cramer Fish Sciences

6 PUBLICATIONS 20 CITATIONS

[SEE PROFILE](#)

Some of the authors of this publication are also working on these related projects:



Delta hydrodynamics [View project](#)

## REPORT:

# INVESTIGATING THE INFLUENCE OF TIDES, INFLOWS, AND EXPORTS ON SUB-DAILY FLOW IN THE SACRAMENTO-SAN JOAQUIN DELTA

*Prepared by:*

**Brad Cavallo<sup>1</sup>**

**Phil Gaskill<sup>2</sup>**

**Jenny Melgo<sup>1</sup>**

1-Cramer Fish Sciences  
13300 New Airport Rd, Suite 102  
Auburn, CA 95602

2-Cramer Fish Sciences  
600 NW Fariss Rd,  
Gresham, OR 97030

*Corresponding author:*

Brad Cavallo, V 530.888.1443, [brad.cavallo@fishsciences.net](mailto:brad.cavallo@fishsciences.net)

**4 June 2013**

Cramer Fish Sciences  
[www.fishsciences.net](http://www.fishsciences.net)

## Table of Contents

List of Figures .....	ii
List of Tables .....	v
<b>Abstract.....</b>	1
<b>Introduction.....</b>	1
<b>Methods.....</b>	3
<b>Results .....</b>	8
Flow Patterns in the Mainstem San Joaquin River .....	8
Direction and Magnitude of Flow at Junctions .....	11
<i>Georgiana Slough</i> .....	11
<i>Head of Old River</i> .....	13
<i>Turner Cut</i> .....	15
<i>Columbia Cut</i> .....	17
<i>Middle River</i> .....	19
<i>Mouth of Old River</i> .....	20
Proportion and Source of Flow to Interior Delta .....	22
<i>Georgiana Slough</i> .....	22
<i>Head of Old River</i> .....	24
<i>Turner Cut</i> .....	25
<i>Columbia Cut</i> .....	26
<i>Middle River</i> .....	28
<i>Mouth of Old River</i> .....	29
Total Proportion of Flow to Interior Delta.....	30
Daily Average Flow vs. 15-minute Flow.....	34
<b>Discussion .....</b>	35
Mainstem San Joaquin River .....	36
Delta Junctions.....	37
Flow Proportion and Fish Routing.....	38
Comparison to PTM Results .....	39
Uncertainties .....	40
Management Implications.....	41
Conclusions.....	42
<b>Acknowledgements .....</b>	42
<b>References .....</b>	43



<b>Appendix 1:</b> FMN, FRV, and JPT Junctions .....	46
Direction and Magnitude of Flow at FMN, FRV, and JPT Junctions .....	46
<i>Fisherman's Cut</i> .....	46
<i>False River</i> .....	47
<i>Jersey Point</i> .....	49
Proportion and Source of Flow to Interior Delta at FMN, FRV, and JPT Junctions .....	51
<i>Fisherman's Cut</i> .....	51
<i>False River</i> .....	53
<i>Jersey Point</i> .....	54
<b>Appendix 2:</b> Details for Total Proportion of Flow to Interior Delta.....	56

## List of Figures

- Figure 1.** Location of Junctions Leading to the Interior Sacramento-San Joaquin Delta. Georgiana Slough, mainstem Sacramento River, and mainstem San Joaquin River are indicated in black. Junction locations are circled in red and designated as follows: GEO=Georgiana Slough, HOR=Head of Old River, TRN=Turner Cut, COL=Columbia Cut: MRV=Middle River, ORV=Mouth of Old River, FMN=Fisherman's Cut, FRV=False River, JPT=Jersey Point. Export facility locations are indicated by blue triangles; SWP is the State Water Project, CVP is the Central Valley Project..... 3
- Figure 2.** Flow Patterns in the Mainstem San Joaquin River over 24 hours. For all graphs, river kilometer is on the x-axis and curve color indicates export level. Junction locations are indicated by dotted vertical lines with junction labels. For the top two rows of graphs, magnitude of flow (in cfs) is on the y-axis. For the bottom row of graphs, y-axis displays percentage of time during which flow is positive. Graphs are arranged from left to right by increasing inflows. .... 9
- Figure 3.** Range of Flow with Varying Exports at Selected Channels in the Mainstem San Joaquin River over 24 hours. Numbered circles on the map indicated DSM2 channel locations. Time of day is on the x-axis, starting at 0000 hours and ending at 2345 hours. Magnitude of flow is on the y-axis. Curve color indicates export level..... 11
- Figure 4.** GEO: Plan-view of Georgiana Slough Junction. Physical channel outlines are shown in gray. DSM2 Hydro channel numbers are given in parentheses, nodes are circled, and positive flow direction in each channel is indicated by blue arrows. Upstream, downstream, and to interior Delta channels are indicated as in Table 2..... 12
- Figure 5.** GEO: Flow in Georgiana Slough Junction Channels over 24 Hours. Time of day in 15-minute increments is on the x-axis, starting at 0000 hours and ending at 2345 hours. Magnitude of flow is on the y-axis. Curve color indicates export level. Chanel designations are as indicated in Table 2. For channel GEO2, all flow is toward the interior Delta. For the other channels, flow displayed in the shaded area is away from the center of the junction. .... 13
- Figure 6.** HOR: Plan-view of Head of Old River Junction. See Figure 4 for description of elements. .... 14
- Figure 7.** HOR: Flow in Head of Old River Junction Channels over 24 Hours. See Figure 5 for description of elements. For channel HOR3, flow displayed in the shaded area is away from the

interior Delta; for the other channels, flow displayed in the shaded area is away from the center of the junction. ....	14
<b>Figure 8.</b> TRN: Plan-view of Turner Cut Junction. <i>See Figure 4 for description of elements.</i> ..	15
<b>Figure 9.</b> TRN: Flow in Turner Cut Junction Channels over 24 Hours. <i>See Figure 5 for description of elements. For channel TRN5, flow displayed in the shaded area is away from the interior Delta; for the other channels, flow displayed in the shaded area is away from the center of the junction.</i> .....	16
<b>Figure 10.</b> COL: Plan-view of Columbia Cut Junction. <i>See Figure 4 for description of elements.</i> .....	17
<b>Figure 11.</b> COL: Flow in Columbia Cut Junction Channels over 24 Hours. <i>See Figure 5 for description of elements. For channel COL7, flow displayed in the shaded area is away from the interior Delta; for the other channels, flow displayed in the shaded area is away from the center of the junction.</i> .....	18
<b>Figure 12.</b> MRV: Plan-view of Middle River Junction. <i>See Figure 4 for description of elements.</i> .....	19
<b>Figure 13.</b> MRV: Flow in Middle River Junction Channels over 24 Hours. <i>See Figure 5 for description of elements. For channel MRV5, flow displayed in the shaded area is away from the interior Delta; for the other channels, flow displayed in the shaded area is away from the center of the junction.</i> .....	20
<b>Figure 14.</b> ORV: Plan-view of Mouth of Old River Junction. <i>See Figure 4 for description of elements.</i> .....	21
<b>Figure 15.</b> ORV: Flow in Mouth of Old River Junction Channels over 24 Hours. <i>See Figure 5 for description of elements. For channel ORV2, flow displayed in the shaded area is away from the interior Delta; for the other channels, flow displayed in the shaded area is away from the center of the junction.</i> .....	22
<b>Figure 16.</b> GEO: Proportion of Flow to Georgiana Slough with Probability of Entrainment. Time of day in 24-hr format is on the x-axis; proportion of flow is on the y-axis. Graphs in the top section display the proportion of water input to the junction which is output to Georgiana Slough (curve), by water source (bars under the curve). Curve color indicates export level. Bar color indicates water source; bar length indicates relative proportion. Gray shading indicates water from more than one source. Black curves superimposed on the proportion of flow graphs are the probability of entrainment into Georgiana Slough, as calculated from equation 6.4 of Perry 2010. Graphs in the top section are arranged by increasing inflows and exports. Graphs in the bottom section compare proportions under varying exports, with the bars removed for clarity. ....	23
<b>Figure 17.</b> HOR: Proportion of Flow to Interior Delta at Head of Old River. Time of day in 24-hr format is on the x-axis; proportion of flow is on the y-axis. Graphs in the top section display the proportion of water input to the junction which is output to the interior Delta (curve), by water source (bars under the curve). Curve color indicates export level. Bar color indicates water source; bar length indicates relative proportion. Gray shading indicates water from more than one source. Graphs in the top section are arranged by increasing inflows and exports. Graphs in the bottom section compare proportions under varying exports, with the bars removed for clarity.....	25
<b>Figure 18.</b> TRN: Proportion of Flow to Interior Delta at Turner Cut. <i>See Figure 17 for description of elements.</i> .....	26



<b>Figure 19.</b> COL: Proportion of Flow to Interior Delta at Columbia Cut. <i>See Figure 17 for description of elements.</i> .....	27
<b>Figure 20.</b> MRV: Proportion of Flow to Interior Delta at Middle River. <i>See Figure 17 for description of elements.</i> .....	28
<b>Figure 21.</b> ORV: Proportion of Flow to Interior Delta at Mouth of Old River. <i>See Figure 17 for description of elements.</i> .....	30
<b>Figure 22.</b> Total Proportion of Flow to Interior Delta over 24 Hours. Data are displayed by junction and export level. Junctions are on the x-axis; proportion of flow is on the y-axis. Bar color indicates export level. Graphs are arranged by increasing inflows, and by water source (i.e., upstream or downstream from the junction).....	31
<b>Figure 23.</b> Change in Total Proportion of Flow to Interior Delta over 24 Hours with Increasing Inflows. Values are for change in total proportion relative to low inflows. Data are displayed by junction and export level. Graphs are arranged by increasing inflows.....	32
<b>Figure 24.</b> Change in Total Proportion of Flow to Interior Delta over 24 Hours with Increasing Exports. Values are for change in percentage of total proportion relative to low exports. Data are displayed by junction and export level. Graphs are arranged by increasing inflows.....	33
<b>Figure 25.</b> Equivalence Test of Metrics for Proportion of Flow to Interior Delta over 24 Hours. Proportion of flow calculated using total flow (upstream and downstream) at 15-minute intervals is displayed on the x-axis. Proportion of flow calculated using daily average flow is displayed on the y-axis. Individual data points are for various inflow and export conditions at each junction. Linear regressions are displayed for the GEO and HOR junctions for clarity. The dotted line indicates equivalence (i.e., unity). .....	35
<b>Figure 26.</b> FMN: Plan-view of Fisherman’s Cut Junction. <i>See Figure 4 for description of elements.</i> .....	46
<b>Figure 27.</b> FMN: Flow in Fisherman’s Cut Junction Channels over 24 Hours. <i>See Figure 5 for description of elements.</i> For channel FMN2, flow displayed in the shaded area is away from the interior Delta; for the other channels, flow displayed in the shaded area is away from the center of the junction. .....	47
<b>Figure 28.</b> FRV: Plan-view of False River Junction. <i>See Figure 4 for description of elements.</i> .....	48
<b>Figure 29.</b> FRV: Flow in False River Junction Channels over 24 Hours. <i>See Figure 5 for description of elements.</i> For channel FRV1, flow displayed in the shaded area is away from the interior Delta; for the other channels, flow displayed in the shaded area is away from the center of the junction. .....	49
<b>Figure 30.</b> JPT: Plan-view of Jersey Point Junction. <i>See Figure 4 for description of elements.</i> .....	50
<b>Figure 31.</b> JPT: Flow in Jersey Point Junction Channels over 24 Hours. <i>See Figure 5 for description of elements.</i> For channels JPT2 and JPT3, flow displayed in the shaded area is away from the interior Delta; for the other channels, flow displayed in the shaded area is away from the center of the junction.....	51
<b>Figure 32.</b> FMN: Proportion of Flow to Interior Delta at Fisherman’s Cut. <i>See Figure 17 for description of elements.</i> .....	52
<b>Figure 33.</b> FRV: Proportion of Flow to Interior Delta at False River. <i>See Figure 17 for description of elements.</i> .....	53
<b>Figure 34.</b> JPT: Proportion of Flow to Interior Delta at Jersey Point. <i>See Figure 17 for description of elements.</i> .....	55
<b>Figure 35.</b> Change in Total Proportion of Flow to Interior Delta over 24 Hours with Increasing Inflows at GEO and HOR. Values are for change in total proportion relative to low inflows.	

Data are displayed by junction and export level. Graphs are arranged by increasing inflows, and by water source (i.e., upstream or downstream from the junction).....	59
<b>Figure 36.</b> Change in Total Proportion of Flow to Interior Delta over 24 Hours with Increasing Inflows at TRN, COL, and MRV. Values are for change in total proportion relative to low inflows. Data are displayed by junction and export level. Graphs are arranged by increasing inflows, and by water source (i.e., upstream or downstream from the junction).....	60
<b>Figure 37.</b> Change in Total Proportion of Flow to Interior Delta over 24 Hours with Increasing Inflows at ORV, FMN, FRV, and JPT. Values are for change in total proportion relative to low inflows. Data are displayed by junction and export level. Graphs are arranged by increasing inflows, and by water source (i.e., upstream or downstream from the junction).....	61
<b>Figure 38.</b> Change in Total Proportion of Flow to Interior Delta over 24 Hours with Increasing Exports at GEO and HOR. Values are for change in total proportion relative to low exports. Data are displayed by junction and export level. Graphs are arranged by increasing inflows, and by water source (i.e., upstream or downstream from the junction).....	62
<b>Figure 39.</b> Change in Total Proportion of Flow to Interior Delta over 24 Hours with Increasing Exports at TRN, COL, and MRV. Values are for change in total proportion relative to low exports. Data are displayed by junction and export level. Graphs are arranged by increasing inflows, and by water source (i.e., upstream or downstream from the junction).....	63
<b>Figure 40.</b> Change in Total Proportion of Flow to Interior Delta over 24 Hours with Increasing Exports at ORV, FMN, FRV, and JPT. Values are for change in total proportion relative to low exports. Data are displayed by junction and export level. Graphs are arranged by increasing inflows, and by water source (i.e., upstream or downstream from the junction).....	64

## List of Tables

<b>Table 1.</b> DSM2 Hydro Simulation Parameters.....	4
<b>Table 2.</b> DSM2 Hydro channels, junction-specific abbreviations, and channel designations. Arrows indicate the direction of positive flows between nodes as defined in the DSM2 Hydro model. Channels leading to the interior Delta are indicated in bold. Channels upstream of a junction are indicated in blue; downstream channels are indicated in red. For Columbia Cut, Disappointment Slough is indicated in aqua; a secondary downstream channel (COL7) is indicated in orange.....	7
<b>Table 3.</b> Total Proportion of Flow to Interior Delta over 24 Hours. Data are displayed by junction and export level. Graphs are arranged by inflow level and water source (i.e., upstream or downstream from the junction).....	56
<b>Table 4.</b> Change in Total Proportion of Flow to Interior Delta over 24 Hours with Increasing Inflows. Values are for change in total proportion relative to low inflows. Data are displayed by junction and export level. Graphs are arranged by inflow level and water source (i.e., upstream or downstream from the junction).....	57
<b>Table 5.</b> Change in Total Proportion of Flow to Interior Delta over 24 Hours with Increasing Exports. Values are for change in percentage of total proportion relative to low exports. Data are displayed by junction and export level. Graphs are arranged by inflow level and water source (i.e., upstream or downstream from the junction).....	58

# Investigating the influence of tides, inflows, and exports on sub-daily flow in the Sacramento-San Joaquin Delta

B. Cavallo, P. Gaskill, and J. Melgo

## Abstract

The relative influence of tides, river inflows, and South Delta exports on hydrodynamics in California's Sacramento-San Joaquin Delta is a source of confusion and uncertainty for resource managers. A particle tracking model (PTM) has been used to characterize water movement in the Delta, to evaluate entrainment risks for larval fishes and, for the first time in the 2009 National Marine Fisheries Service OCAP Biological Opinion, to evaluate hydrodynamic effects on juvenile salmonids. While the fate of particles depicts the cumulative effects of net water movement (i.e., average flow) over longer time periods (>days), recent findings from acoustic telemetry studies suggest migrating juvenile salmonids respond more strongly to sub-daily hydrodynamic conditions. Hydrodynamic variables of interest are readily available and provided by the Delta Simulation Model-2 hydrodynamics model with considerable spatial-temporal resolution (every 15 minutes for 500+ channel locations). Our analysis based on DSM2 Hydro data provides the first detailed description of flow patterns in the mainstem San Joaquin River and at key Delta junctions. Our results for the proportion of flow which enters the interior Delta at Georgiana Slough are consistent with the calculated probability of fish and flow entrainment into Georgiana Slough. We found little evidence that river inflows or South Delta exports—within the range typically controlled by managers—could substantially alter hydrodynamic conditions likely to cause juvenile salmonids to enter the interior Delta from the mainstem Sacramento or San Joaquin rivers. Additional acoustic telemetry studies and perhaps more detailed hydrodynamic data are necessary to more thoroughly test the relative importance of hypothesized mechanisms. However, our analysis suggests available hydrodynamic data can further understand and help inform management actions intended to enhance juvenile salmonid survival in the Sacramento-San Joaquin Delta.

**Keywords:** hydrodynamics, flow, salmon, Delta, estuary, tides, behavior, exports, PTM

## Suggested citation:

Cavallo, B., P. Gaskill, and J. Melgo. 2013. Investigating the influence of tides, inflows, and exports on sub-daily flow in the Sacramento-San Joaquin Delta. Cramer Fish Sciences Report. 64 pp. Available online at: [http://www.fishsciences.net/reports/2013/Cavallo\\_et\\_al\\_Delta\\_Flow\\_Report.pdf](http://www.fishsciences.net/reports/2013/Cavallo_et_al_Delta_Flow_Report.pdf).

## Introduction

An understanding of hydrodynamics within California's Sacramento-San Joaquin Delta (Delta) is critical to evaluating how altered river inflows, South Delta water diversions (exports), and other management actions may impact the Delta ecosystem. The potential for impacts to sensitive fish species from export pumping in particular remains highly contentious, having been the focus of two recently remanded Endangered Species Act Section 7 biological opinions (USFWS 2008; NMFS 2009). A Particle Tracking Model (PTM) has been used to characterize Delta flow patterns, evaluate entrainment risks for larval fishes (Culberson et al. 2004; USFWS 2008; Kimmerer and Nobriga 2008) and, recently, to evaluate hydrodynamic effects on juvenile salmonids (NMFS 2009).

The PTM is typically applied by injecting particles at locations within a simulated Delta; the fate of particles after one or more months is then reported (e.g., Kimmerer and Nobriga 2008). The transport of particles to their ultimate destination is often a gradual process, such that reliance upon PTM as an indicator of generalized hydrodynamic conditions has left sub-daily variations in hydrodynamic conditions largely un-described. Whereas PTM may be applicable to larvae with more passive drifting behavior (Kimmerer and Nobriga 2008), sub-daily flow conditions are more likely to be important for fishes with directed swimming behavior. Salmon smolts are known to be strong swimmers and to move through the Delta more quickly than tracer particles, with larger smolts migrating more quickly than smaller ones (Baker and Morhardt 2001). Furthermore, recent acoustic telemetry studies of juvenile salmonids have shown flows to influence route selection and survival rates (Perry 2010).

Kimmerer and Nobriga (2008) demonstrated that particle fate, both in terms of destination and arrival timing, was very sensitive to river inflows and, to a somewhat lesser extent, exports. They observed tides acted only to “spread out and delay the passage of particles” and thus, the fate of particles largely reflects net, non-tidal flow, and does not describe sub-daily hydrodynamics resulting from the interaction of tides with river inflows and exports. Yet, sub-daily tidal flow in the Delta is much larger than tidally-averaged net flow (Baker and Morhardt 2001). In addition, tidal flow and stage have been observed to strongly influence discharge and water velocities within Delta channels and junctions (Burau et al. 2007). These tidally-driven variations are known to influence salmon migration, and recent studies have pointed out that the interaction of complex fish behaviors and sub-daily changes in flow is the key to understanding migration and entrainment, particularly at junctions (Blake and Horn 2003; Vogel 2004; Burau et al. 2007; Perry and Skalski 2008; Perry 2010).

In this paper, we take a new approach to analyzing water movement in the Delta, building upon the analyses provided by Kimmerer and Nobriga (2008) but representing Delta hydrodynamics in terms of short time horizons (daily or sub-daily conditions) which are typically not represented by PTM. This approach is potentially more useful in describing water movement relevant to migrating juvenile salmonids. Informed by insights gained from recent acoustic tagging studies (particularly Holbrook et al. 2009; Perry 2010, SJRG 2011), and starting with inflow and export scenarios used in Kimmerer and Nobriga (2008), we used flow data taken at 15-minute intervals from the Delta Simulation Model-2 hydrodynamics model (DSM2 Hydro) to analyze sub-daily flow patterns in the Delta.

We follow a systematic approach, beginning at the broadest scale by describing flow patterns in the mainstem San Joaquin River and in the channels associated with eight mainstem San Joaquin River junctions, as well as the Georgiana Slough junction on the Sacramento River. We then use this data to determine the proportion of flow entering the interior Delta at 15-minute time intervals, and to compare the proportion of flow to the proportion of fish entrained at the Georgiana Slough junction on the Sacramento River. Finally, we calculate total proportion of flow as a hypothesized “roll-up” metric for assessing entrainment vulnerability at all nine junctions leading to the interior Delta. In this manner, we provide a detailed description of how tides, river inflows, and exports interact to produce hydrodynamic conditions experienced by juvenile salmonids and other Delta fishes. Though potentially important for management, we are unaware of any prior efforts to provide such an assessment of Delta hydrodynamics.

## Methods

Our investigation focused on the mainstem San Joaquin River between Head of Old River and Jersey Point; an important migration corridor for juvenile salmonids originating from all Central Valley tributaries, but particularly for those of the Southern Sierra Nevada Diversity Group (Lindley et al. 2007). We identified and conducted additional analyses for eight junctions along the San Joaquin River to evaluate how tides, inflows, and exports may divert migrating fish from the San Joaquin River into the interior Delta (Figure 1). We also included the junction at Georgiana Slough because it is the primary waterway by which migrating salmonids enter the interior Delta from the Sacramento River, and because juvenile salmonid migration behavior and route selection at Georgiana Slough is well studied.

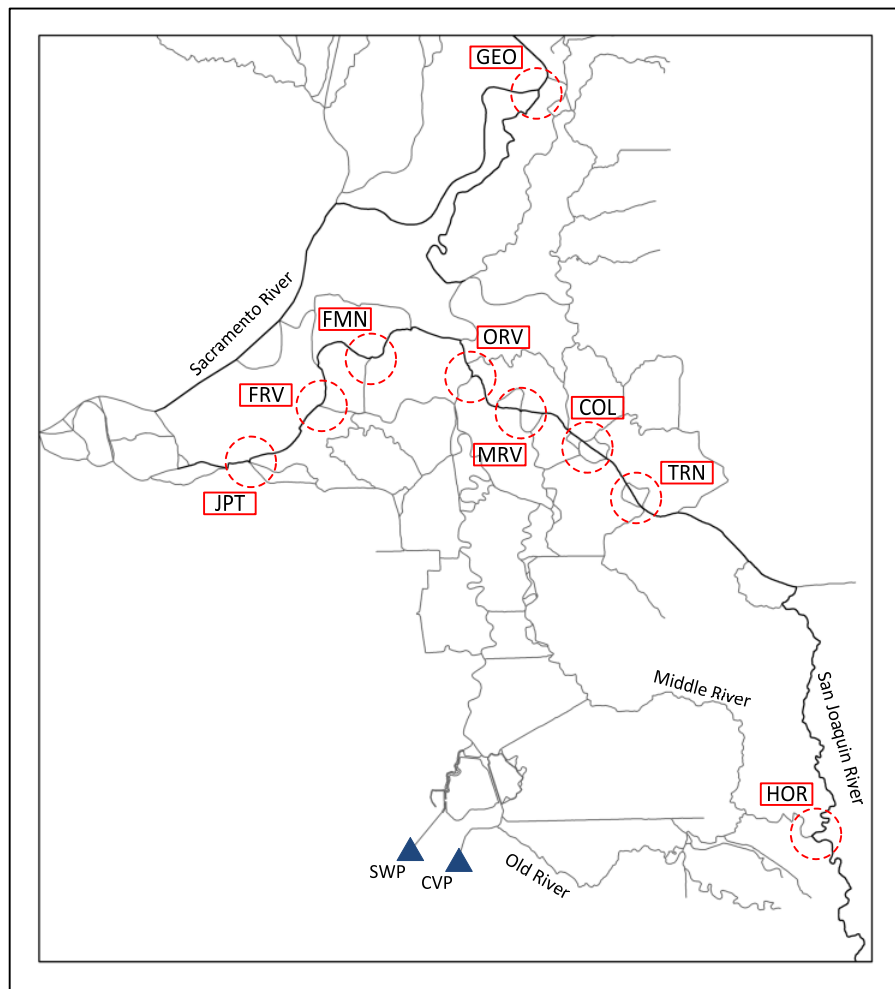


**Figure 1.** Location of Junctions Leading to the Interior Sacramento-San Joaquin Delta. Georgiana Slough, mainstem Sacramento River, and mainstem San Joaquin River are indicated in black. Junction locations are circled in red and designated as follows: GEO=Georgiana Slough, HOR=Head of Old River, TRN=Turner Cut, COL=Columbia Cut: MRV=Middle River, ORV=Mouth of Old River, FMN=Fisherman’s Cut, FRV=False River, JPT=Jersey Point. Export facility locations are indicated by blue triangles; SWP is the State Water Project, CVP is the Central Valley Project.

Flow patterns in the San Joaquin River and at these nine junctions were analyzed using simulated flow data from DSM2 Hydro. The DSM2 Hydro model is a one-dimensional hydrodynamic model that simulates flows in the Delta's network of riverine and estuarine channels. For a given set of boundary conditions (including tides, river inflows, and exports) DSM2 Hydro provides stage and flow data at 15-minute intervals for hundreds of channels in the Delta. The model has been calibrated to observed flow and stage data and validated by comparing simulated data with field data from a different time period (Kimmerer and Nobriga 2008). DSM2 Hydro has been extensively tested by the California Department of Water Resources and is used for planning and operation of the State Water Project and Central Valley Project export pumping. More detailed information about the DSM2 Hydro model can be found at: <http://baydeltaoffice.water.ca.gov/modeling/deltamodeling/index.cfm>.

For our analysis of sub-daily flow patterns, we used DSM2 Hydro data from a subset of scenarios and model runs specified and used by Kimmerer and Nobriga (2008) as inputs for their PTM analysis. We used “base” model runs (defined by Kimmerer and Nobriga 2008) encompassing nine combinations of river inflow and export levels in the Delta (Table 1). As described in Kimmerer and Nobriga (2008), these scenarios were based upon synthetic hydrologies consisting of constant river inflow, constant exports, and repeating spring tides. Diversions from the North Bay Aqueduct, Contra Costa Canal, and from within-Delta agriculture, were included but did not vary within or among scenarios considered. Our nine scenarios represent a subset of those evaluated by Kimmerer and Nobriga (2008) and include the range of export and river inflows within operational control of water project managers. Though river inflows of  $67,000 \text{ m}^3 \text{ sec}^{-1}$  ( $\text{ft}^3 \text{ sec}^{-1}$  or cfs) or  $120,000 \text{ m}^3 \text{ sec}^{-1}$  (cfs)—the highest inflows considered by Kimmerer and Nobriga (2008)—likely have ecological significance, events of this magnitude currently occur only as a result of heavy precipitation and related reservoir storage and flood management, not as part of managed flow pulses intended to provide ecological benefits for juvenile salmonids or other aquatic organisms.

**Table 1.** DSM2 Hydro Simulation Parameters.

Total Inflow	Inflow Sacramento	Inflow San Joaquin	DCC Gate Position	Total Exports	OMR
Low (12,000 cfs)	Low (10,595 cfs)	Low (1,405 cfs)	Closed	Low (2000 cfs)	-2298
Low (12,000 cfs)	Low (10,595 cfs)	Low (1,405 cfs)	Closed	Med (6,000 cfs)	-5400
Low (12,000 cfs)	Low (10,595 cfs)	Low (1,405 cfs)	Closed	High (10,000 cfs)	-8503
Med (21,000 cfs)	Med (18,264 cfs)	Med (2,736 cfs)	Closed	Low (2000 cfs)	-1511
Med (21,000 cfs)	Med (18,264 cfs)	Med (2,736 cfs)	Closed	Med (6,000 cfs)	-4614
Med (21,000 cfs)	Med (18,264 cfs)	Med (2,736 cfs)	Closed	High (10,000 cfs)	-7717
High (38,000 cfs)	High (32,288 cfs)	High (5,712 cfs)	Closed	Low (2000 cfs)	246
High (38,000 cfs)	High (32,288 cfs)	High (5,712 cfs)	Closed	Med (6,000 cfs)	-2856
High (38,000 cfs)	High (32,288 cfs)	High (5,712 cfs)	Closed	High (10,000 cfs)	-5959



For our analysis of flow patterns along the contiguous San Joaquin River we used 15-minute interval data for every mainstem channel from the Head of Old River to Jersey Point. These DSM2 Hydro channels are: 7-16, 18-25, 30, 31, 34-38, 41-48, 83, 49, and 50—where channel 7 is the channel immediately upstream of the Head of Old River junction, and channel 50 is the channel immediately downstream of the Jersey Point junction—corresponding to river kilometer 84 through river kilometer 12. For this section of the San Joaquin River, we analyzed 15-minute data to calculate: average flows, range of flows (difference between 24-hour max and min), and percent positive flows (percentage of 15-minute time intervals during which flows are toward San Francisco Bay). In order to clearly depict the influence of exports in the lower portion of the San Joaquin River, we plotted 15-minute flow data for nine DSM2 Hydro channels (37, 42-49) under medium total inflow and with all three export levels. These channels were selected because they represent the portion of the San Joaquin River with the largest export influence and where adverse export effects on juvenile salmonids have been hypothesized to occur (Newman and Brandes 2010). The channels analyzed include all un-branched portions of the San Joaquin River (as represented in DSM2 Hydro) between the Mouth of Old River and the confluence with the Sacramento River.

For our analysis of hydrodynamics at Delta junctions, we chose every junction at which water can flow from the mainstem San Joaquin River into the interior Delta, and also the junction on the Sacramento River at which water can flow into Georgiana Slough. We constructed a schematic plan-view for each junction and labeled channels sequentially in a clockwise fashion (for example, see Figure 8). A summary of channel labels and corresponding DSM2 Hydro designations can be found in Table 2 below. DSM2 channel 31, shared by Turner Cut and Columbia Cut junctions, was given a separate designation for each of these junctions. The plan-view depictions of channel junctions were an essential step in interpreting DSM2 Hydro data; they were used to visually identify upstream and downstream channels, and to determine physical flow directions for which water from upstream and/or downstream could be diverted into the interior Delta at each junction.

In order to describe hydrodynamic conditions relevant to fish at Delta junctions, we analyzed the proportion of flow entering the interior Delta at 15-minute intervals to obtain proportion of flow patterns over 24 hours. Our approach was informed by analyses of Holbrook et al. (2009) and Perry (2010), which found the proportion of acoustically-tagged fish diverted at Delta junctions—from the San Joaquin River into Old River and from the Sacramento River into Georgiana Slough, respectively—tracked the proportion of flow diverted at these junctions.

For calculation purposes, water which flowed into a junction—when the direction of flow was toward (rather than away from) the center of the junction—was termed “input” ( $I$ ); water which flowed into the interior Delta from the junction was termed “output” ( $O$ ). At each 15-minute time interval provided by DSM2 Hydro, the proportion of flow entering the interior Delta ( $\rho_{jt}$ ) was calculated as:

$$(1) \quad \rho_{jt} = \frac{O_{jt}}{I_{jt}},$$

where  $O_{jt}$  is the flow in  $\text{m}^3 \text{ sec}^{-1}$  (cfs) entering the interior Delta at junction  $j$  at 15-minute time interval  $t$ , and where  $I_{jt}$  is the total inflow in  $\text{m}^3 \text{ sec}^{-1}$  (cfs) entering from junction  $j$  channels at 15-minute time interval  $t$ . Calculations were made with the following assumptions:

- a)  $\rho$  could not exceed 1.

- b) When  $O_{jt}$  was toward the center of the junction (i.e., when flow was leaving the interior Delta instead of entering it),  $\rho$  was set to zero.

Regarding the source(s) of water flowing into the interior Delta ( $I_{jt}$ ), we assumed:

- c)  $I_j$  and  $O_j$  balanced at each time interval  $t$  such that there was no delay in balance of flows entering and exiting the junction.
- d) A channel could only contribute to  $I_j$  at time interval  $t$  if the physical direction of flow in that channel was toward the center of the junction at time interval  $t$ .
- e) If only one channel contributed to  $I_j$  at time interval  $t$ , then all water flowing into the interior Delta ( $O_{jt}$ ) was from that channel at time interval  $t$ .
- f) If multiple channels contributed to  $I_j$  at time interval  $t$ , then water flowing into the interior Delta ( $O_{jt}$ ) was assumed to be a mixture of water from the channels, where the relative contribution of each input channel was proportional to the relative magnitude of flow in that channel at time interval  $t$ .

Inspection of the junction plan-views and analysis of hydrodynamic data indicates that assumption (c) did not hold in some circumstances. For example, the Colombia Cut junction is large and includes a number of internal channels not directly accounted for in our calculations of junction flow flux; as a result, flow exiting the Colombia Cut junction may lag behind flow entering the junction. However, these were transitory discrepancies that are not likely to bias estimates of  $\rho$  among scenarios. Other assumptions (a, b, d-f) were necessary in part to prevent time lags resulting from violation of assumption (c) from generating erroneous results. Though our analysis is admittedly a simplification of reality, it provides a useful first look at flow proportion dynamics at Delta junctions which are consequential for the management of juvenile salmonids.

In order to meaningfully relate flow patterns in the junctions to the migration routing of juvenile salmon, we compared our calculated flow proportion into Georgiana Slough to the predicted probability of fish entrainment into Georgiana Slough based upon acoustic tagging studies. To represent the probability of entrainment into Georgiana Slough ( $\pi_{GEO}$ ) based upon acoustic tag studies, we applied the following equation developed and described by Perry (2010):

$$(2) \quad \pi_{GEO} = \frac{\exp(\beta_{G0} + (\beta_{G1} * Q_S) + (\beta_{G2} * Q_G) + (\beta_{G4} * U))}{1 + (\exp(\beta_{G0} + (\beta_{G1} * Q_S) + (\beta_{G2} * Q_G) + (\beta_{G4} * U)))},$$

where  $\beta_{G0}$ ,  $\beta_{G1}$ ,  $\beta_{G2}$ , and  $\beta_{G4}$  are constants with values -0.9, -1.163, 0.852, and 1.595, respectively. Where  $Q_S$  is (Sacramento River flow at time  $t$ )—(mean Sacramento River flow/Std. Dev. of Sacramento River flow), and where  $Q_G$  is (Georgiana Slough flow at time  $t$ )—(mean Georgiana Slough flow/Std. Dev. of Georgiana Slough flow).  $U$  is a dummy variable (0 or 1) indicating the direction of flow in Georgiana Slough. See Perry (2010) for details of parameter definitions and for explanation for coefficient estimation methods.

**Table 2.** DSM2 Hydro channels, junction-specific abbreviations, and channel designations. Arrows indicate the direction of positive flows between nodes as defined in the DSM2 Hydro model. Channels leading to the interior Delta are indicated in bold. Channels upstream of a junction are indicated in blue; downstream channels are indicated in red. For Columbia Cut, Disappointment Slough is indicated in aqua; a secondary downstream channel (COL7) is indicated in orange.

Junction	Jct. Abbrev.	DSM2 Nodes	DSM2 Channel	Designation
Georgiana Slough	GEO	343→288	366	<b>GEO2</b>
		342→343	422	<b>GEO1</b>
		343→344	423	<b>GEO3</b>
Head of Old River	HOR	7→8	7	HOR2
		8→9	8	HOR1
		8→48	<b>54</b>	<b>HOR3</b>
Turner Cut	TRN	25→26	25	<b>TRN3</b>
		26→27	26	TRN1
		26←28	27	TRN7
		27→29	28	TRN2
		28←29	29	TRN6
		26→29	30	TRN4
		29→30	31	<b>TRN8</b>
		26←140	<b>172</b>	<b>TRN5</b>
		29→30	31	<b>COL4</b>
Columbia Cut	COL	30→31	32	COL6
		32→31	33	COL10
		30→32	34	COL5
		31→33	35	<b>COL8</b>
		32→33	36	<b>COL9</b>
		31←133	<b>160</b>	<b>COL7</b>
		243→244	<b>314</b>	<b>COL1</b>
		30←244	315	COL2
		32←244	316	COL3
		33→34	37	<b>MRV3</b>
Middle River	MRV	34→35	38	MRV4
		35→36	39	MRV1
		36→37	40	MRV2
		35→37	41	MRV8
		37→38	42	<b>MRV9</b>
		133→134	<b>161</b>	<b>MRV5</b>
		34←134	162	MRV7
		35←134	163	MRV6
		37→38	42	<b>ORV1</b>
Mouth of Old River	ORV	38→39	43	<b>ORV3</b>
		38←103	<b>124</b>	<b>ORV2</b>
		37→38	42	<b>FMN1</b>
Fisherman's Cut	FMN	42→43	47	<b>FMN3</b>
		42→226	<b>280</b>	<b>FMN2</b>
		43→44	48	<b>FRV3</b>
False River	FRV	44→469	83	<b>FRV2</b>
		44→226	<b>279</b>	<b>FRV1</b>
		45←469	49	<b>JPT1</b>
Jersey Point	JPT	45→461	50	<b>JPT4</b>
		45←76	<b>260</b>	<b>JPT3</b>
		45←223	<b>275</b>	<b>JPT2</b>



To further describe hydrodynamic conditions relevant to fish, we calculated the total proportion of flow or *daily 15-minute flow proportion* entering the interior Delta ( $\rho_j$ ) at each junction over 24 hours; calculated as:

$$(3) \quad \rho_j = \frac{\sum_{t=1}^{96} O_{jt}}{I_{jt}} / 96.$$

For purposes of comparison, we also calculated values for an alternative total proportion of flow metric we termed *daily average flow proportion*; calculated as:

$$(4) \quad \rho'_j = \frac{\sum_{t=1}^{96} |O_{jt}|}{\sum_{t=1}^{96} |I_{jt}|}.$$

Therefore, the *daily 15-minute flow proportion* represents flow proportion to the interior Delta based upon the average of 96 individual flow ratios (every 15-minutes) whereas the *daily average flow proportion* metric represents flow proportion to the interior by summing all 96 observations and then calculating a pooled, 24-hour flow ratio. *Daily average flow proportion* is a fish entrainment metric evaluated by Perry (2010) and proposed by biologists as potentially applicable to other Delta junctions. For our analysis, both  $\rho_j$  and  $\rho'_j$  were calculated for  $I_{jt}$  for all nine scenarios with two different treatments of junction inflow: 1) including upstream inflow only, and 2) including inflow originating from upstream and downstream.

## Results

We found the relative influence of river inflows and exports on flow magnitude, direction, and proportion of flow varied markedly by location (longitudinally along the San Joaquin River and among Delta junctions) and that no single hydrodynamic metric (average flow, range of flow, or percent positive flow) could thoroughly characterize observed patterns in the mainstem San Joaquin River. In the interest of brevity, only data for the mainstem San Joaquin River and for those junctions generally considered most important for management are reported in Results. Additional results are described in the Appendices.

### ***Flow Patterns in the Mainstem San Joaquin River***

The relative influence of river inflows and exports on each hydrodynamic metric (average flow, range of flow, and percent positive flow) varied by river kilometer (Figure 2).

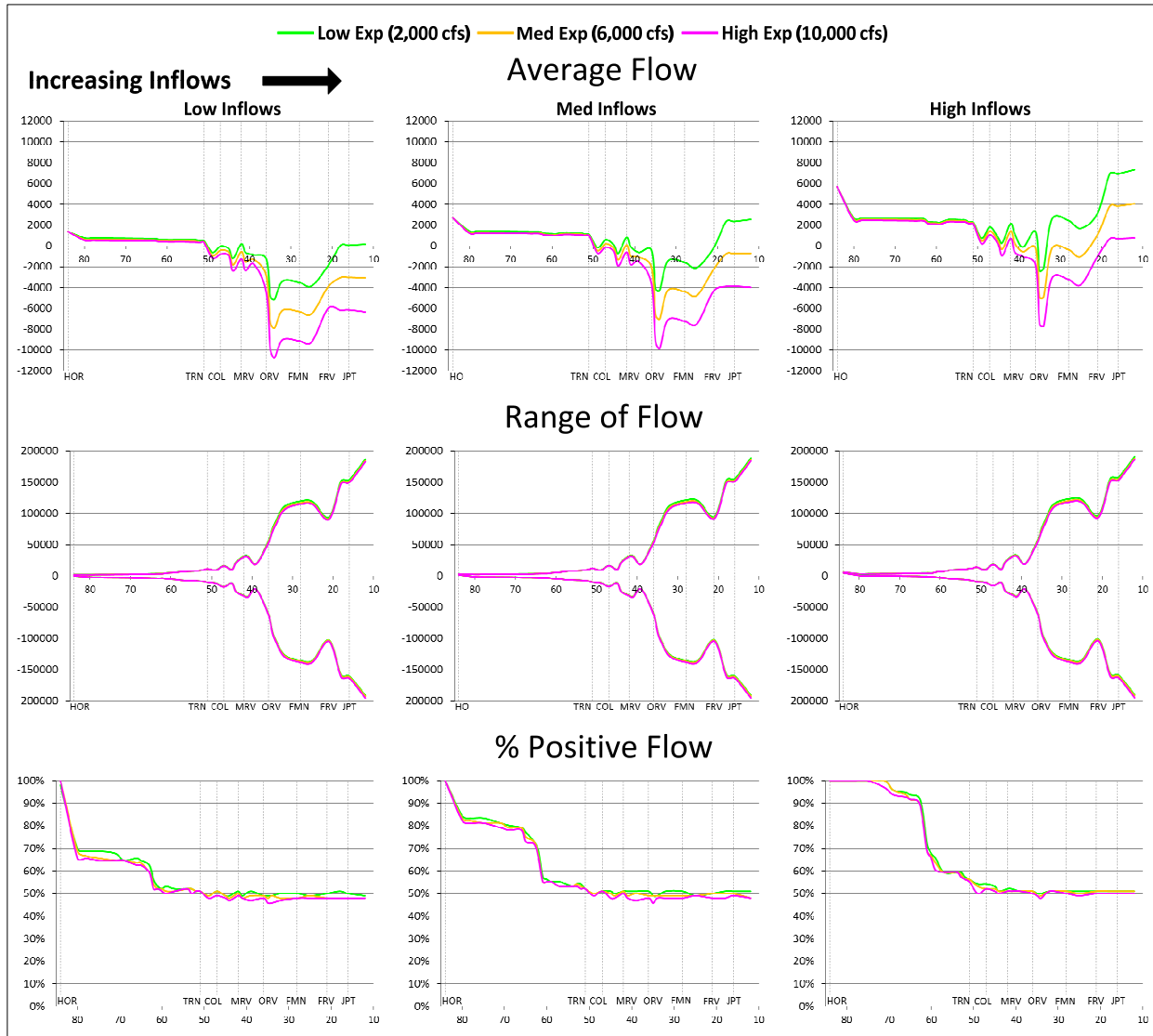


**Figure 2.** Flow Patterns in the Mainstem San Joaquin River over 24 hours. For all graphs, river kilometer is on the x-axis and curve color indicates export level. Junction locations are indicated by dotted vertical lines with junction labels. For the top two rows of graphs, magnitude of flow (in cfs) is on the y-axis. For the bottom row of graphs, y-axis displays percentage of time during which flow is positive. Graphs are arranged from left to right by increasing inflows.

Average flow at river kilometer (rkm) 84 varied between  $1,373 \text{ m}^3 \text{ sec}^{-1}$  (cfs) for low inflows/low exports and  $5,697 \text{ m}^3 \text{ sec}^{-1}$  (cfs) for high inflows/high exports. Between rkm 80 and rkm 52, average flow remained relatively flat with increasing distance downstream. Increasing inflows raised average flow in this reach from  $\sim 570 \text{ m}^3 \text{ sec}^{-1}$  (cfs) at low inflows to  $\sim 1,220 \text{ m}^3 \text{ sec}^{-1}$  (cfs) at medium inflows and  $\sim 2,420 \text{ m}^3 \text{ sec}^{-1}$  (cfs) at high inflows. Increasing exports decreased average flow in this reach by approximately  $-220 \text{ m}^3 \text{ sec}^{-1}$  (cfs) at low inflows,  $-175 \text{ m}^3 \text{ sec}^{-1}$  (cfs) at medium inflows, and  $-190 \text{ m}^3 \text{ sec}^{-1}$  (cfs) at high inflows. Downstream of rkm 52, increasing inflows raised average flow by as much as  $1,792 \text{ m}^3 \text{ sec}^{-1}$  (cfs) at rkm 51, as much as  $3,034 \text{ m}^3 \text{ sec}^{-1}$  (cfs) at rkm 34, and as much as  $7,239 \text{ m}^3 \text{ sec}^{-1}$  (cfs) at rkm 12. Increasing exports had a growing influence on average flow downstream of rkm 52, accounting for maximum

differences in average flow of  $-169 \text{ m}^3 \text{ sec}^{-1}$  (cfs) at rkm 51,  $-5,583 \text{ m}^3 \text{ sec}^{-1}$  (cfs) at rkm 34, and  $-6,544 \text{ m}^3 \text{ sec}^{-1}$  (cfs) at rkm 12.

At low inflows, flow ranged between  $2,122 \text{ m}^3 \text{ sec}^{-1}$  (cfs) and  $-30 \text{ m}^3 \text{ sec}^{-1}$  (cfs) at rkm 84, and between  $187,138 \text{ m}^3 \text{ sec}^{-1}$  (cfs) and  $-195,539 \text{ m}^3 \text{ sec}^{-1}$  (cfs) at rkm 12. At medium inflows, flow ranged between  $3,278 \text{ m}^3 \text{ sec}^{-1}$  (cfs) and  $1,474 \text{ m}^3 \text{ sec}^{-1}$  (cfs) at rkm 84 and from  $188,822 \text{ m}^3 \text{ sec}^{-1}$  (cfs) to  $-195,367 \text{ m}^3 \text{ sec}^{-1}$  (cfs) at rkm 12. At high inflows, flow ranged between  $6,121 \text{ m}^3 \text{ sec}^{-1}$  (cfs) and  $4,828 \text{ m}^3 \text{ sec}^{-1}$  (cfs) at rkm 84 and from  $191,161 \text{ m}^3 \text{ sec}^{-1}$  (cfs) to  $-195,022 \text{ m}^3 \text{ sec}^{-1}$  (cfs) at rkm 12. In general, the range of flow (difference between maximum and minimum) increased with distance downstream across all inflow and export levels.

Percent positive flow varied from 100% at rkm 84 (under all inflow/export conditions except low inflows/low exports) to just below 50% on average between rkm 51 and rkm 12. Percent positive flow was most variable between rkm 80 and rkm 59, increasing by 10% to 35% with increasing inflows. Between rkm 57 and rkm 52 (the vicinity of the TRN junction), percent positive flow increased between 5% and 8% with increasing inflows. Percent positive flow remained relatively flat between rkm 51 and rkm 12, increasing by a maximum of 5% with increasing inflows. Increasing exports decreased the percent positive flow between rkm 84 and rkm 12 by a maximum of 4% at low inflows (at rkm 80, 75, 62, and 39), a maximum of 4% at medium inflows (at rkm 65 and 39), and a maximum of 5% at high inflows (at rkm 59).

Moving westward from Channel 37, sub-daily flows in channels of the lower San Joaquin River showed increasing tidal influence (Figure 3), but despite average flows approaching  $-10,000 \text{ m}^3 \text{ sec}^{-1}$  (cfs) (see Figure 2), sub-daily flows seemingly exhibited little sensitivity to export levels (Figure 3).

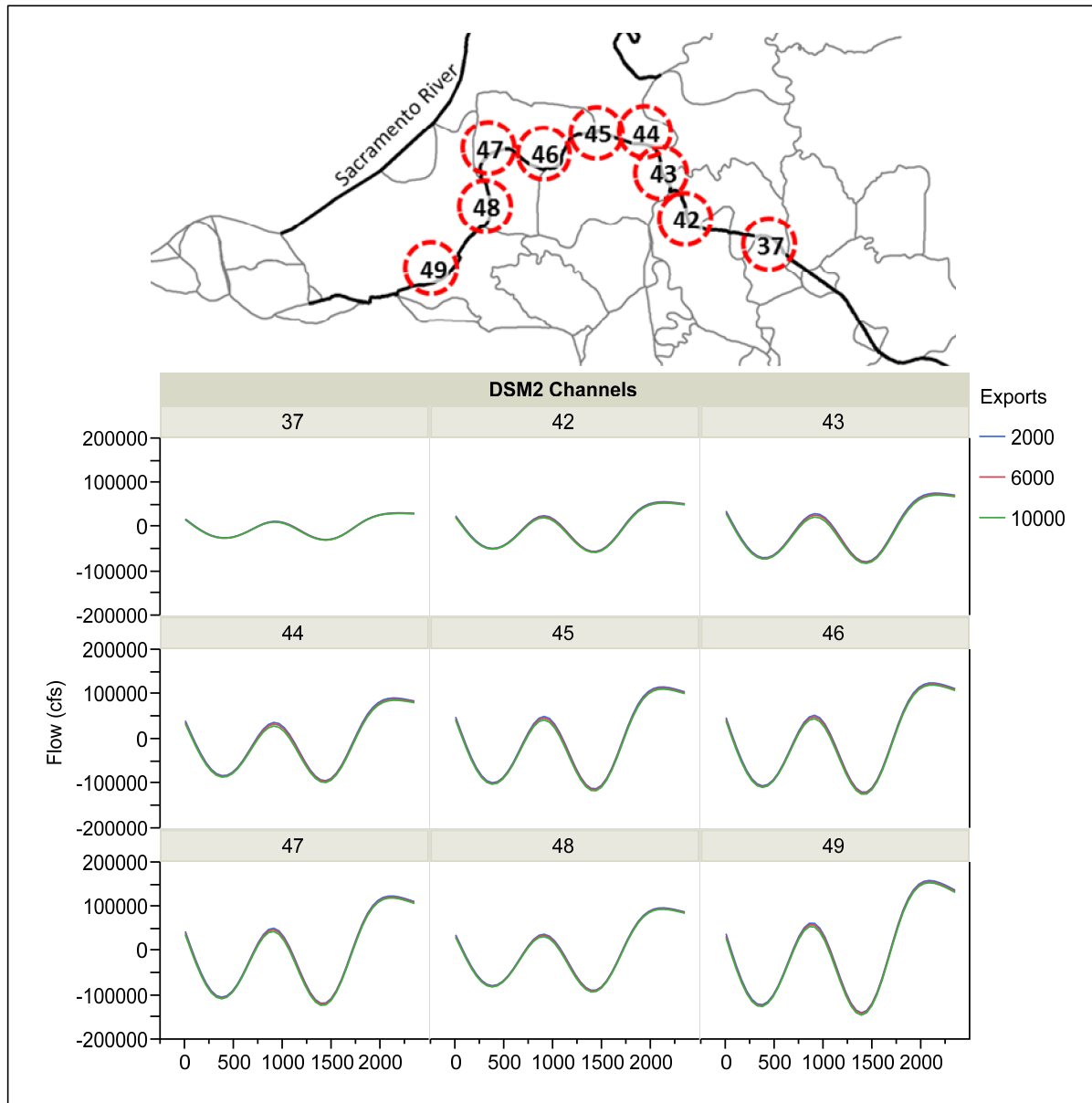


**Figure 3.** Range of Flow with Varying Exports at Selected Channels in the Mainstem San Joaquin River over 24 hours. Numbered circles on the map indicated DSM2 channel locations. Time of day is on the x-axis, starting at 0000 hours and ending at 2345 hours. Magnitude of flow is on the y-axis. Curve color indicates export level.

#### ***Direction and Magnitude of Flow at Junctions***

**Georgiana Slough:** The Georgiana Slough junction (GEO) is located on the mainstem Sacramento River and is comprised of three DSM2 Hydro channels (Figure 4). At low inflows, flow in the mainstem Sacramento River upstream of the GEO junction (GEO1) ranged from  $12,472 \text{ m}^3 \text{ sec}^{-1}$  (cfs) (downstream flow with the ebb tide) to  $-3,083 \text{ m}^3 \text{ sec}^{-1}$  (cfs) (upstream flow with the flood tide) over 24 hours (Figure 5). At medium and high inflows, flow in the mainstem Sacramento River upstream of the GEO junction was always directed downstream (i.e., always

positive), regardless of tidal state, and reached a maximum of  $19,481 \text{ m}^3 \text{ sec}^{-1}$  (cfs) under high inflow/high export conditions. Flow in the mainstem Sacramento River downstream of the GEO junction (GEO3) at low inflows ranged from  $11,336 \text{ m}^3 \text{ sec}^{-1}$  (cfs) to  $-8,395 \text{ m}^3 \text{ sec}^{-1}$  (cfs); at medium inflows, flow ranged from  $12,555 \text{ m}^3 \text{ sec}^{-1}$  (cfs) to  $-4,580 \text{ m}^3 \text{ sec}^{-1}$  (cfs). At high inflows, flow in the mainstem Sacramento River downstream of the GEO junction was always directed downstream and reached a maximum of  $15,505 \text{ m}^3 \text{ sec}^{-1}$  (cfs) under high inflow/low export conditions. Increasing inflows influenced flow patterns in the mainstem Sacramento at GEO by altering both the direction and magnitude of flow. Increasing exports did not alter direction of flow, but altered magnitude of flow by a maximum of  $193 \text{ m}^3 \text{ sec}^{-1}$  (cfs) upstream of GEO, and a maximum of  $302 \text{ m}^3 \text{ sec}^{-1}$  (cfs) downstream of GEO.

Flow in the channel leading to the interior Delta (GEO2) ranged from  $7,358 \text{ m}^3 \text{ sec}^{-1}$  (cfs) to  $593 \text{ m}^3 \text{ sec}^{-1}$  (cfs) over 24 hours (Figure 5). Maximum flow toward the interior Delta (i.e., into GEO2) occurred at time 1430 under flood tide, high inflow/high export conditions, during which all of the water entering Georgiana Slough was from upstream (GEO1) and physical flow direction in GEO3 was away from the center of the junction. Minimum flow into Georgiana Slough (GEO2) occurred at time 1800 under ebb tide, low inflow/low export conditions, during which all of the water entering Georgiana Slough was from upstream (GEO1) and physical flow direction in GEO3 was again away from the center of the junction. Increasing inflows altered magnitude of flow in GEO2 across the tidal cycle, but did not alter direction of flow. Increasing exports did not alter direction of flow in GEO2, but accounted for changes to magnitude of flow in GEO2 ranging from  $30 \text{ m}^3 \text{ sec}^{-1}$  (cfs) under high inflow conditions at time 0230 to  $241 \text{ m}^3 \text{ sec}^{-1}$  (cfs) under low inflow conditions at time 1100. Increasing exports resulted in smaller changes at other times, accounting for an average change of  $124 \text{ m}^3 \text{ sec}^{-1}$  (cfs) (i.e., more flow into Georgiana Slough) across all inflow levels.

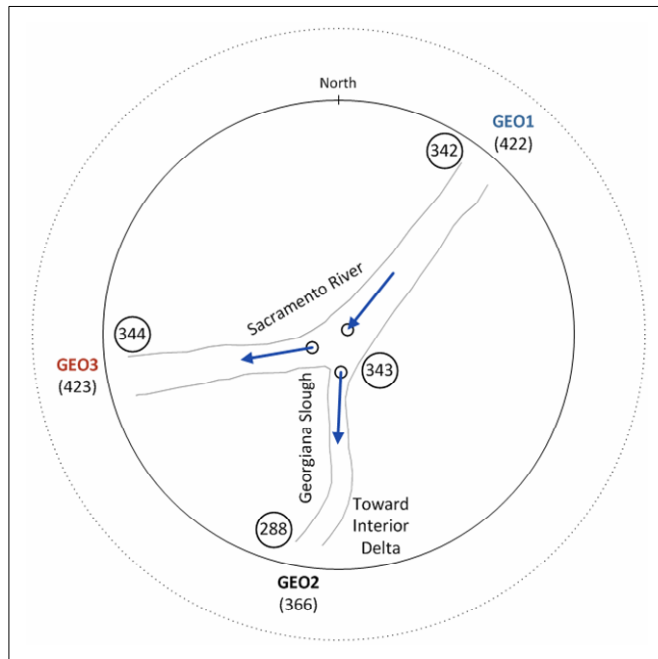


**Figure 4.** GEO: Plan-view of Georgiana Slough Junction. Physical channel outlines are shown in gray. DSM2 Hydro channel numbers are given in parentheses, nodes are circled, and positive flow direction in each channel is indicated by blue arrows. Upstream, downstream, and to interior Delta channels are indicated as in Table 2.

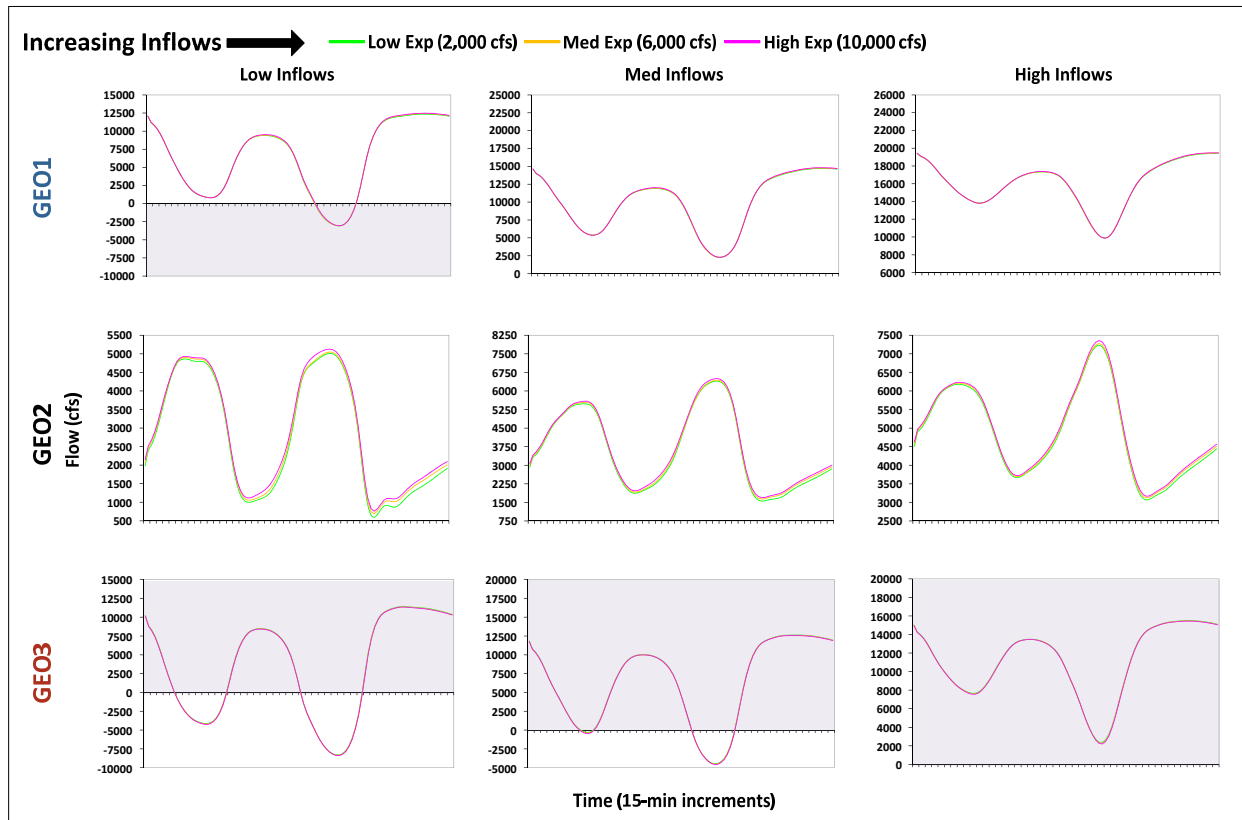


**Figure 5.** GEO: Flow in Georgiana Slough Junction Channels over 24 Hours. Time of day in 15-minute increments is on the x-axis, starting at 0000 hours and ending at 2345 hours. Magnitude of flow is on the y-axis. Curve color indicates export level. Channel designations are as indicated in Table 2. For channel GEO2, all flow is toward the interior Delta. For the other channels, flow displayed in the shaded area is away from the center of the junction.

**Head of Old River:** The Head of Old River junction (HOR) is located on the mainstem San Joaquin River and is comprised of three DSM2 Hydro channels (Figure 6). At low inflows, flow in the mainstem San Joaquin River upstream of the HOR junction (HOR2) ranged from  $2,122 \text{ m}^3 \text{ sec}^{-1}$  (cfs) to  $-30 \text{ m}^3 \text{ sec}^{-1}$  (cfs) over 24 hours (Figure 7). At medium and high inflows, flow direction was always downstream regardless of tidal state, and reached a maximum of  $6,041 \text{ m}^3 \text{ sec}^{-1}$  (cfs) under high inflow/high export conditions. Flow in the mainstem San Joaquin River downstream of the HOR junction (HOR1) at low inflows ranged from  $2,070 \text{ m}^3 \text{ sec}^{-1}$  (cfs) to  $-2,042 \text{ m}^3 \text{ sec}^{-1}$  (cfs); at medium inflows, flow ranged from  $2,442 \text{ m}^3 \text{ sec}^{-1}$  (cfs) to  $-1,404 \text{ m}^3 \text{ sec}^{-1}$  (cfs). At high inflows, flow direction in the mainstream San Joaquin River downstream of the HOR junction was always downstream (positive) and reached a maximum of  $3,233 \text{ m}^3 \text{ sec}^{-1}$  (cfs) under high inflow/low export conditions. Increasing inflows influenced flow patterns in the mainstem San Joaquin at HOR by altering both direction and magnitude of flow. Increasing exports altered direction of flow upstream of the junction (HOR2) at ebb tide under low inflow/low export conditions. Increasing exports altered magnitude of flow by a maximum of  $348 \text{ m}^3 \text{ sec}^{-1}$  (cfs) upstream of the HOR junction and by a maximum of  $950 \text{ m}^3 \text{ sec}^{-1}$  (cfs) downstream of the junction.

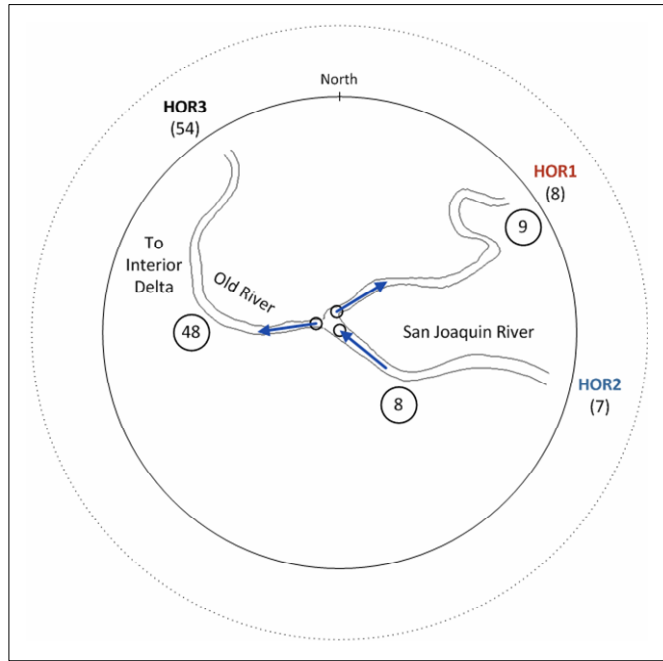


**Figure 6.** HOR: Plan-view of Head of Old River Junction. See Figure 4 for description of elements.

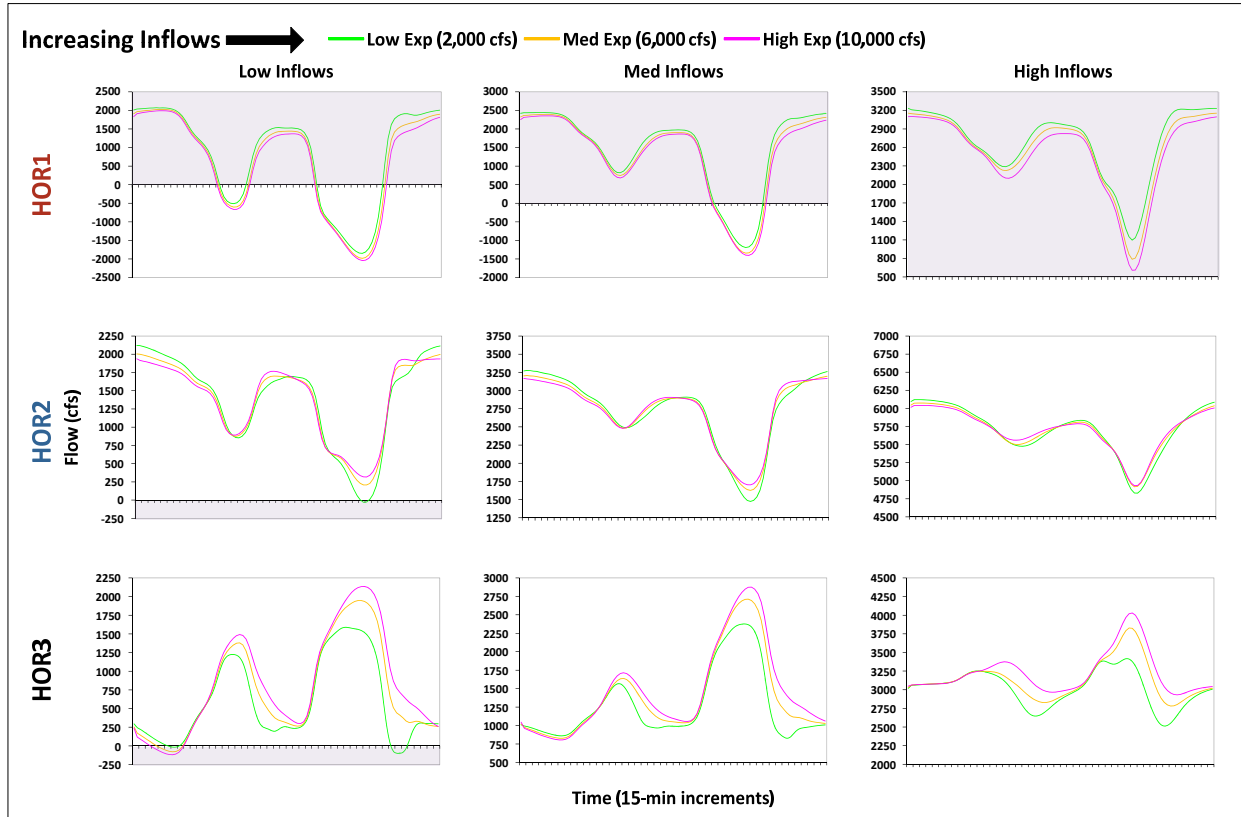


**Figure 7.** HOR: Flow in Head of Old River Junction Channels over 24 Hours. See Figure 5 for description of elements. For channel HOR3, flow displayed in the shaded area is away from the interior Delta; for the other channels, flow displayed in the shaded area is away from the center of the junction.

Flow in the channel leading to the interior Delta at HOR junction (HOR3) ranged from  $4,030 \text{ m}^3 \text{ sec}^{-1}$  (cfs) toward the interior Delta to  $-118 \text{ m}^3 \text{ sec}^{-1}$  (cfs) away from the interior Delta over 24 hours (*see Figure 7*). Maximum flow toward the interior Delta occurred at time 1730 under flood tide, high inflow/high export conditions, during which all of the water entering the interior Delta was from upstream (HOR2) and physical flow direction in HOR1 was away from the center of the junction. Maximum flow away from the interior Delta (i.e., out of HOR3 and into the mainstem San Joaquin River) occurred at time 0300 under ebb tide, low inflow/high export conditions; physical flow direction in HOR1 was again away from the center of the junction. Increasing inflows influenced flow patterns in the channel leading to the interior Delta (HOR3) by altering both direction and magnitude of flow. Increasing exports altered flow direction, resulted in separation of flow curves across most of the tidal cycle, and accounted for changes to magnitude of flow in HOR3 ranging from  $-131 \text{ m}^3 \text{ sec}^{-1}$  (cfs) under low inflow conditions at time 0045 to  $1,033 \text{ m}^3 \text{ sec}^{-1}$  (cfs) under low inflow conditions at time 1945. Increasing exports resulted in smaller changes at other times, accounting for an average change of  $217 \text{ m}^3 \text{ sec}^{-1}$  (cfs) (i.e., more flow into the interior Delta) across all inflow levels.

**Turner Cut:** The Turner Cut junction (TRN) is located on the mainstem San Joaquin River and is comprised of eight DSM2 Hydro channels (Figure 8). Our analysis focused on three of these channels (TRN3, TRN5, and TRN8) which represent all flows entering or exiting the junction. Flow in the mainstem San Joaquin River upstream of the TRN junction (TRN3) ranged from  $14,361 \text{ m}^3 \text{ sec}^{-1}$  (cfs) to  $-10,015 \text{ m}^3 \text{ sec}^{-1}$  (cfs) over 24 hours (Figure 9). Flow in the mainstem San Joaquin River downstream of the TRN junction (TRN8) ranged from  $18,607 \text{ m}^3 \text{ sec}^{-1}$  (cfs) to  $-17,549 \text{ m}^3 \text{ sec}^{-1}$  (cfs). Increasing inflows had little influence on flow patterns in the mainstem San Joaquin at TRN; direction and magnitude of flow appeared to largely track the tidal cycle. Increasing exports altered magnitude of flow by a maximum of  $1,014 \text{ m}^3 \text{ sec}^{-1}$  (cfs) upstream of the TRN junction and by a maximum of  $1,690 \text{ m}^3 \text{ sec}^{-1}$  (cfs) downstream of the junction.

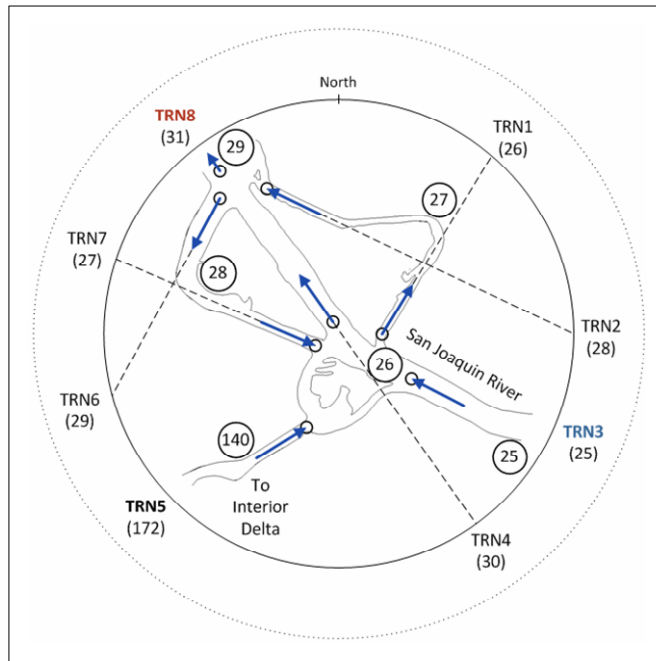


**Figure 8.** TRN: Plan-view of Turner Cut Junction. *See Figure 4 for description of elements.*

Flow in the channel leading to the interior Delta at TRN junction (TRN5) ranged from  $-5,069 \text{ m}^3 \text{ sec}^{-1}$  (cfs) toward the interior Delta to  $3,611 \text{ m}^3 \text{ sec}^{-1}$  (cfs) away from the interior Delta over 24 hours (Figure 9). Maximum flow toward the interior Delta occurred at time 1515 under flood tide, high inflow/high export conditions, during which all of the water entering the interior Delta was from downstream (TRN8) and physical flow direction in TRN3 was away from the center of the junction. Maximum flow away from the interior Delta occurred at time 2115 under ebb tide, high inflow/low export conditions. During this time, physical flow direction in TRN8 was away from the center of the junction. Increasing inflows had little influence on flow patterns in the channel leading to the interior Delta at TRN (TRN5); direction and magnitude of flow were largely dependent on the tidal cycle. Increasing exports resulted in separation of flow curves across most of the tidal cycle, and accounted for changes to magnitude of flow in TRN5 ranging from  $-99 \text{ m}^3 \text{ sec}^{-1}$  (cfs) under high inflow conditions at time 0430 to  $-1,449 \text{ m}^3 \text{ sec}^{-1}$  (cfs) under medium inflow conditions at time 0915. Increasing exports resulted in smaller changes at other times, accounting for an average change of  $-589 \text{ m}^3 \text{ sec}^{-1}$  (cfs) (i.e., more flow into the interior Delta) across all inflow levels.

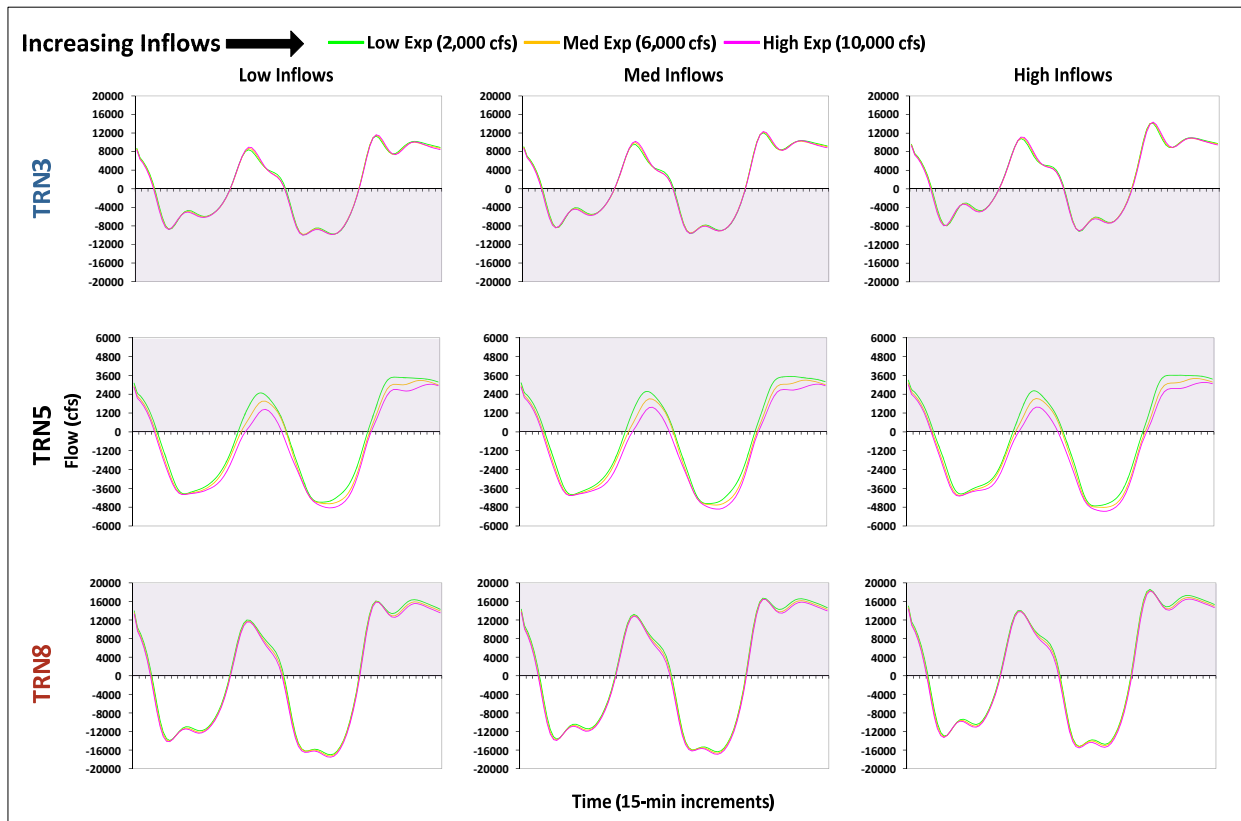


**Figure 9.** TRN: Flow in Turner Cut Junction Channels over 24 Hours. See Figure 5 for description of elements. For channel TRN5, flow displayed in the shaded area is away from the interior Delta; for the other channels, flow displayed in the shaded area is away from the center of the junction.

**Columbia Cut:** The Columbia Cut junction (COL) is located at the confluence of the mainstem San Joaquin River and Disappointment Slough. COL is comprised of ten channels, as defined in DSM2 Hydro (Figure 10). The COL junction is unique in having two channels entering the junction from upstream (COL1 and COL4) and two parallel channels exiting the junction (COL8 and COL9). Our analysis focused on a subset of the ten channels which represented total inflow and outflow from the junction (COL1, COL4, COL7, COL8, and COL9). Flow in the mainstem San Joaquin River upstream of the COL junction (COL4) ranged from  $18,607 \text{ m}^3 \text{ sec}^{-1}$  (cfs) to  $-17,549 \text{ m}^3 \text{ sec}^{-1}$  (cfs) over 24 hours (Figure 11). Flow in the mainstem San Joaquin River downstream of the COL junction (COL8 and COL9) ranged from  $32,239 \text{ m}^3 \text{ sec}^{-1}$  (cfs) to  $-33,541 \text{ m}^3 \text{ sec}^{-1}$  (cfs)— $9,587 \text{ m}^3 \text{ sec}^{-1}$  (cfs) to  $-8,410 \text{ m}^3 \text{ sec}^{-1}$  (cfs) for COL8 and  $22,652 \text{ m}^3 \text{ sec}^{-1}$  (cfs) to  $-25,131 \text{ m}^3 \text{ sec}^{-1}$  (cfs) for COL9. Increasing inflows had little influence on flow patterns in the mainstem San Joaquin at COL; direction and magnitude of flow appeared to primarily track the tidal cycle. Increasing exports altered magnitude of flow by a maximum of  $1,736 \text{ m}^3 \text{ sec}^{-1}$  (cfs) upstream of COL and by a maximum of  $2,644 \text{ m}^3 \text{ sec}^{-1}$  (cfs) downstream of the junction.

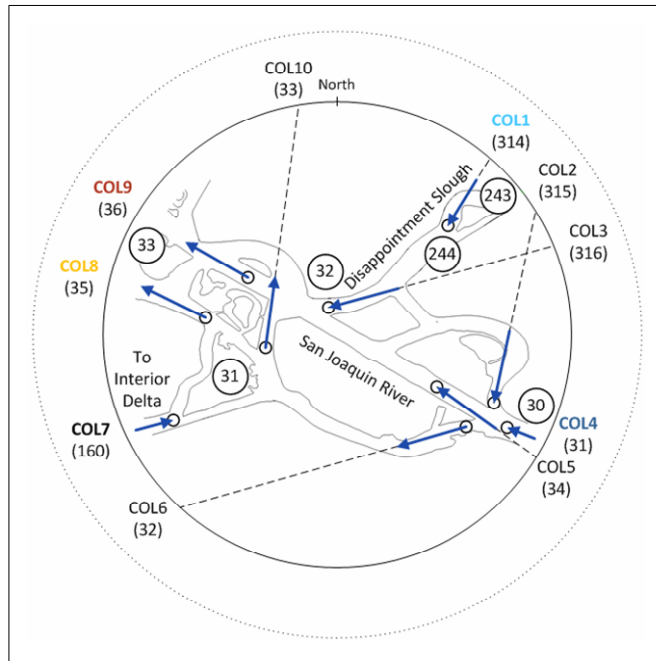


**Figure 10.** COL: Plan-view of Columbia Cut Junction. See Figure 4 for description of elements.

Flow in the channel leading to the interior Delta at COL junction (COL7) ranged from  $-9,980 \text{ m}^3 \text{ sec}^{-1}$  (cfs) toward the interior Delta to  $6,375 \text{ m}^3 \text{ sec}^{-1}$  (cfs) away from the interior Delta over 24 hours (Figure 11). Maximum flow toward the interior Delta occurred at time 1745 under ebb tide, high inflow/low export conditions, during which all of the water entering the interior Delta was from upstream, and was likely a mix of water originating from Disappointment Slough (COL1) and the San Joaquin River (COL4). Maximum flow away from the interior Delta occurred at time 0130 under flood tide, high inflow/high export conditions. During this time, physical flow direction in both COL1 and COL4 was away from the center of the junction. Increasing inflows had little influence on flow patterns in the channel leading to the interior Delta (COL7); direction and magnitude of flow varied largely with the tidal cycle. Increasing

exports resulted in separation of flow curves across most of the tidal cycle, and accounted for changes to magnitude of flow in COL7 ranging from  $-261 \text{ m}^3 \text{ sec}^{-1}$  (cfs) under low inflow conditions at time 0430 to  $-3,141 \text{ m}^3 \text{ sec}^{-1}$  (cfs) under medium inflow conditions at time 0915. Increasing exports resulted in smaller changes at other times, accounting for an average change of  $-1,360 \text{ m}^3 \text{ sec}^{-1}$  (cfs) (i.e., more flow into the interior Delta) across all inflow levels.

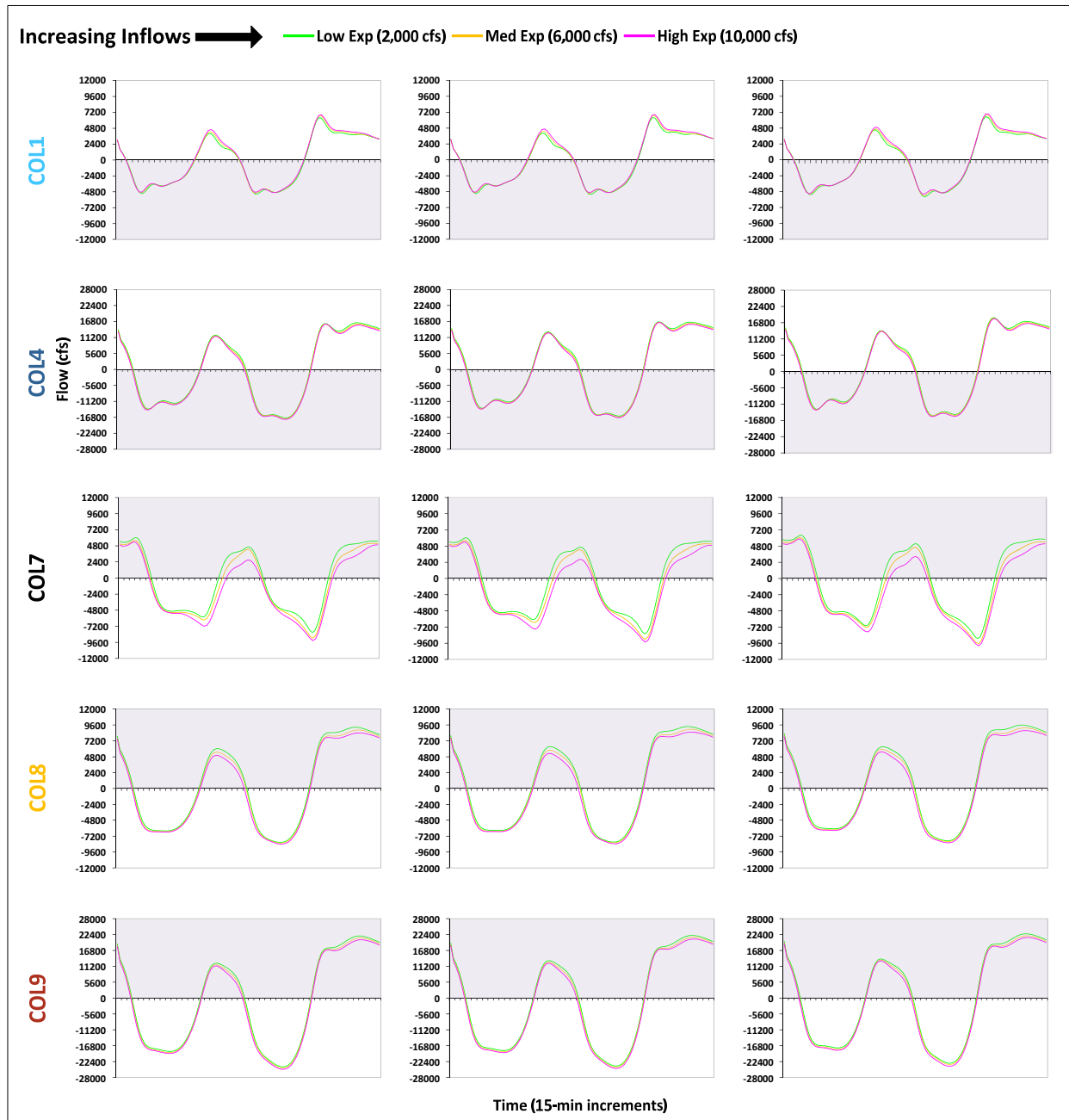


**Figure 11.** COL: Flow in Columbia Cut Junction Channels over 24 Hours. See Figure 5 for description of elements. For channel COL7, flow displayed in the shaded area is away from the interior Delta; for the other channels, flow displayed in the shaded area is away from the center of the junction.

**Middle River:** The Middle River junction (MRV) is located on the mainstem San Joaquin River and is comprised of nine DSM2 Hydro channels (Figure 12). However, total flow into and out of the junction is represented by just three channels (MRV3, MRV5, and MRV9). Flow in the mainstem San Joaquin River upstream of the MRV junction (MRV3) ranged from  $33,129 \text{ m}^3 \text{ sec}^{-1}$  (cfs) to  $-32,310 \text{ m}^3 \text{ sec}^{-1}$  (cfs) over 24 hours (Figure 13). Flow in the mainstem San Joaquin River downstream of the MRV junction (MRV9) ranged from  $57,170 \text{ m}^3 \text{ sec}^{-1}$  (cfs) to  $-61,960 \text{ m}^3 \text{ sec}^{-1}$  (cfs). Increasing inflows had little influence on flow patterns in MRV3 and MRV9; direction and magnitude of flow largely tracked the tidal cycle. Increasing exports altered magnitude of flow by a maximum of  $3,307 \text{ m}^3 \text{ sec}^{-1}$  (cfs) upstream of the MRV junction and by a maximum of  $7,468 \text{ m}^3 \text{ sec}^{-1}$  (cfs) downstream of the junction.

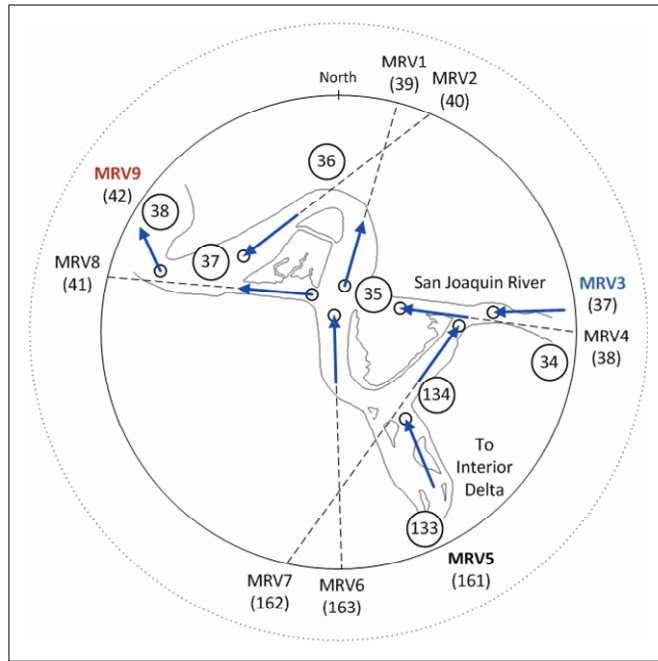


**Figure 12.** MRV: Plan-view of Middle River Junction. See Figure 4 for description of elements.

Flow in the channel leading to the interior Delta at MRV junction (MRV5) ranged from  $-20,769 \text{ m}^3 \text{ sec}^{-1}$  (cfs) toward the interior Delta to  $17,890 \text{ m}^3 \text{ sec}^{-1}$  (cfs) away from the interior Delta over 24 hours (Figure 13). Maximum flow toward the interior Delta occurred at time 1445 under flood tide, medium inflow/high export conditions, during which all of the water entering the interior Delta was from downstream (MRV9) and physical flow direction in MRV3 was away from the center of the junction. Maximum flow away from the interior Delta occurred at time 1830 under ebb tide, high inflow/low export conditions. During this time, physical flow direction in MRV9 was away from the center of the junction. Increasing inflows had little influence on flow patterns in the channel leading to the interior Delta (MRV5); direction and magnitude of flow largely tracked the tidal cycle. Increasing exports resulted in separation of flow curves across nearly half of the tidal cycle, and accounted for changes to magnitude of flow in MRV5 ranging from  $124 \text{ m}^3 \text{ sec}^{-1}$  (cfs) under low inflow conditions at time 1315 to  $-3,845 \text{ m}^3 \text{ sec}^{-1}$  (cfs) under medium inflow conditions at time 0800. Increasing exports resulted in smaller

changes at other times, accounting for an average change of  $-1,765 \text{ m}^3 \text{ sec}^{-1}$  (cfs) (i.e., more flow into the interior Delta) across all inflow levels.

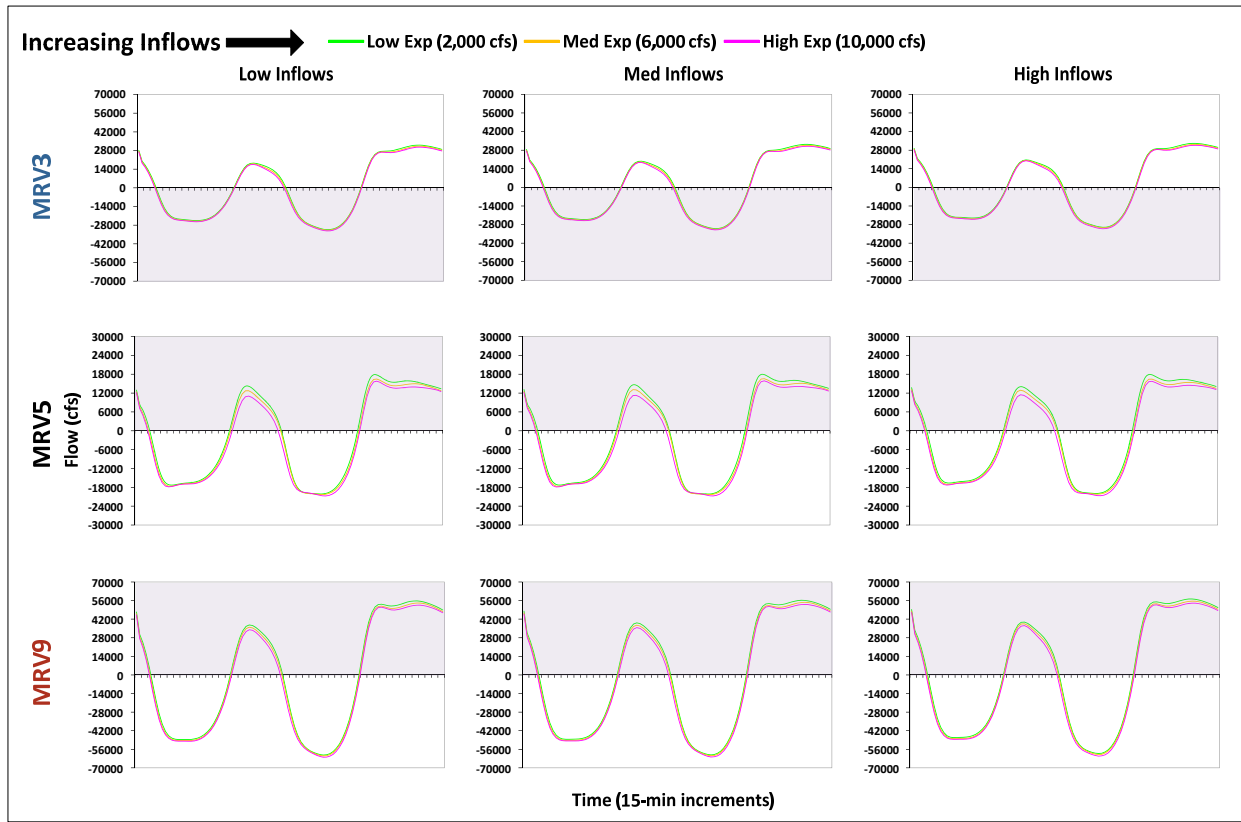


**Figure 13.** MRV: Flow in Middle River Junction Channels over 24 Hours. See Figure 5 for description of elements. For channel MRV5, flow displayed in the shaded area is away from the interior Delta; for the other channels, flow displayed in the shaded area is away from the center of the junction.

**Mouth of Old River:** The Mouth of Old River junction (ORV) is located on the mainstem San Joaquin River just upstream of its confluence with Potato Slough. The junction is comprised of three DSM2 Hydro channels (Figure 14). Flow in the mainstem San Joaquin River upstream of the ORV junction (ORV1) ranged from  $57,170 \text{ m}^3 \text{ sec}^{-1}$  (cfs) to  $-61,960 \text{ m}^3 \text{ sec}^{-1}$  (cfs) over 24 hours (Figure 15). Flow in the mainstem San Joaquin River downstream of the ORV junction (ORV3) ranged from  $75,852 \text{ m}^3 \text{ sec}^{-1}$  (cfs) to  $-90,746 \text{ m}^3 \text{ sec}^{-1}$  (cfs). Increasing inflows had little influence on flow patterns in the mainstem San Joaquin at ORV; direction and magnitude of flow largely tracked tidal variation. Increasing exports altered the magnitude of flow by a maximum of  $7,468 \text{ m}^3 \text{ sec}^{-1}$  (cfs) upstream of the ORV junction and by a maximum of  $11,305 \text{ m}^3 \text{ sec}^{-1}$  (cfs) downstream of the junction.

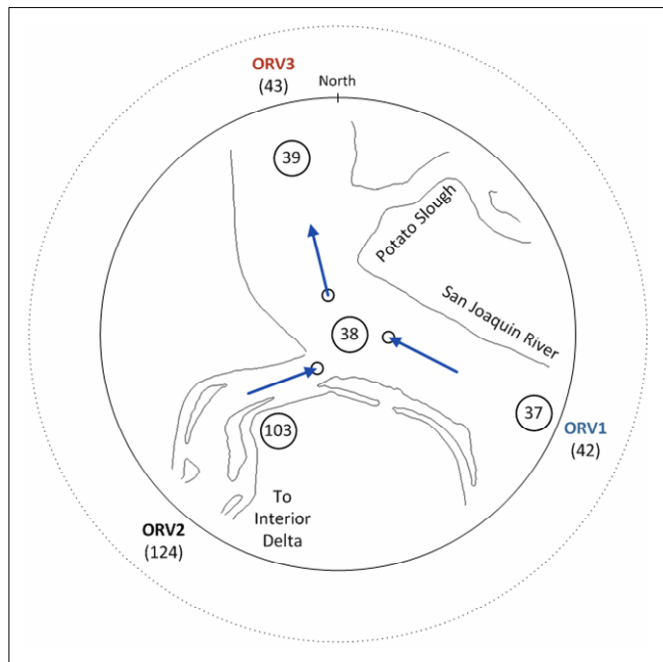


**Figure 14.** ORV: Plan-view of Mouth of Old River Junction. See Figure 4 for description of elements.

Flow in the channel leading to the interior Delta at ORV junction (ORV2) ranged from  $-23,140 \text{ m}^3 \text{ sec}^{-1}$  (cfs) toward the interior Delta to  $13,597 \text{ m}^3 \text{ sec}^{-1}$  (cfs) away from the interior Delta over 24 hours (Figure 15). Maximum flow toward the interior Delta occurred at time 1430 under flood tide, high inflow/high export conditions, during which all of the water entering the interior Delta was from downstream. Maximum flow away from the interior Delta occurred at time 2045 under ebb tide, low inflow/low export conditions. During this time, physical flow direction in ORV3 was away from the center of the junction. Increasing inflows had little influence on flow patterns in the channel leading to the interior Delta (ORV2); direction and magnitude of flow appeared to largely track tidal variations. Increasing exports resulted in separation of flow curves across more than half of the tidal cycle, and accounted for changes to magnitude of flow in ORV2 ranging from  $-506 \text{ m}^3 \text{ sec}^{-1}$  (cfs) under low inflow conditions at time 0445 to  $-4,268 \text{ m}^3 \text{ sec}^{-1}$  (cfs) under high inflow conditions at time 1200. Increasing exports resulted in smaller changes at other times, accounting for an average change of  $-1,932 \text{ m}^3 \text{ sec}^{-1}$  (cfs) (i.e., more flow into the interior Delta) across all inflow levels.

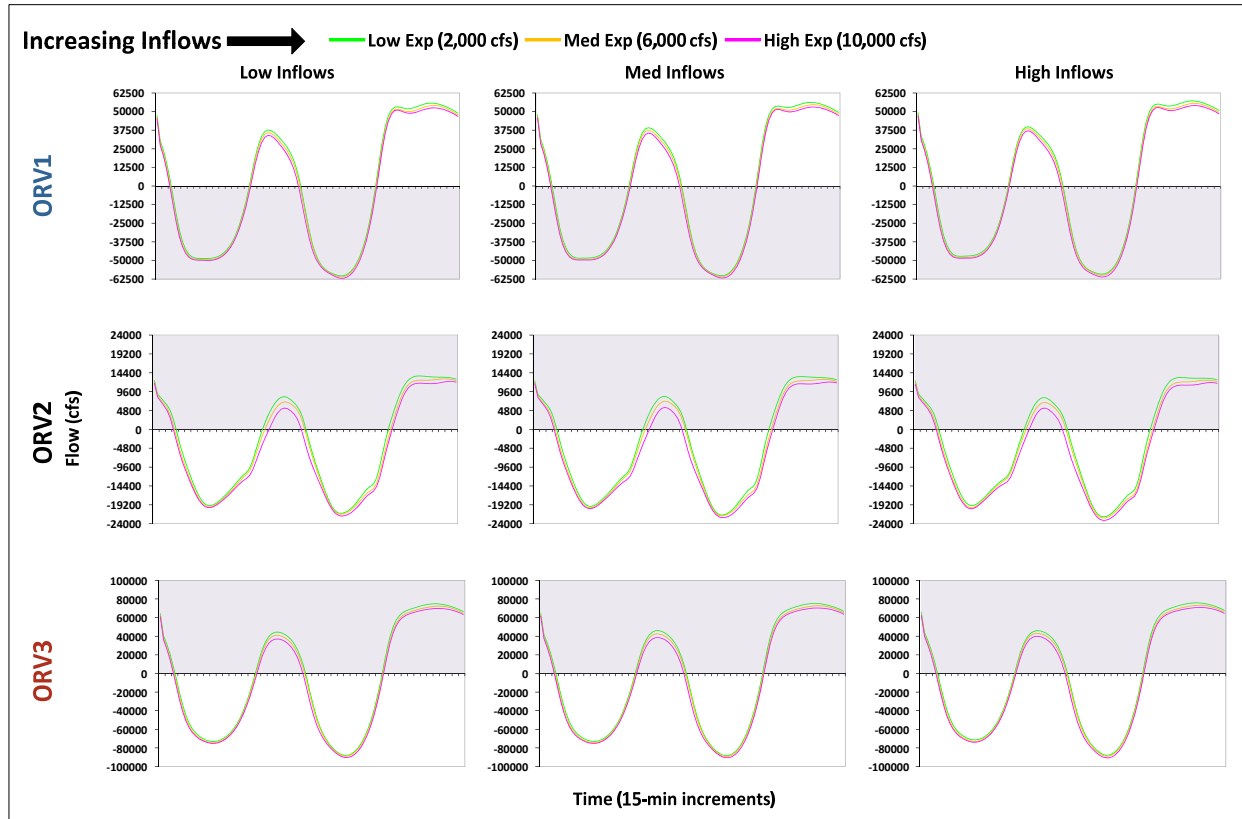


**Figure 15.** ORV: Flow in Mouth of Old River Junction Channels over 24 Hours. See Figure 5 for description of elements. For channel ORV2, flow displayed in the shaded area is away from the interior Delta; for the other channels, flow displayed in the shaded area is away from the center of the junction.

### ***Proportion and Source of Flow to Interior Delta***

***Georgiana Slough:*** The proportion of flow which entered GEO varied from 5.9% to 100% over 24 hours (Figure 16), depending on inflow and export conditions. At low exports, increasing inflows from low to high accounted for changes in proportion of flow into Georgiana Slough (GEO2) ranging from -70.2% (at time 1645) to 12.5% (at time 1445). At high exports, increasing inflows from low to high accounted for changes in proportion of flow ranging from -69.4% (at time 1645) to 13.2% (at time 1445). Increasing inflows resulted in smaller changes at other times, accounting for an average change of -13.2% across all export levels. Increasing inflows also resulted in decreased proportion of flow and decreased variation in proportion of flow across the tidal cycle. At low inflows, increasing exports from low to high accounted for changes in proportion of flow ranging from -0.3% (at time 1615) to 5.7% (at time 1700). At high inflows, increasing exports from low to high accounted for changes in proportion of flow ranging from 0.1% (at time 1245) to 1.7% (at time 1600). Increasing exports resulted in smaller changes at other times, accounting for an average change of 0.9% across all inflow levels. Increasing exports had little influence on proportion of flow patterns over 24 hours.

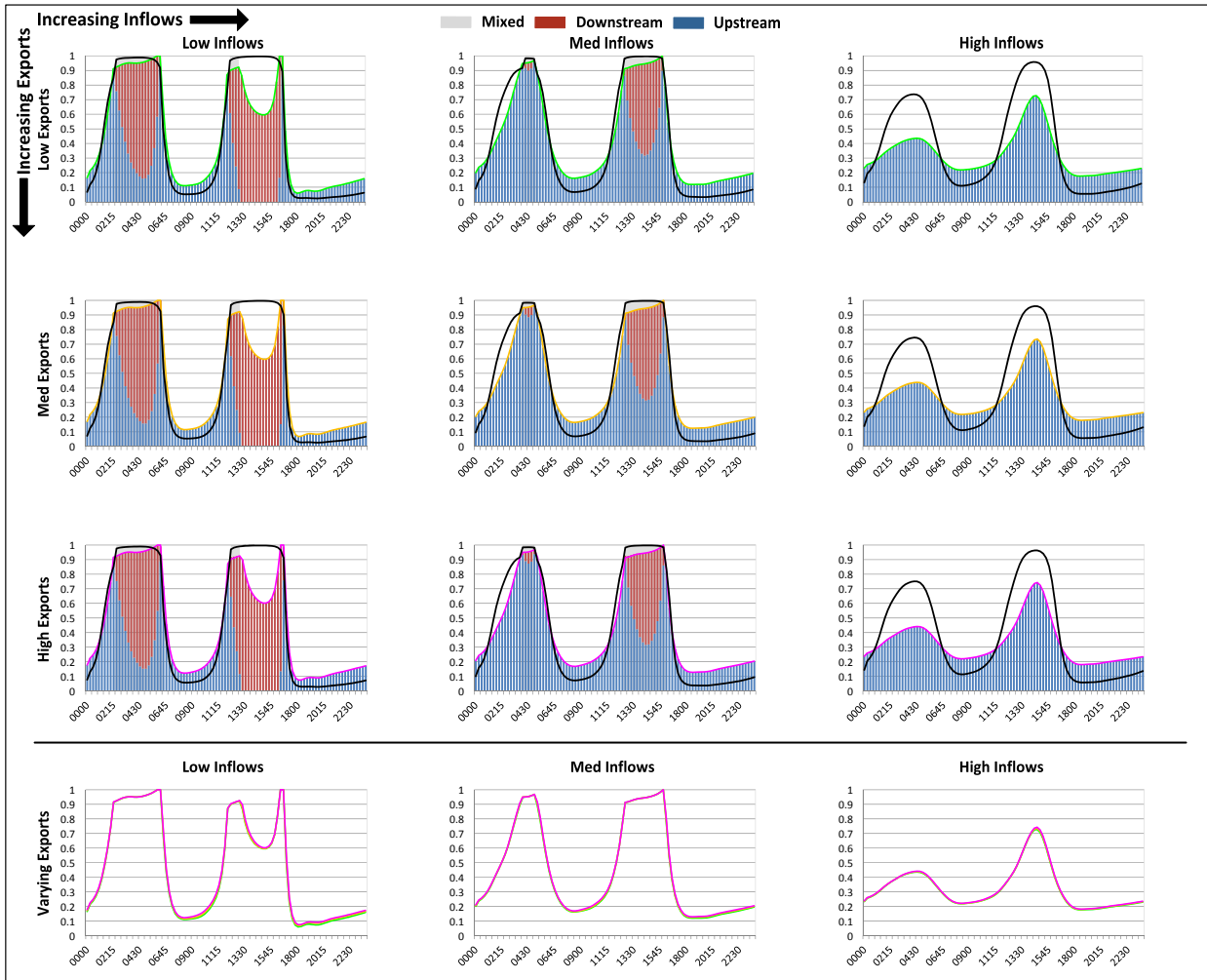


**Figure 16.** GEO: Proportion of Flow to Georgiana Slough with Probability of Entrainment. Time of day in 24-hr format is on the x-axis; proportion of flow is on the y-axis. Graphs in the top section display the proportion of water input to the junction which is output to Georgiana Slough (curve), by water source (bars under the curve). Curve color indicates export level. Bar color indicates water source; bar length indicates relative proportion. Gray shading indicates water from more than one source. Black curves superimposed on the proportion of flow graphs are the probability of entrainment into Georgiana Slough, as calculated from equation 6.4 of Perry 2010. Graphs in the top section are arranged by increasing inflows and exports. Graphs in the bottom section compare proportions under varying exports, with the bars removed for clarity.

At low inflows, water entered Georgiana Slough (GEO2) from the upstream direction for nearly the entire tidal cycle and from both upstream and downstream directions for most of the first flood tide and at the beginning of the second flood tide. Flow from downstream (i.e., water entering the GEO junction from downriver and flowing into Georgiana Slough) accounted for most of the water which entered Georgiana Slough during high tides. As inflows increased, relative proportion of flow from downstream decreased. At high inflows, all of the water which entered Georgiana Slough was from upstream. Increasing exports had little effect on the relative proportion of flow from upstream versus from downstream.

Overall, inflows had a stronger influence than exports on proportion of flow and direction of flow entering the interior Delta at GEO junction.

In order to meaningfully relate the proportion of flow patterns at GEO to the migration routing of juvenile salmon at that junction, we compared our results for the proportion of water which entered Georgiana Slough to the observed probability of fish entrainment into Georgiana Slough from Perry (2010) (*see equation 2 for details*). The proportion of flow and probability of entrainment were closely correlated at low and medium inflows. At high inflows, the proportion of flow which entered Georgiana Slough and the probability of entrainment into Georgiana Slough diverged in absolute value but exhibited a similar pattern, with peaks and troughs in the curves occurring at the same times.

**Head of Old River:** The proportion of flow which entered the interior Delta at HOR varied from 0% to 100% over 24 hours (Figure 17), depending on inflow and export conditions. At low exports, increasing inflows from low to high accounted for changes in proportion of flow into the interior Delta (HOR3) ranging from -49.7% (at time 1915) to 51.4% (at time 0330). At high exports, increasing inflows from low to high accounted for changes in proportion of flow into the interior Delta ranging from -42.3% (at time 0900) to 52.3% (at time 0345). Increasing inflows resulted in smaller changes at other times, accounting for an average change of 11.5% across all export levels. Increasing inflows resulted in decreased variation in proportion of flow across the tidal cycle. At low inflows, increasing exports from low to high accounted for changes in proportion of flow ranging from -6.3% (at time 0115) to 74.5% (at time 1945). At high inflows, increasing exports from low to high accounted for changes in proportion of flow ranging from 0.3% (at time 0515) to 12.6% (at time 1800). Increasing exports resulted in smaller changes at other times, accounting for an average change of 6.3% across all inflow levels. Increasing exports resulted in separation of proportion of flow curves over 24 hours—mostly during ebb tides.

At low inflows, water entered the interior Delta via HOR3 from the upstream direction for nearly the entire tidal cycle and from both the upstream and downstream directions for nearly the entire duration of high tides (0630-0900 and 1415-1930). As inflows increased, relative proportion of flow from downstream decreased. At high inflows, all of the water which entered the interior Delta was from the upstream direction. As exports increased, relative proportion of flow from upstream increased slightly.

Overall, inflows had a stronger influence than exports on proportion of flow and on direction of flow entering the interior Delta at the HOR junction.

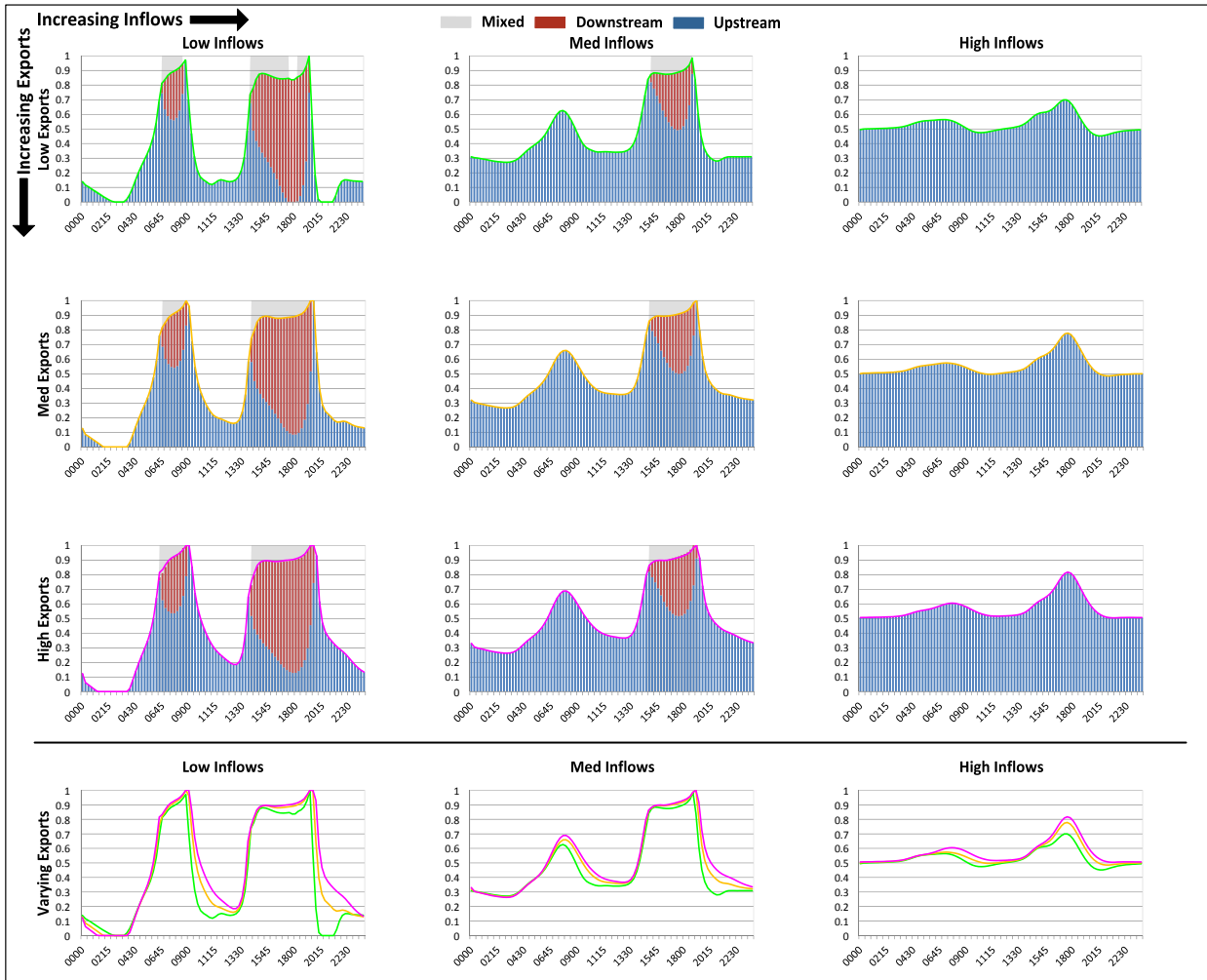


**Figure 17.** HOR: Proportion of Flow to Interior Delta at Head of Old River. Time of day in 24-hr format is on the x-axis; proportion of flow is on the y-axis. Graphs in the top section display the proportion of water input to the junction which is output to the interior Delta (curve), by water source (bars under the curve). Curve color indicates export level. Bar color indicates water source; bar length indicates relative proportion. Gray shading indicates water from more than one source. Graphs in the top section are arranged by increasing inflows and exports. Graphs in the bottom section compare proportions under varying exports, with the bars removed for clarity.

***Turner Cut:*** The proportion of flow which entered the interior Delta at TRN varied from 0% to 100% over 24 hours (Figure 18), depending on inflow and export conditions. At low exports, increasing inflows from low to high accounted for changes in proportion of flow into the interior Delta (TRN5) ranging from -69.4% (at time 0730) to 47.5% (at time 0700). At high exports, increasing inflows from low to high accounted for changes in proportion of flow into the interior Delta ranging from -57.0% (at time 0730) to 41.9% (at time 0700). Increasing inflows resulted in smaller changes at other times, accounting for an average change of 1.1% across all export levels. At low inflows, increasing exports from low to high accounted for changes in proportion of flow ranging from -1.7% (at time 0715) to 25.8% (at time 0745). At high inflows, increasing exports from low to high accounted for changes in proportion of flow ranging from -3.9% (at time 1700) to 25.5% (at time 1730). Increasing exports resulted in smaller changes at other

times, accounting for an average change of 3.6% across all inflow levels. Neither increasing inflows nor increasing exports substantially altered proportion of flow patterns over 24 hours.

At all inflow levels, water entered the interior Delta via TRN5 mostly from the downstream direction and primarily during flood/high tides; flow from upstream (i.e., water entering the TRN junction from upriver and flowing into the interior Delta) entered the interior Delta only briefly—on ebb tides. As inflows increased from low to high, relative proportion of flow from upstream increased only slightly. Relative proportion of flow from upstream also increased only slightly with increasing exports.

Overall, inflows and exports caused relatively little change in proportion of flow and direction of flow entering the interior Delta at the TRN junction.

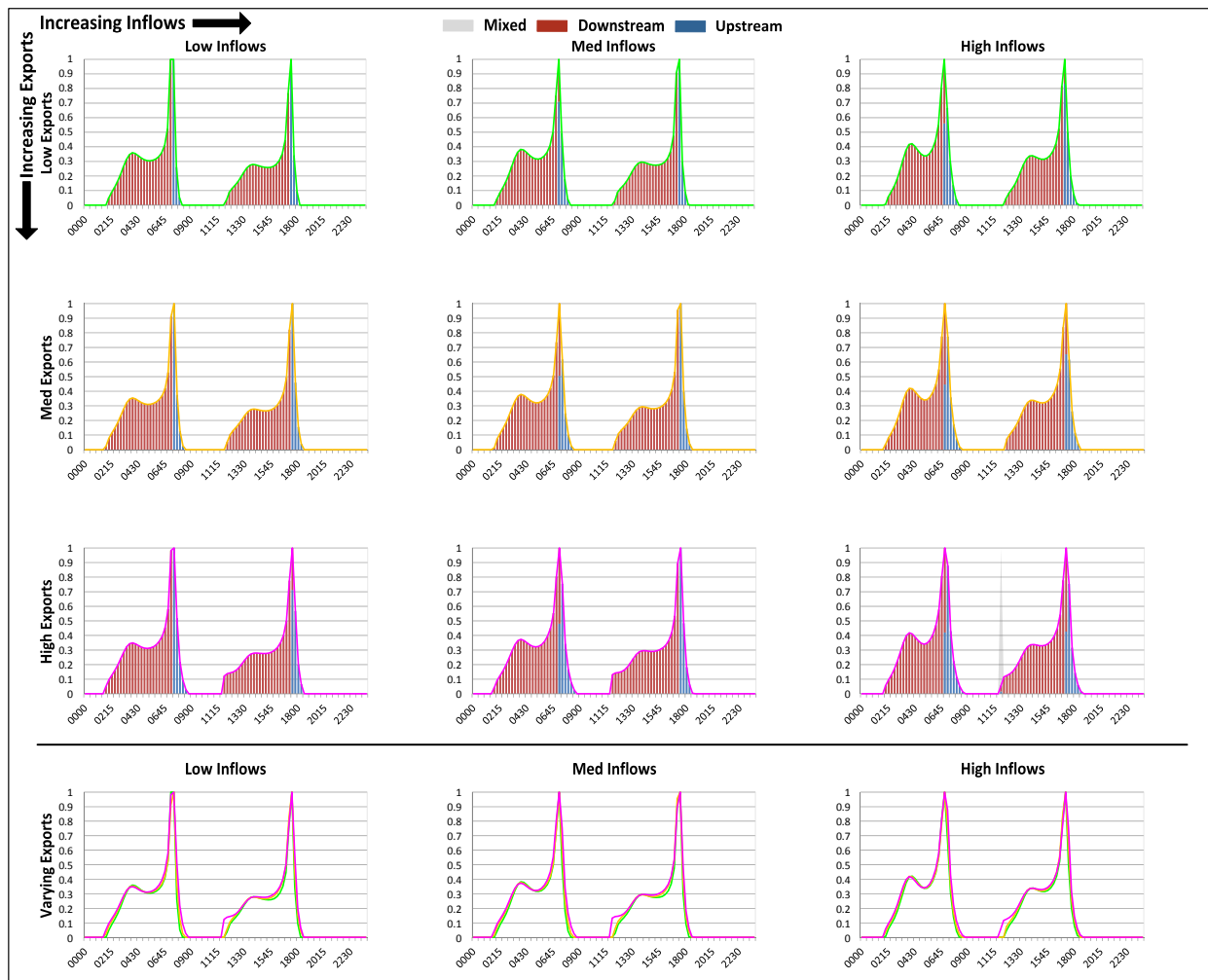


**Figure 18.** TRN: Proportion of Flow to Interior Delta at Turner Cut. See Figure 17 for description of elements.

**Columbia Cut:** The proportion of flow which entered the interior Delta at COL varied from 0% to 100% over 24 hours (Figure 19), depending on inflow and export conditions. At low exports, increasing inflows from low to high accounted for changes in proportion of flow into the interior Delta (COL7) ranging from -24.2% (at time 0745) to 44.8% (at time 0700). At high exports, increasing inflows from low to high accounted for changes in proportion of flow into the interior

Delta ranging from -37.2% (at time 0745) to 35.5% (at time 0700). Increasing inflows resulted in smaller changes at other times, accounting for an average change of 0.6% across all export levels. At low inflows, increasing exports from low to high accounted for changes in proportion of flow ranging from -6.4% (at time 0715) to 25.5% (at time 0745). At high inflows, increasing exports from low to high accounted for changes in proportion of flow ranging from -6.6% (at time 0700) to 19.3% (at time 0730). Increasing exports resulted in smaller changes at other times, accounting for an average change of 4.6% across all inflow levels. Neither increasing inflows nor increasing exports substantially altered proportion of flow patterns over 24 hours.

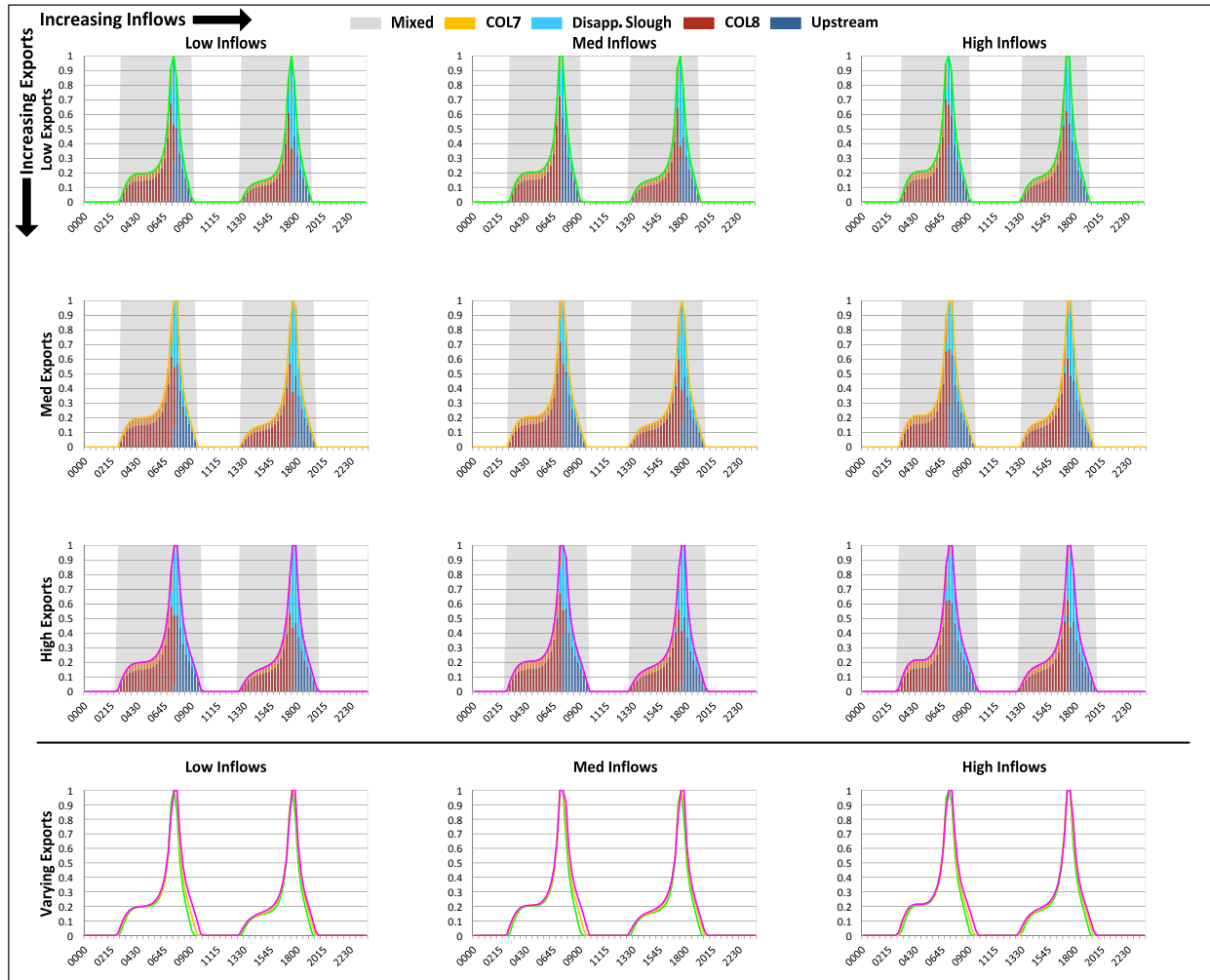


**Figure 19.** COL: Proportion of Flow to Interior Delta at Columbia Cut. See Figure 17 for description of elements.

At all inflow levels, water entered the interior Delta via COL7 from more than one source simultaneously. Flow from downstream (COL8/COL9) entered the interior Delta primarily during flood/high tides and accounted for about 59% of the water which entered the interior Delta at COL under all inflow/export scenarios. Flow from upstream (COL4/COL5) generally entered the interior Delta during ebb tides. As inflows increased, relative proportion of flow from upstream increased only slightly—less than 1%. Relative proportion of flow from upstream versus from downstream also increased only slightly with increasing exports.

Overall, inflows and exports caused relatively little change in proportion of flow and direction of flow entering the interior Delta at the COL junction.

**Middle River:** The proportion of flow which entered the interior Delta at MRV varied from 0% to 100% over 24 hours (Figure 20), depending on inflow and export conditions. At low exports, increasing inflows from low to high accounted for changes in proportion of flow into the interior Delta (MRV5) ranging from -34.7% (at time 1715) to 13.0% (at time 0700). At high exports, increasing inflows from low to high accounted for changes in proportion of flow ranging from -31.6% (at time 0100) to 43.3% (at time 0715). Increasing inflows resulted in smaller changes at other times, accounting for an average change of 0.2% across all export levels. At low inflows, increasing exports from low to high accounted for changes in proportion of flow ranging from -0.9% (at time 1300) to 49.0% (at time 0715). At high inflows, increasing exports from low to high accounted for changes in proportion of flow into the interior Delta ranging from -0.4% (at time 1330) to 100% (at time 0715 and time 1715). Increasing exports resulted in smaller changes at other times, accounting for an average change of 5.3% across all inflow levels. Neither increasing inflows nor increasing exports substantially altered proportion of flow patterns over 24 hours.

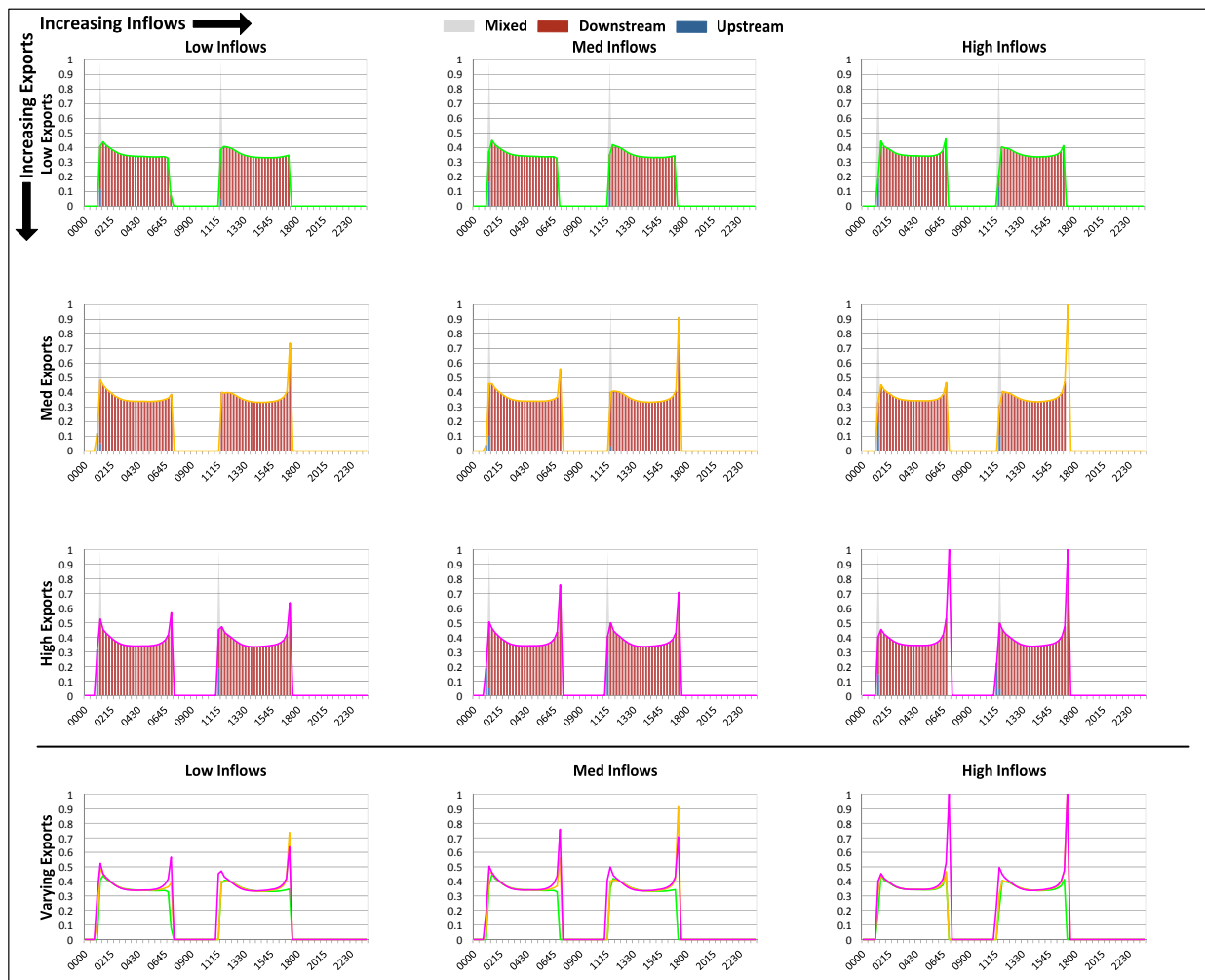


**Figure 20.** MRV: Proportion of Flow to Interior Delta at Middle River. See Figure 17 for description of elements.

Water entered the interior Delta via MRV5 almost exclusively from the downstream direction at all inflow levels and for the entire duration of flood/high tides; water entered the interior Delta at MRV from upstream only very briefly at the beginning of flood tides. Increasing inflows had little effect on the relative proportion of flow from upstream. Increasing exports also had little effect on the relative proportion of flow from upstream versus from downstream.

Overall, inflows and exports caused relatively little change in proportion of flow and direction of flow entering the interior Delta at the MRV junction.

***Mouth of Old River:*** The proportion of flow which entered the interior Delta at ORV varied from 0% to 100% over 24 hours (Figure 21), depending on inflow and export conditions. At low exports, increasing inflows from low to high accounted for changes in proportion of flow into the interior Delta (ORV2) ranging from -38.3% (at time 0730) to 26.1% (at time 0700). At high exports, increasing inflows from low to high accounted for changes in proportion of flow ranging from -24.0% (at time 0745) to 18.1% (at time 0715). Increasing inflows resulted in smaller changes at other times, accounting for an average change of 0.2% across all export levels. At low inflows, increasing exports from low to high accounted for changes in proportion of flow to the interior Delta ranging from -18.1% (at time 0715) to 29.8% (at time 0745). At high inflows, increasing exports from low to high accounted for changes in proportion of flow ranging from -13.0% (at time 0700) to 34.3% (at time 0730). Increasing exports resulted in smaller changes at other times, accounting for an average change of 3.0% across all inflow levels. Neither increasing inflows nor increasing exports substantially altered proportion of flow patterns over 24 hours.

Water entered the interior Delta via ORV2 mostly from the downstream direction and primarily on flood tides. Flow from upstream generally entered the interior Delta during ebb tides. As inflows increased, relative proportion of flow from upstream increased only slightly. Relative proportion of flow from upstream also increased only slightly with increasing exports.

Overall, inflows and exports caused relatively little change in proportion of flow and direction of flow entering the interior Delta at the ORV junction.



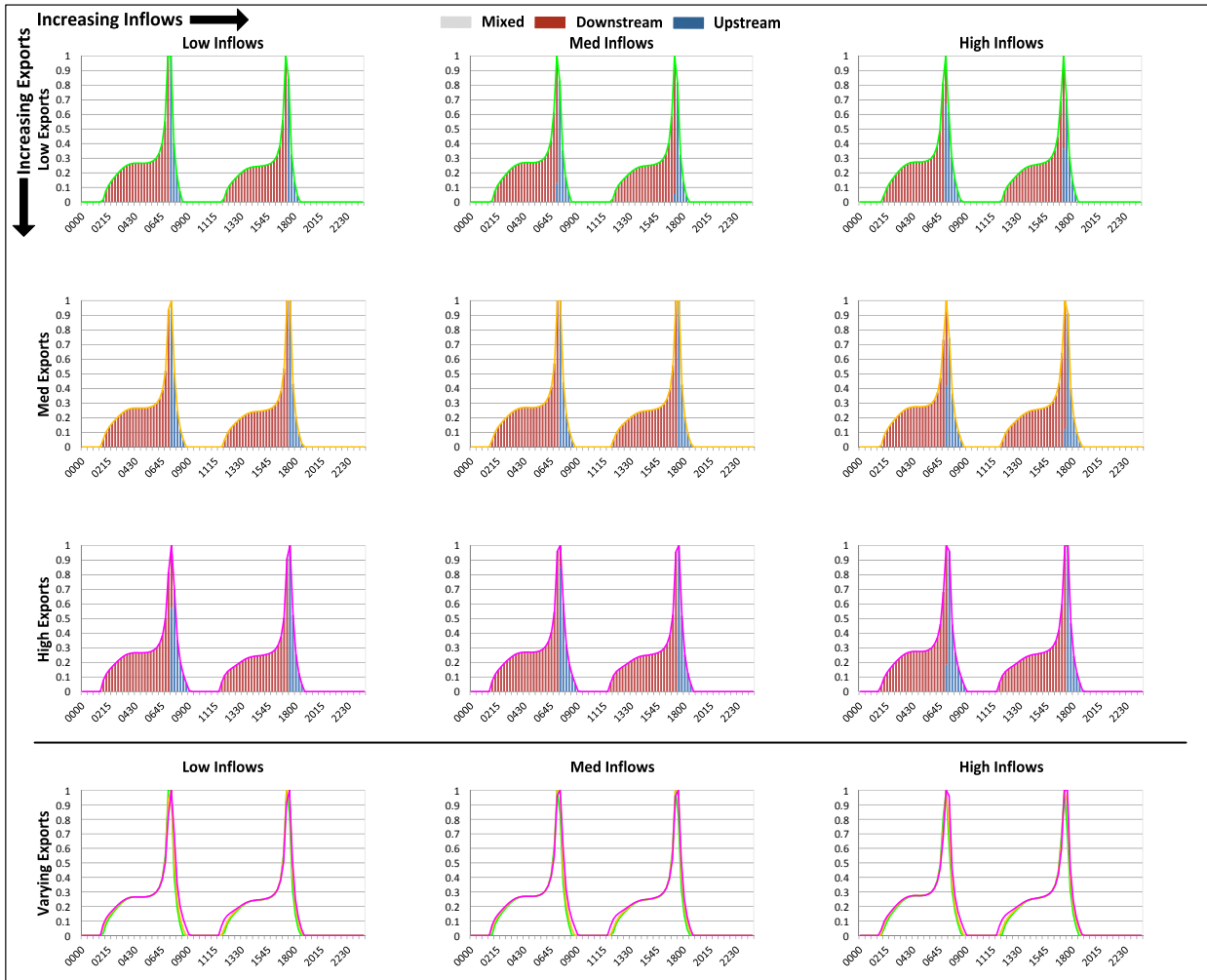


**Figure 21.** ORV: Proportion of Flow to Interior Delta at Mouth of Old River. See Figure 17 for description of elements.

### Total Proportion of Flow to Interior Delta

The GEO and HOR junctions had the highest total proportion of flow (calculated as the *daily 15-minute flow proportion*;  $\rho_j$ ) to the interior Delta (Figure 22; Appendix 2, Table 3). The total proportion of flow to the interior Delta at GEO ranged from 32.4% to 46.6%. The total proportion of flow at HOR ranged from 38.5% to 57.0%. By comparison, the total proportion of flow to the interior Delta at all of the other junctions we analyzed ranged from 2.4% to 20.7%.

Changes in total proportion of flow to the interior Delta occurred with increasing inflows and with increasing exports, but the direction and magnitude of the effect varied among junctions (Figures 23 and 24; Appendix 2). Increasing inflows from low to high accounted for decreases in proportion of flow at GEO ranging from -12.8% at low exports to -13.6% at high exports, and increasing exports from low to high accounted for increases in proportion of flow at GEO ranging from 1.28% at low inflows to 0.6% at high inflows. At HOR, increasing inflows from low to high accounted for increases in proportion of flow into the interior Delta ranging from 14.6% at low exports to 8.9% at high exports; increasing exports from low to high accounted for

increases in proportion of flow ranging from 9.5% at low inflows to 3.8% at high inflows. At TRN, COL, and MRV, increasing inflows from low to high accounted for changes in proportion of flow into the interior Delta ranging from -0.4% at low exports, to 1.1% at medium exports, to 1.0% at high exports. Increasing exports from low to high accounted for increases in proportion of flow into the interior Delta ranging from 2.1% at low inflows to 3.3% at high inflows. At ORV, FMN, FRV, and JPT, increasing inflows from low to high accounted for changes in proportion of flow into the interior Delta ranging from -0.4% at low exports to 1.9% at high exports.

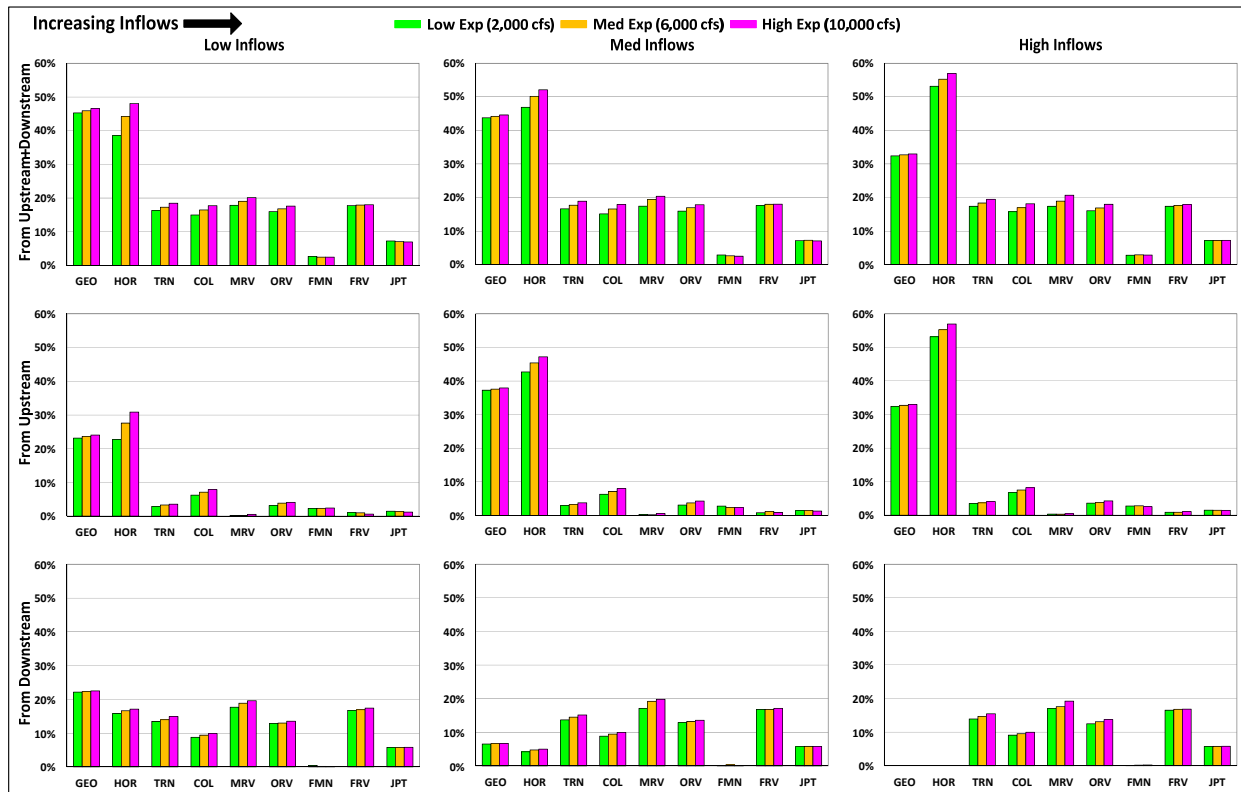


**Figure 22.** Total Proportion of Flow to Interior Delta over 24 Hours. Data are displayed by junction and export level. Junctions are on the x-axis; proportion of flow is on the y-axis. Bar color indicates export level. Graphs are arranged by increasing inflows, and by water source (i.e., upstream or downstream from the junction).



**Figure 23.** Change in Total Proportion of Flow to Interior Delta over 24 Hours with Increasing Inflows. Values are for change in total proportion relative to low inflows. Data are displayed by junction and export level. Graphs are arranged by increasing inflows.

The GEO and HOR junctions also had the highest proportion of flow into the interior Delta from upstream (*see* Figure 22; Appendix 2, Table 3); the proportion of flow into the interior Delta from upstream reached a maximum of 37.9% at GEO (under medium inflow conditions) and a maximum of 57.0% at HOR (under high inflow conditions). GEO also had the highest proportion of flow into the interior Delta from downstream under low inflow conditions (22.5%), but MRV had the highest proportion of flow from downstream under medium and high inflow conditions—19.8% and 19.2%, respectively. By comparison, the proportion of flow into the interior Delta from upstream at the other junctions we analyzed ranged from 0.6% to 8.2%. The proportion of flow into the interior Delta from downstream at the other junctions ranged from 0.6% to 17.9%.

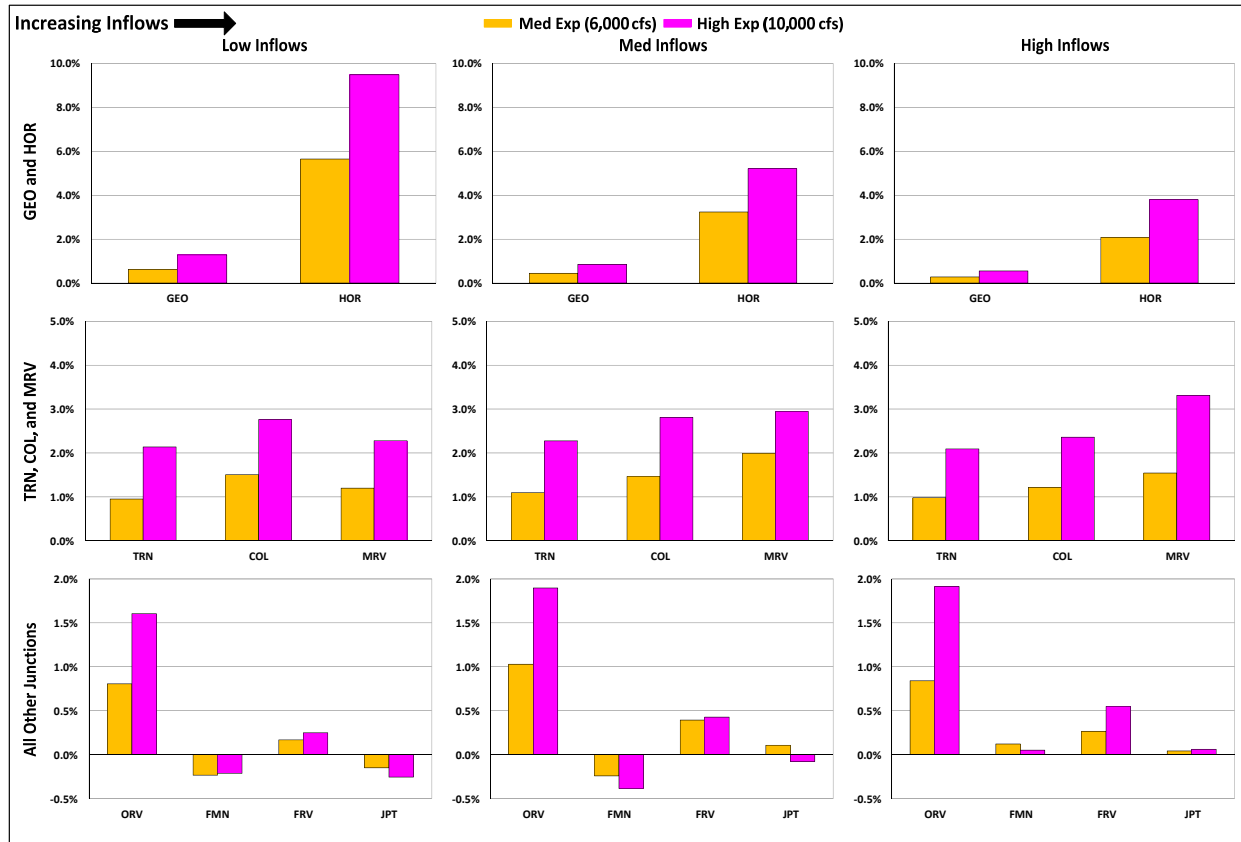


**Figure 24.** Change in Total Proportion of Flow to Interior Delta over 24 Hours with Increasing Exports. Values are for change in percentage of total proportion relative to low exports. Data are displayed by junction and export level. Graphs are arranged by increasing inflows.

Changes in proportion of flow to the interior Delta from upstream and downstream occurred with increasing inflows and with increasing exports, but the direction and magnitude of the effect varied among junctions (Appendix 2). Increasing inflows from low to high accounted for increases in proportion of flow from upstream into Georgiana Slough at GEO ranging from 9.3% at low exports to 8.9% at high exports, and for decreases in proportion of flow from downstream into Georgiana Slough ranging from -22.1% at low exports to -22.5% at high exports. Increasing exports from low to high accounted for increases in proportion of flow into Georgiana Slough from upstream ranging from 0.9% at low inflows to 0.6% at high inflows, and for increases in proportion of flow from downstream ranging from 0.4% at low inflows to 0% at high inflows.

At HOR, increasing inflows from low to high accounted for increases in proportion of flow from upstream into the interior Delta ranging from 30.4% at low exports to 26.1% at high exports, and for decreases in proportion of flow from downstream into the interior Delta ranging from -15.8% at low exports to -17.1% at high exports. Increasing exports from low to high accounted for increases in proportion of flow from upstream ranging from 8.1% at low inflows to 3.8% at high inflows, and for increases in proportion of flow from downstream ranging from 1.3% at low inflows to 0% at high inflows.

At the other junctions we analyzed, increasing inflows from low to high accounted for changes in proportion of flow into the interior Delta from upstream ranging from -0.2% (FRV) to

0.6% (TRN) at low exports, from -0.1% (FRV) to 0.5% (FMN) at medium exports, and from -0.1% (MRV) to 0.5% (TRN) at high exports. Changes in proportion of flow into the interior Delta from downstream with increasing inflows ranged from -0.6% (MRV) to 0.5% (TRN) at low exports, -1.3% (MRV) to 0.8% (TRN) at medium exports, and -0.5% (FRV) to 0.6% (TRN) at high exports. Increasing exports from low to high accounted for changes in proportion of flow into the interior Delta from upstream ranging from -0.4% (FRV) to 1.7% (COL) at low inflows, -0.4% (FMN) to 1.7% (COL) at medium inflows, and -0.2% (FMN) to 1.5% (COL) at high inflows. Changes in proportion of flow from downstream with increasing exports ranged from -0.3% (FMN) to 1.9% (MRV) at low inflows, 0% (FMN) to 2.7% (MRV) at medium inflows, and 0.1% (JPT) to 2.2% (MRV) at high inflows.

Overall, the influence of inflows on total proportion of flow to the interior Delta was weak ( $\leq 1\%$ ) at all junctions except Georgiana Slough (GEO) and Head of Old River (HOR). Exports had the strongest influence on total proportion of flow at the HOR junction (up to 10% increase), but accounted for less than a 3% change at all other junctions. The proportion of flow to the interior Delta from upstream versus downstream differed among junctions, but the GEO and HOR junctions were unique in diverting a large and increasing proportion of flow from upstream during higher inflows. Changes in relative proportion of flow from upstream versus downstream were relatively insensitive to inflows and exports at all other junctions.

#### **Daily Average Flow vs. 15-minute Flow**

The *daily average flow proportion* ( $\rho'_j$ ) and *daily 15-minute flow proportion* ( $\rho_j$ ) metrics were nearly equivalent for the GEO and HOR junctions when analyzing only flow entering the junctions from upstream (Figure 25, upper panel), but diverged when flow entering the junctions from both upstream and downstream was considered (Figure 25, lower panel). The two metrics were not equivalent for any other junction, whether considering upstream flow alone or together with downstream flow. Further, the two metrics showed no apparent relationship to each other for these junctions. Therefore, our approach to analyzing 15-minute flow data was generally not equivalent to an approach based on daily average flow.



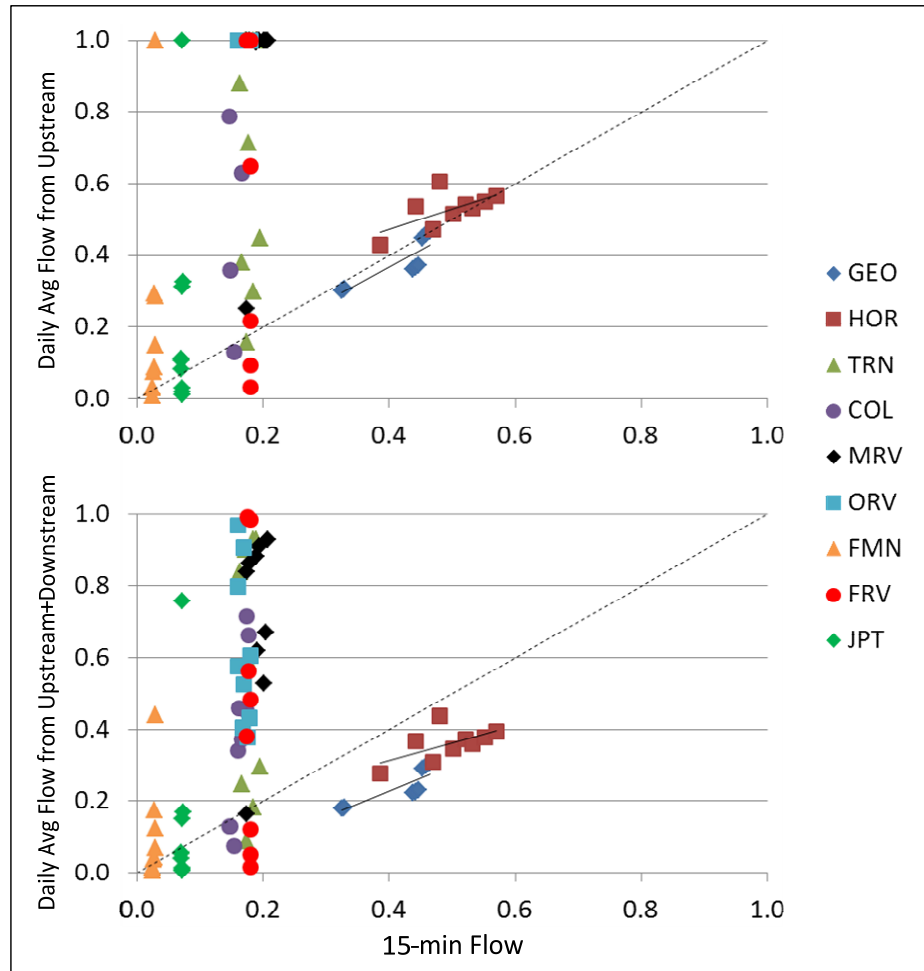


**Figure 25.** Equivalence Test of Metrics for Proportion of Flow to Interior Delta over 24 Hours. Proportion of flow calculated using total flow (upstream and downstream) at 15-minute intervals is displayed on the x-axis. Proportion of flow calculated using daily average flow is displayed on the y-axis. Individual data points are for various inflow and export conditions at each junction. Linear regressions are displayed for the GEO and HOR junctions for clarity. The dotted line indicates equivalence (i.e., unity).

## Discussion

Kimmerer and Nobriga (2008) applied a particle tracking model (PTM) to provide a detailed accounting of how location, river inflows and diversions influence the long-term fate of particles in the Delta. Using the same baseline simulation data, scenarios and assumptions we have described how tides, river inflows, and exports influence Delta daily and sub-daily hydrodynamics (i.e., over shorter time intervals not typically shown in PTM results). We followed a systematic approach to describing daily and sub-daily Delta hydrodynamics. We began at the broadest scale, using all available DSM2 Hydro channels (41 total) to describe longitudinal patterns in the mainstem San Joaquin River from its entry to the Delta (at Head of Old River) to its confluence with the Sacramento River (at Jersey Point). Next we plotted hydrodynamic time series (at 15-minute intervals) for channels entering and exiting eight mainstem San Joaquin River junctions and for the Georgiana Slough junction on the Sacramento

River. We then used hydrodynamic data to calculate and plot the proportion of flow entering the interior Delta at 15-minute time intervals from each of the nine junctions. To test the validity of flow proportion as a predictor of juvenile salmonid routing, we compared our calculated flow proportions with patterns of observed fish routing behavior at the Georgiana Slough junction. We then calculated and reported total flow proportion (contrasting  $\rho_j$  and  $\rho'_j$ ); a hypothesized “roll up” metric which may be useful for assessing entrainment vulnerability at all nine junctions leading to the interior Delta.

### **Mainstem San Joaquin River**

Our results indicate that the mainstem San Joaquin River between rkm 80 and rkm 12 can be broadly divided into two segments with very different characteristics. The first segment—from rkm 80 to rkm 52—exhibits relatively little tidal fluctuation (i.e., small differences between maximum and minimum flows), and exports appeared to have little influence on flow patterns in this reach. The percentage of time with positive flow direction (i.e., percent positive flow) was almost always greater than 50% in this segment, and percent positive flow increased (up to maximum of 100%) as river inflows increased and pushed further downstream. Consistent with prior observations by Cavallo et al. (2012), river inflows appeared to have a large influence on percent positive flow in this reach; accounting for increases of ~5% to ~35% with increasing inflows, depending on inflow level and river kilometer. The dominance of river inflows may be influenced by the relatively simple and narrow channel morphology characteristic of this segment. The upper portion of the San Joaquin River (i.e., the first segment) consists of a single channel with no significant side channels or tributaries. Further downstream in the vicinity of Stockton, the San Joaquin River becomes six times wider (Dauble et al. 2010) and includes more sloughs and tributary channels. The abrupt decrease in percent positive flow between rkm 63 and rkm 60 (see Figure 2) may largely be attributable to increase in channel width, depth and area (i.e., volume) which occurs in this area.

The second segment—from rkm 51 to rkm 12—is characterized by relatively stable percent positive flow (between 50% and 60%) and a greater range of flow (i.e., the difference between daily minimum and maximum flow) which increased with distance downstream. In contrast to the first segment, exports appeared to have a large influence on average flow in this reach, increasing negative average flow by as much as  $\sim 6,000 \text{ m}^3 \text{ sec}^{-1}$  (cfs) between rkm 34 and at rkm 12 (see Figure 2). Relatively strong negative average daily flow in this area occurs because it represents the primary corridor by which Sacramento River water flows “downhill” to balance large water volumes pumped from the South Delta export facilities. River inflows also had a relatively large influence on average flow in this segment, reducing negative average flow by  $\sim 3,000 \text{ m}^3 \text{ sec}^{-1}$  (cfs) at rkm 34 and  $\sim 7,000 \text{ m}^3 \text{ sec}^{-1}$  (cfs) at rkm 12 in changing from low to high inflows. Though exports clearly increased net negative flows downstream of rkm 34, the effect of exports was not evident in complete time series hydrographs (see Figure 3) suggesting the effect of exports on hydrodynamics (and therefore fish behavior) may be more subtle than indicated by calculated daily average or net flows.

Neither exports nor river inflows appeared to have much influence on range of flow or percent positive flow in the second segment of the mainstem San Joaquin River.

The influence of tides on mainstem San Joaquin River hydrodynamics is clearly seen in our results for range of flow. The range of flow steadily increased with distance downstream, and became quite large from rkm 39 to rkm 12 (see Figure 2). At rkm 51, for example, positive flow

(i.e., toward San Francisco Bay) exceeded  $14,000 \text{ m}^3 \text{ sec}^{-1}$  (cfs), and negative flows exceeded  $-10,000 \text{ m}^3 \text{ sec}^{-1}$  (cfs)—a range of over  $24,000 \text{ m}^3 \text{ sec}^{-1}$  (cfs). At rkm 12, positive flows exceeded  $180,000 \text{ m}^3 \text{ sec}^{-1}$  (cfs), and negative flows exceeded  $195,000 \text{ m}^3 \text{ sec}^{-1}$  (cfs)—a range of over  $375,000 \text{ m}^3 \text{ sec}^{-1}$  (cfs). These values exceeded changes in flow due to river inflows and exports by one or two orders of magnitude.

The dominant influence of tidal flows is also apparent from percent positive flows. These values were close to 50% for the entire length of the second river segment (rkm 51 to rkm 12) under all inflow and export conditions which we investigated. This would tend to indicate that the volume and duration of positive and negative flows in this reach were nearly equal, as would be expected in a tidally-driven system.

### ***Delta Junctions***

Paralleling our results from the longitudinal analysis of the mainstem San Joaquin River, the junction analysis revealed two groups with very different characteristics. The first group—consisting of GEO and HOR—was primarily influenced by river inflows. Most of the water entering Georgiana Slough (and therefore flowing toward the interior Delta) entered the GEO junction from upstream. Flow direction in the Sacramento River, both above and below the entrance to Georgiana Slough, was always positive (i.e., downstream, toward San Francisco Bay) at high inflows. Flow upstream of the entrance to Georgiana Slough was always positive at medium inflows and almost always positive at low inflows. At the HOR junction, flow direction on the San Joaquin River was dependent on inflow, and proportion of flow into the interior Delta at HOR paralleled the pattern observed at GEO; ~44% of the water which entered the HOR junction flowed into the interior Delta when San Joaquin River inflows were low. However, in contrast to GEO, the proportion of flow which entered the interior Delta increased to ~55% at high inflows. Also, exports had a stronger influence on magnitude, direction, and proportion of flow at HOR. The difference in export influence may be due in large part to the difference in proximity to the export facilities; HOR is the closest junction to the export facilities while GEO is the furthest away.

The second group of junctions—TRN, COL, MRV, ORV, FMN, FRV, and JPT—were primarily influenced by tides. Most of the water entering the interior Delta at these junctions entered the interior Delta on flood tides, except for at FMN. The magnitude and direction of flow was largely dependent on the tidal cycle, with changes in direction of flow tracking with tides in the channels leading to the interior Delta and in the mainstem San Joaquin River at all of these junctions. In contrast to the strong influence of tides, river inflows at these junctions did not appreciably alter magnitude and direction of flow or daily 15-minute flow proportion (i.e., total proportion of flow). Exports altered sub-daily proportion of flow at these junctions—sometimes considerably—but these changes were temporary; when total proportion of flow to the interior Delta was calculated, the overall influence of exports was slight (~3%, at most; see Appendix 2, Table 5). Though it may appear to be a discrepancy in results, the relatively weak influence of exports on total proportion of flow merely reflects the fact that changes in sub-daily flow conditions attributable to exports were most often short-lived or occurred at low flow magnitude, and so did not influence total proportion of flow as much as might be expected.

### **Flow Proportion and Fish Routing**

The two junctions with the highest total proportion of flow to the interior Delta (calculated as the *daily 15-minute flow proportion, or  $\rho_j$* ) were GEO and HOR (*see Figure 22*). Under most inflow and export conditions, around half of the water entering these junctions over 24 hours was diverted from the mainstem river to the interior Delta. This was ~12% to ~36% higher than observed at any other junction, depending on inflow and export levels. In contrast, less than one third of the water entering other junctions over 24 hours was diverted from the mainstem river; total proportion values ranged from ~2% to ~21% among all other junctions (*see Appendix 2, Table 3*). This suggests GEO and HOR may have the greatest potential to route (or “entrain”) migrating juvenile salmonids into the interior Delta.

Though data on routing of juvenile salmonids at Delta junctions has only recently become available, our metric  $\rho_j$  (*daily 15-minute flow proportion*) appears consistent with limited observations of fish entrainment available to date for the Georgiana Slough and Head of Old River junctions, and possibly for the Turner Cut junction as well. Georgiana Slough is the best studied of the Delta junctions we investigated, and we observed general agreement between our results for the proportion of water flowing into Georgiana Slough and the probability of fish entrainment into Georgiana Slough estimated by Perry (2010) (*see Figure 16*). Holbrook et al. (2009)—in which the study authors found that the proportion of fish entrained into the interior Delta at the Head of Old River junction was similar to the proportion of water flowing into the interior Delta—provides additional support for a correlation between the proportion of water and of fish diverted to the interior Delta. In addition, Holbrook et al. (2009) calculated entrainment probabilities for the Turner Cut junction of  $0.32 \pm 0.05$  for week 1 of their study and  $0.11 \pm 0.03$  for week 2; our results for the proportion of water flowing into the interior Delta at Turner Cut—approximately 16% to 20%, depending on inflow and export conditions—fall within this range of probabilities. However, the 2010 Vernalis Adaptive Management Program study (SJRG 2011) estimated an entrainment probability of only  $0.09 \pm 0.03$  for migrating juvenile salmonids entering Turner Cut. Admittedly, direct comparison of our results with either Holbrook et al. (2009) or the Vernalis Adaptive Management Program study is difficult because—as our analysis implies—routing of individual fish will depend on hydrodynamic conditions at the time fish arrive at the junction and neither Holbrook et al. (2009) nor SJRG (2011) provide the information necessary for a detailed comparison. Our analysis of flow proportion at junctions of the interior Delta provides an example of how hydrodynamic data might be summarized and used to develop testable hypotheses. Additional field testing, validation and refinement are undoubtedly needed.

We also investigated an alternative metric ( $\rho'_j$  or *daily average flow proportion*) for proportion of flow diverted at junctions. In simplest terms,  $\rho'_j$  is the proportion of average daily flow which enters the interior Delta at each junction. While we observed a near-equivalence of  $\rho'_j$  and *daily 15-minute flow proportion* ( $\rho_j$ ) for the river-inflow driven junctions GEO and HOR, this equivalence broke down entirely at junctions primarily influenced by tides (*see Figure 25*). The contribution of average river inflows to total proportion of flow likely diminishes in these tidally-driven junctions because the large magnitude of tidal flows—alternating from positive to negative repeatedly over 24 hours—simply overwhelms it. That  $\rho_j$  and  $\rho'_j$  were nearest to unity when *only* average flow from upstream (the source of inflows) was considered,

supports this interpretation. Thus, while  $\rho_j$  captures sub-daily patterns in flow proportion,  $\rho'_j$  does not. Therefore  $\rho'_j$  cannot adequately describe daily flow proportions, which are determinative of the total proportion of flow which enters the interior Delta.

The non-equivalence of the 15-minute and average flow metrics implies that sub-daily variations in flow proportion—not average flows—likely have the greatest potential to influence the migration and entrainment of fish. It should be noted that the total proportion of flow which entered the interior Delta at the tide-dominated junctions was not appreciably altered by increasing inflows or exports (*see* Figures 22, 23, and 24; Appendix 2). Though we observed a strong effect of increasing inflows and increasing exports on average flow downstream of rkm 52 on the mainstem San Joaquin River (*see* Figure 2, top row), these effects were correlated with increasing tidal influence (*see* Figure 2, middle row) and resulted in greatly diminished influence of average flow on percent positive flow (*see* Figure 2, bottom row) and total proportion of flow to the interior Delta (*see* Figure 16). Though average flow in a predominantly tidal environment has been suggested to have important biological and ecological consequences for juvenile salmonids (Newman and Brandes 2010, Dauble et al. 2010, NRC 2012), the mechanism for this effect has not to our knowledge been hypothesized or investigated.

### ***Comparison to PTM Results***

Kimmerer and Nobriga (2008) demonstrated that particle fate, both in terms of destination and arrival timing, was very sensitive to river inflows and, to a somewhat lesser extent, exports. They observed tides acted only to “spread out and delay the passage of particles” and thus, the fate of particles largely reflects net, non-tidal flow and does not describe sub-daily hydrodynamics resulting from the interaction of tides with river inflows and exports. . In the San Joaquin River, low inflows and low exports led to residence times of more than 80 days for particles released at Stockton. Under the same circumstances, except with high exports, particle residence time was less than 20 days. Thus, Kimmerer and Nobriga (2008) observed a profound influence of exports on particle residence time within the region evaluated in the present study. Yet, in directly evaluating sub-daily hydrodynamic data from the same DSM2 Hydro data used as PTM inputs for Kimmerer and Nobriga (2008), we observed a relatively minor influence of exports. What explains this discrepancy? It appears the answer is found in the interaction of two related factors: advection and time horizon.

Kimmerer and Nobriga (2008) defined time horizon as the number of days over which the fate of particles is evaluated, and defined advection as the process by which the PTM moves particles in relation to daily average flows. Demonstrating the importance of time horizon, Kimmerer and Nobriga concluded that for the evaluation of the proportion of particles entrained under a given set of conditions, the PTM could provide "no clear answer" because the answer depended on the time period considered. San Joaquin River average flow is often low (as depicted in the present study), and thus we would expect particle movements to be very sensitive to time horizon, with longer time horizons being necessary to allow particles to reach destinations via the slow and gradual advective process. Our findings differ from PTM results because average flow is the primary driver of net particle movement in the PTM (particles are also dispersed by tides and junctions, but this does not influence the net movement of particles), yet our study shows that: 1) average flow is largely unrelated to sub-daily hydrodynamics; and 2) sub-daily hydrodynamics appear, with information available to date, most closely related to observed patterns and mechanisms of juvenile salmonid migration behavior.

Though average flow and related advective particle movements may be hypothesized as important drivers and indicators of juvenile salmonid behavior, researchers using the PTM to assess hydrodynamic effects on juvenile salmonids have not to our knowledge proposed a testable mechanistic hypothesis for how this relationship might function. In contrast, findings from the present study describe a specific mechanism by which sub-daily flows may influence migration behavior; a mechanism which appears at least generally consistent with available empirical evidence from acoustic telemetry studies to date (e.g., Perry 2010; Holbrook et al. 2009; SJRG 2011).

### ***Uncertainties***

Considerable effort has been devoted to calibrating DSM2 Hydro, and the model is regularly employed to accurately represent Delta salinity and flow conditions; a testament to the model's value and validity. More complex hydrodynamics models are available for the Delta (e.g., RMA Multidimensional Models, TRIM, and UnTrim) and for other estuaries. However, we believe that weaknesses of DSM2 Hydro relative to other hydrodynamic models are likely to be minor relative to the challenges of linking any hydrodynamic model to the behavior of migrating juvenile salmonids. Kimmerer and Nobriga (2008) made the same point, and though they presented PTM results, DSM2 Hydro data (presented here for the first time) was an essential precursor to their analysis. Given the relative novelty of relating complex hydrodynamics to juvenile salmonid behavior, the use of relatively coarse DSM2 Hydro data is a reasonable first step. The use of more sophisticated hydrodynamic models will undoubtedly follow if subsequent analyses show two or three dimensional flow resolution are needed to evaluate the influence of water project operations on juvenile salmonid migratory behavior.

We have provided a complete set of hydrodynamic data for the mainstem San Joaquin River and for nine associated junctions. However, there are other regions of the Delta which also warrant consideration, and other hydrodynamic metrics which might be considered. Future studies might explore other regions and metrics, but a broader analysis of such additional factors was simply beyond the scope of this already lengthy paper.

All the flow metrics used in our analysis are calculated from 15-minute flow data. Flow is a standard metric for assessing broad-scale salmonid habitat characteristics (e.g., Poff and Zimmerman 2010) and thus was an obvious choice for our analysis. Velocity is another hydrodynamic metric provided by DSM2 Hydro. Though velocity is often assessed for microhabitat investigation, it is less commonly associated with broad scale evaluations (such as the present study). Furthermore, since flow is the product of velocity and stage-dependent cross sectional area we expect velocity patterns would largely mimic flow patterns already described.

We evaluated nine combinations of river inflow and South Delta exports, which represent a subset of the twenty-hour flow-export scenarios evaluated by Kimmerer and Nobriga (2008). Inflows greater than  $1,077 \text{ m}^3 \text{ sec}^{-1}$  (38,000 cfs), exports below  $57 \text{ m}^3 \text{ sec}^{-1}$  (2,000 cfs), inflows with the Delta Cross Channel gates open, and the differential effect of neap tides were not considered in our analysis. Also, as with all scenarios considered by Kimmerer and Nobriga (2008), the proportion of inflow between the Sacramento and San Joaquin River were fixed. Though all of these factors are potentially important for ecological or management reasons, it was not possible to consider these additional dimensions for our analysis. However, we are hopeful that future efforts can build upon the foundations provided in this paper to evaluate and concisely report the influence of factors such as higher San Joaquin River flows,

placement of a physical barrier at the Head of Old River, or use of a barrier at Georgiana Slough—as recently described by Perry et al. (2012).

### **Management Implications**

Among the many assessments of Delta environmental conditions, altered hydrodynamics caused by South Delta exports have almost universally been identified as a significant adverse effect for juvenile salmonids. Brandes and McLain (2001) identified Delta channels with net negative, or “reverse flows”—which are thought to be problematic for migrating juvenile salmonids—in the introduction of their paper. In fact, the view that net flows exert a strong influence on juvenile salmonid behavior and survival appears to be an assumption underlying decades of study (Newman and Brandes 2010; Dauble et al. 2010). Most recently, the National Research Council of the National Academies (NRC 2012) concluded “losses [of juvenile salmonids] are substantive and are at least in part attributable to pump operations that alter current patterns into and through the channel complex, drawing smolts into the interior waterways and toward the pumps.” As Kimmerer (2008) indicated, given the large volumes of water diverted and the large numbers of juvenile salmonids salvaged at South Delta export facilities, such a conclusion appears reasonable and well justified. Yet, given the importance of the issue, the absence, prior to this study, of a spatially detailed assessment of daily and sub-daily Delta hydrodynamics is surprising. In the 2009 Biological Opinion for operations of the SWP and CVP, the National Marine Fisheries Service used PTM simulation results to evaluate general hydrodynamic conditions and as a primary basis for setting export restrictions. The need for a thorough and appropriately-scaled hydrodynamic assessment of the Delta was not identified as a critical research need in the Biological Opinion. In a Delta Science Program review of the Vernalis Adaptive Management Program (VAMP), Dauble et al. (2010) provided some data assessing the influence of tides and river inflows at Stockton, but the panel generally accepted the premise of spatially extensive and significant alteration of Delta hydrodynamics resulting from South Delta exports. Like the Biological Opinion before it, the VAMP review panel did not identify hydrodynamic analysis such as that reported here as a priority for future studies.

Regardless of the reason, it is undeniable that assessing and describing the influence of exports and river inflows on sub-daily hydrodynamics has not been a priority research topic in the Delta. Our analysis demonstrates the hydrodynamic complexity of the Delta, and therefore illustrates the potential weakness of Delta studies and management actions which assume average daily flows alone are a sufficient representation of conditions experienced by fishes. Studies of juvenile salmonid survival in the Delta have for nearly three decades sought evidence for a hypothesized strong influence from river inflows and exports, but results have been equivocal. Newman and Brandes (2010) found exports were negatively associated with survival, but their model without exports fit observed juvenile salmon survival data nearly as well as a model with exports; thus there was little support for exports as a “significant” effect using a standard model selection approach (Burnham and Anderson 2002) . Newman (2008) in an analysis of VAMP studies since 1987, found some evidence for a positive association with river inflow for tagged fish released upstream of the Delta, but did not find the expected negative association with exports. Study authors and others interpreting these findings have attributed equivocal results to an inherently low signal to noise ratio for the Delta. The results of our analysis suggest ambiguous study findings may have occurred not just because of “noise”, but

also because the hydrodynamic "signal" produced by varying exports and river inflows is weaker, or at least different, than many researchers have assumed.

Though other studies have shown increased river flows can yield benefits to juvenile salmonids (e.g., Perry 2010) our analysis suggests that hydrodynamic benefits of higher inflows are likely to attenuate or be absent in tidal portions of the Delta. For the mainstem San Joaquin River, we observed a diminished influence on sub-daily hydrodynamics at points downstream of Turner Cut for river inflows up to  $5,712 \text{ m}^3 \text{ sec}^{-1}$  (cfs). On the Sacramento River, Cavallo et al. (2012) showed that the point of tidal transition (where flow becomes bidirectional) occurs near the mouth of Cache Slough at Sacramento River inflows of  $38,000 \text{ m}^3 \text{ sec}^{-1}$  (cfs). Of course, factors like turbidity, water quality and food availability which can be associated with higher river inflows may still influence survival and behavior of juvenile salmonids even if hydrodynamic factors do not.

### **Conclusions**

The potential for river inflows and exports to influence Delta hydrodynamics, and therefore to influence juvenile salmonids and other fish species, should neither be accepted nor dismissed based upon generalizations. Rather, our findings demonstrate the need for testable hypotheses for specific conditions and locations, and which propose a specific mechanism by which flow metrics might reasonably influence juvenile salmonid survival and behavior. Illustrating the point, studies on San Joaquin River tributaries (upstream of the Delta) have found relatively consistent evidence for increased river flows to enhance apparent survival of juvenile salmon (e.g., Dauble et al. 2010; CDFG 2005). The potential mechanisms for these benefits are relatively well understood; increased flow can increase available habitat, reduce predation losses, and decrease water temperatures, for example. The present study hypothesizes a mechanism within the Delta by which flow direction, magnitude, and duration can influence fish behavior (i.e., flow proportion). In contrast, the mechanism by which increased or decreased average daily flows could yield significant hydrodynamic benefits to juvenile salmonids in the *tidal portions* (where tidal flux greatly exceeds average flows) of the Delta have not to our knowledge been proposed or explained.

The hydrodynamic analyses presented here are not conclusive; similar analyses for other portions of the Delta under different boundary conditions—and perhaps with different hydrodynamic metrics estimated by different modeling tools—would help to provide a more complete picture. Juvenile salmonid telemetry studies, particularly Perry (2010), have been invaluable in helping define key hydrodynamic variables; additional telemetry studies which can help define and describe juvenile salmonid behavior in relation to hydrodynamic conditions in tidal portions of the Delta will be particularly important.

### **Acknowledgements**

This report was inspired and made possible by the contributions of many people. Comments and suggestions for the emerging analysis were provided by Lenny Grimaldo, Barbara Byrne, Matt Nobriga, Pete Smith, Ted Sommer, Gardner Jones, Kevin Clark, Kevin Reece, James Newcomb, Rachel Johnson, Tara Smith and Steve Cramer. Constructive comments on early drafts of the report were provided by Tara Smith, Kijin Nam, Rick Sitts, and Ted Sommer. Funding for development of this report was provided by the California Department of Water Resources. We

are also grateful to Aaron Miller and Mark Teply for providing their expertise with FORTRAN programming, and lastly, to Aaron Miller for sharing the DSM2 hydro data.

## References

- Baker P.F. and J.E. Morhardt. 2001. Survival of Chinook salmon smolts in the Sacramento-San Joaquin Delta and Pacific Ocean. Pages 163-182 in R.L. Brown, Editor. Contributions to the Biology of Central Valley Salmonids, Volume 2, Fish Bulletin 179. California Department of Fish and Game, Sacramento, California.
- Blake, A. and M.J. Horn. 2003. Acoustic Tracking of Juvenile Chinook Salmon Movement in the Vicinity of the Delta Cross Channel, Sacramento River, California – 2001 Study Results. Draft Report. U.S. Department of the Interior, U.S. Geological Survey.
- Brandes, Patricia L., and Jeffrey S. McLain. 2001. Juvenile Chinook Salmon Abundance, Distribution, and Survival in the Sacramento-San Joaquin Estuary. Intranet, Series: California Department of Fish and Game Fish Bulletin, Vol. 179, Page(s): 39-136
- Burau, J., A. Blake, and R. Perry. 2007. Sacramento/San Joaquin River Delta regional salmon outmigration study plan: Developing understanding for management and restoration. 72 pp. plus appendices. Available online at: [http://deltarevision.com/images/pdfs/2008workshop\\_outmigration\\_reg\\_study\\_plan\\_011608.pdf](http://deltarevision.com/images/pdfs/2008workshop_outmigration_reg_study_plan_011608.pdf). Accessed October 17, 2011.
- Burnham, K. P. and D. R. Anderson. 2002. Model Selection and Multimodel Inference: A Practical Information-Theoretical Approach (2<sup>nd</sup> Edition). Springer-Verlag, New York, NY.
- California Department of Fish and Game (CDFG). 2005. “San Joaquin River Fall-run Chinook Salmon Population Model”. California Department of Fish and Game report.
- Cavallo B., J. Merz, and J. Setka. 2012. Effects of predator and flow manipulation on Chinook salmon (*Oncorhynchus tshawytscha*) survival in an imperiled estuary. Environmental Biology of Fishes DOI 10.1007/s10641-012-9993-5.
- Culberson, S.D., C.B. Harrison, C. Enright, and M.L. Nobriga. 2004. Sensitivity of larval fish transport to location, timing, and behavior using a particle tracking model in Suisun Marsh, California. American Fisheries Society Symposium 39:257-267.
- Dauble D., D. Hankin, J.J. Pizzimenti, and P. Smith. 2010. The Vernalis Adaptive Management Program: Report of the 2010 Review Panel. Prepared for the Delta Science Program.
- Holbrook, C.M., R.W. Perry, and N.S. Adams. 2009. Distribution and Joint Fish-Tag Survival of Juvenile Chinook Salmon Migrating through the Sacramento-San Joaquin River Delta, California, 2008. Intranet, Series: U.S. Geological Survey Open-File Report 2009-1204. 30 pp.

**REPORT – Investigating the influence of tides, inflows, and exports on sub-daily flow in the Delta**

- Kimmerer, Wim J. 2008. Losses of Sacramento River chinook salmon and Delta smelt to entrainment in water diversions in the Sacramento-San Joaquin delta. San Francisco Estuary and Watershed Science. 6(2).
- Kimmerer, W. and M. Nobriga. 2008. Investigating particle transport and fate in the Sacramento-San Joaquin Delta using a particle tracking model. San Francisco Estuary and Watershed Science. 6(1).
- Lindley, S.T., R.S. Schick, E. Mora, P.B. Adams, J.J. Anderson, S. Greene, C. Hanson, B.P. May, D.R. McEwan, R.B. MacFarlane, C. Swanson, and J.G. Williams. 2007. Framework for Assessing Viability of Threatened and Endangered Chinook Salmon and Steelhead in the Sacramento-San Joaquin Basin. San Francisco Estuary and Watershed Science. 5(1).
- National Marine Fisheries Service (NMFS). 2009 (amended 2011). NMFS Final 2009 Biological Opinion on the Long-Term Central Valley Project and State Water Project Operation, Criteria, and Plan. June 4, 2009. Available at: [http://swr.nmfs.noaa.gov/sac/myweb8/BiOpFiles/2009/Draft\\_OCAP\\_Opinion.pdf](http://swr.nmfs.noaa.gov/sac/myweb8/BiOpFiles/2009/Draft_OCAP_Opinion.pdf).
- National Research Council (NRC). 2012. Sustainable Water and Environmental Management in the California Bay-Delta. Washington, DC: The National Academies Press, 2012a. Available at: <http://dels.nas.edu/Report/Sustainable-Water-Environment/13394>.
- Newman, K.B. 2008. An evaluation of four Sacramento-San Joaquin River Delta juvenile salmon survival studies. US Fish and Wildlife Service, Stockton California. Available at: [http://www.science.calwater.ca.gov/pdf/psp/PSP\\_2004\\_final/PSP\\_CalFed\\_FWS\\_salmon\\_studies\\_final\\_033108.pdf](http://www.science.calwater.ca.gov/pdf/psp/PSP_2004_final/PSP_CalFed_FWS_salmon_studies_final_033108.pdf).
- Newman, K.B and P.L. Brandes. 2010. Hierarchical modeling of juvenile Chinook salmon survival as a function of Sacramento–San Joaquin Delta water exports. North American Journal of Fisheries Management 30(1):157-169.
- Perry R.W. 2010. Survival and Migration Dynamics of Juvenile Chinook Salmon in the Sacramento–San Joaquin River Delta. Doctoral dissertation. University of Washington.
- Perry, R.W. and J.R. Skalski. 2008. Migration and Survival of Juvenile Chinook Salmon through the Sacramento-San Joaquin River Delta during the Winter of 2006-2007. Report prepared for U.S. Fish and Wildlife Service, Stockton, California. 32 pp.
- Perry, R.W., P.L. Brandes, P.T. Sandstrom, A. Ammann, B. MacFarlane, A.P. Klimley, and J. R. Skalski. 2010. Estimating survival and migration route probabilities of juvenile Chinook salmon in the Sacramento–San Joaquin River Delta. North American Journal of Fisheries Management 30:142-152.

**REPORT – Investigating the influence of tides, inflows, and exports on sub-daily flow in the Delta**

Perry, R.W., P.L. Brandes, J.R. Burau, A.P. Klimley, B. MacFarlane, C. Michel, and J.R. Skalski. 2012. Sensitivity of survival to migration routes used by juvenile Chinook salmon to negotiate the Sacramento-San Joaquin River Delta. Series: Environmental Biology of Fishes, Vol. Online First, 9 February 2012.

Poff, N.L. and J.K.H. Zimmerman. 2010. Ecological responses to altered flow regimes: a literature review to inform environmental flows science and management. Freshwater Biology 55:194-20.

San Joaquin River Group Authority (SJRGA). 2011. 2010 Annual Technical Report on Implementation and Monitoring of the San Joaquin River Agreement and the Vernalis Adaptive Management Plan (VAMP). 167 pp.

USFWS (U.S. Fish and Wildlife Service). 2008. Formal Endangered Species Act Consultation on the Proposed Coordinated Operations of the Central Valley Project (CVP) and State Water Project (SWP). Available at: [http://www.fws.gov/sacramento/delta\\_update.htm](http://www.fws.gov/sacramento/delta_update.htm).

Vogel, D.A. 2004. Juvenile Chinook Salmon Radio-Telemetry Studies in the Northern and Central Sacramento-San Joaquin Delta 2002-2003. Report to the National Fish and Wildlife Foundation, Southwest Region. 44 pp.

## **Appendix 1: FMN, FRV, and JPT Junctions**

### ***Direction and Magnitude of Flow at FMN, FRV, and JPT Junctions***

***Fisherman's Cut:*** The Fisherman's Cut junction (FMN) is located on the mainstem San Joaquin River and is comprised of three DSM2 Hydro channels (Figure 26). Flow in the mainstem San Joaquin River upstream of the FMN junction (FMN1) ranged from  $123,779 \text{ m}^3 \text{ sec}^{-1}$  (cfs) to  $-138,333 \text{ m}^3 \text{ sec}^{-1}$  (cfs) over 24 hours (Figure 27). Flow in the mainstem San Joaquin River downstream of the FMN junction (FMN3) ranged from  $122,284 \text{ m}^3 \text{ sec}^{-1}$  (cfs) to  $-137,659 \text{ m}^3 \text{ sec}^{-1}$  (cfs). Increasing inflows had little influence on overall flow patterns in the mainstem San Joaquin; direction and magnitude of flow appeared to largely track the tidal cycle. Increasing exports altered the magnitude of flow by a maximum of  $13,338 \text{ m}^3 \text{ sec}^{-1}$  (cfs) upstream of the FMN junction and by a maximum of 12,794 cfs downstream of the junction.

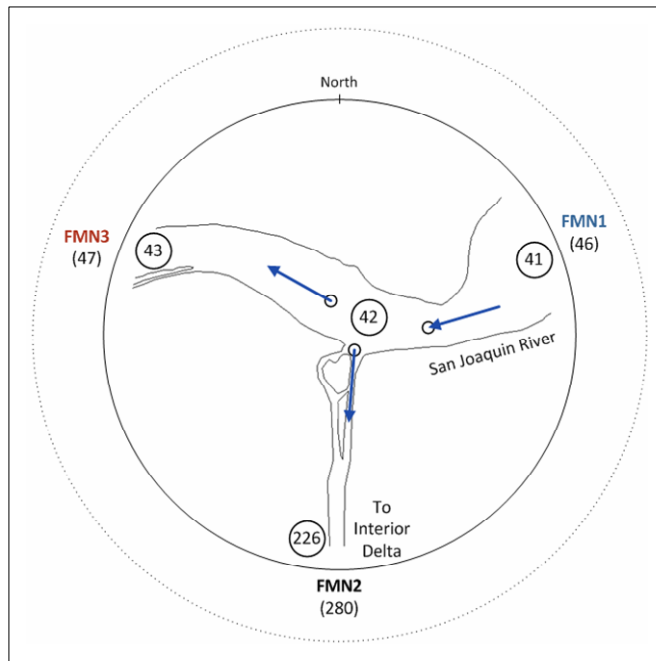


**Figure 26.** FMN: Plan-view of Fisherman's Cut Junction. *See Figure 4 for description of elements.*

Flow in the channel leading to the interior Delta at FMN junction (FMN2) ranged from  $6,178 \text{ m}^3 \text{ sec}^{-1}$  (cfs) toward the interior Delta to  $-5,259 \text{ m}^3 \text{ sec}^{-1}$  (cfs) away from the interior Delta over 24 hours (*see Figure 27*). Maximum flow toward the interior Delta occurred at time 1915 under ebb tide, high inflow/low export conditions, during which all of the water entering the interior Delta was from upstream (FMN2) and physical flow directions in FMN3 was away from the center of the junction. Maximum flow away from the interior Delta occurred at time 1445 under flood tide, low inflow/high export conditions. During this time, physical flow direction in FMN1 was away from the center of the junction. Increasing inflows had little influence on flow patterns in the channel leading to the interior Delta at FMN (FMN2); direction and magnitude of flow were largely dependent on the tidal cycle. Increasing exports also had little influence on flow patterns, but accounted for changes to magnitude of flow in FMN2 ranging from

$-66 \text{ m}^3 \text{ sec}^{-1}$  (cfs) under low inflow conditions at time 0345 to  $-554 \text{ m}^3 \text{ sec}^{-1}$  (cfs) under medium inflow conditions at time 1130. Increasing exports resulted in smaller changes at other times, accounting for an average change of  $-123 \text{ m}^3 \text{ sec}^{-1}$  (cfs) (i.e., less flow into the interior Delta) across all inflow levels.

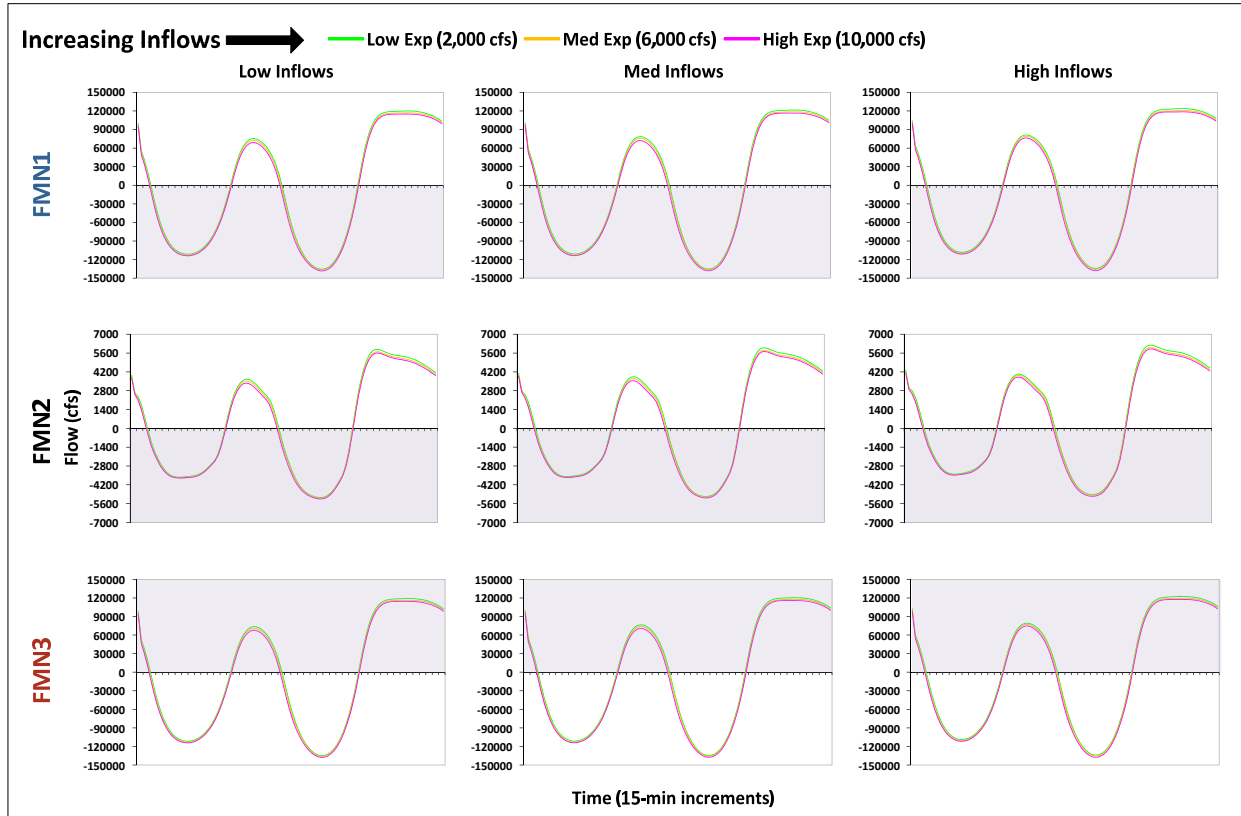


**Figure 27.** FMN: Flow in Fisherman’s Cut Junction Channels over 24 Hours. See Figure 5 for description of elements. For channel FMN2, flow displayed in the shaded area is away from the interior Delta; for the other channels, flow displayed in the shaded area is away from the center of the junction.

**False River:** The False River junction (FRV) is located on the mainstem San Joaquin River and is comprised of three DSM2 Hydro channels (Figure 28). Flow in the mainstem San Joaquin River upstream of the FRV junction (FRV3) ranged from  $96,420 \text{ m}^3 \text{ sec}^{-1}$  (cfs) to  $-104,865 \text{ m}^3 \text{ sec}^{-1}$  (cfs) over 24 hours (Figure 29). Flow in the mainstem San Joaquin River downstream of the FRV junction (FRV2) ranged from  $155,875 \text{ m}^3 \text{ sec}^{-1}$  (cfs) to  $-161,686 \text{ m}^3 \text{ sec}^{-1}$  (cfs). Increasing inflows had little influence on flow patterns in the mainstem San Joaquin; direction and magnitude of flow were largely dependent on the tidal cycle. Increasing exports altered the magnitude of flow by a maximum of  $9,348 \text{ m}^3 \text{ sec}^{-1}$  (cfs) upstream of the FRV junction and by a maximum of  $14,021 \text{ m}^3 \text{ sec}^{-1}$  (cfs) downstream of the junction.

Flow in the channel leading to the interior Delta at FRV junction (FRV1) ranged from  $-52,475 \text{ m}^3 \text{ sec}^{-1}$  (cfs) toward the interior Delta to  $55,316 \text{ m}^3 \text{ sec}^{-1}$  (cfs) away from the interior Delta over 24 hours (Figure 29). Maximum flow toward the interior Delta occurred at time 1400 under flood tide, high inflow/high export conditions, during which all of the water entering the interior Delta was from downstream (FRV2) and physical flow direction in FRV3 was away from the

center of the junction. Maximum flow away from the interior Delta occurred at time 1915 under ebb tide, high inflow/low export conditions. During this time, physical flow direction in FRV2 was away from the center of the junction. Increasing inflows had little influence on flow patterns in the channel leading to the interior Delta at FRV (FRV1); direction and magnitude of flow largely tracked the tidal cycle. Increasing exports also had little influence on flow patterns, but accounted for changes to magnitude of flow in FRV1 ranging from  $-723 \text{ m}^3 \text{ sec}^{-1}$  (cfs) under low inflow conditions at time 0230 to  $-5,622 \text{ m}^3 \text{ sec}^{-1}$  (cfs) under medium inflow conditions at time 1100. Increasing exports resulted in smaller changes at other times, accounting for an average change of  $-2,106 \text{ m}^3 \text{ sec}^{-1}$  (cfs) (i.e., more flow into the interior Delta) across all inflow levels.

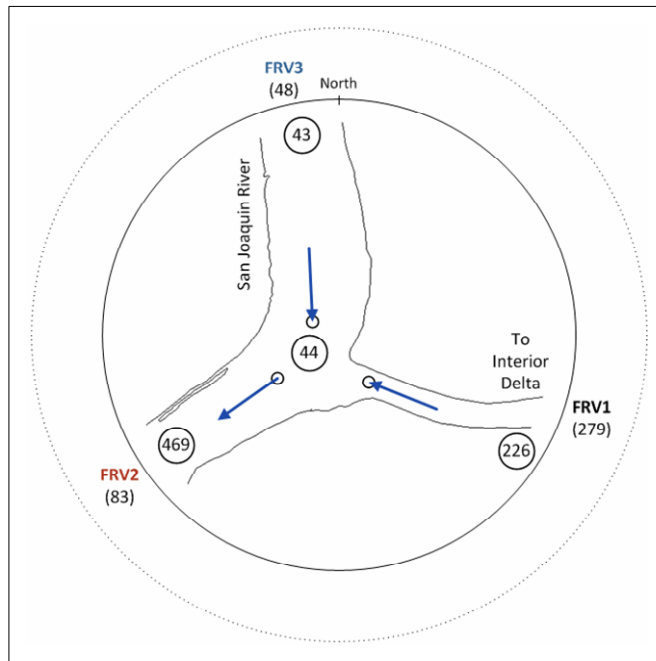


**Figure 28.** FRV: Plan-view of False River Junction. See Figure 4 for description of elements.

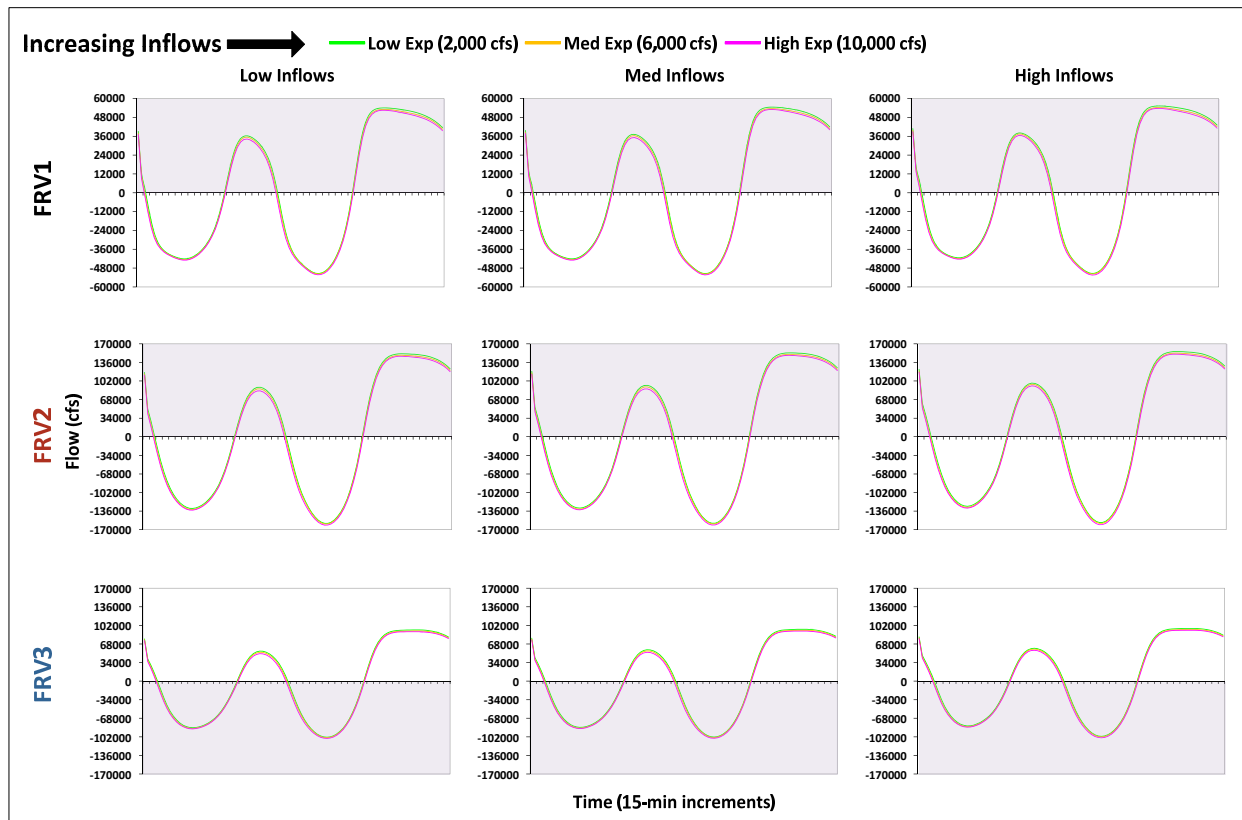


**Figure 29.** FRV: Flow in False River Junction Channels over 24 Hours. See Figure 5 for description of elements. For channel FRV1, flow displayed in the shaded area is away from the interior Delta; for the other channels, flow displayed in the shaded area is away from the center of the junction.

***Jersey Point:*** The Jersey Point junction (JPT) is located on the mainstem San Joaquin River and is comprised of four DSM2 channels (Figure 30). Flow in the mainstem San Joaquin River upstream of the JPT junction (JPT1) ranged from  $157,917 \text{ m}^3 \text{ sec}^{-1}$  (cfs) to  $-163,476 \text{ m}^3 \text{ sec}^{-1}$  (cfs) over 24 hours (Figure 31). Flow in the mainstem San Joaquin River downstream of the JPT junction (JPT4) ranged from  $191,161 \text{ m}^3 \text{ sec}^{-1}$  (cfs) to  $-195,539 \text{ m}^3 \text{ sec}^{-1}$  (cfs). Increasing inflows had little influence on flow patterns in the mainstem San Joaquin; direction and magnitude of flow were largely dependent on the tidal cycle. Increasing exports altered the magnitude of flow by a maximum of  $13,973 \text{ m}^3 \text{ sec}^{-1}$  (cfs) upstream of the JPT junction and by a maximum of  $14,380 \text{ m}^3 \text{ sec}^{-1}$  (cfs) downstream of the junction.

Flow in the channels leading to the interior Delta at JPT junction (JPT2 and JPT3) ranged from  $-3,089 \text{ m}^3 \text{ sec}^{-1}$  (cfs) toward the interior Delta to  $3,447 \text{ m}^3 \text{ sec}^{-1}$  (cfs) away from the interior Delta for JPT2, and from  $-19,452 \text{ m}^3 \text{ sec}^{-1}$  (cfs) toward the interior Delta to  $17,460 \text{ m}^3 \text{ sec}^{-1}$  (cfs) away from the interior Delta for JPT3 over 24 hours (Figure 31). Calculations for flow to the interior Delta were made after adding the flow in JPT2 and JPT3 together. Maximum flow toward the interior Delta occurred at time 1315 under flood tide, high inflow/high export conditions, during which all of the water entering the interior Delta was from downstream (JPT4) and physical flow direction in JPT1 was away from the center of the junction. Maximum flow away from the interior Delta occurred at time 2000 under ebb tide, low inflow/low export conditions. During this time, physical flow direction in JPT4 was away from the center of the

junction. Increasing inflows had little influence on flow patterns in the channels leading to the interior Delta at JPT (JPT2 and JPT3); direction and magnitude of flow largely tracked the tidal cycle. Increasing exports also had little influence on flow patterns, but accounted for changes to magnitude of flow in JPT2 and JPT3 combined ranging from  $254 \text{ m}^3 \text{ sec}^{-1}$  (cfs) under high inflow conditions at time 0130 to  $-1,184 \text{ m}^3 \text{ sec}^{-1}$  (cfs) under medium inflow conditions at time 1045. Increasing exports resulted in smaller changes at other times, accounting for an average change of  $-342 \text{ m}^3 \text{ sec}^{-1}$  (cfs) (i.e., more flow into the interior Delta) across all inflow levels.

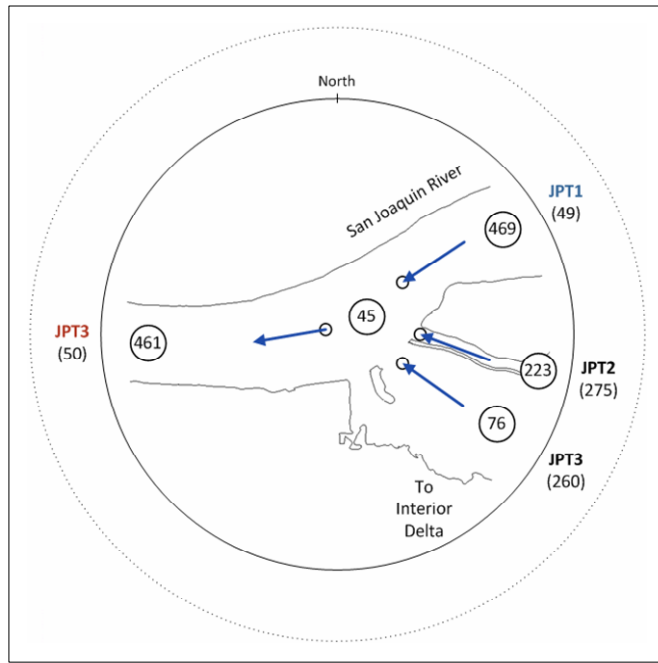


**Figure 30.** JPT: Plan-view of Jersey Point Junction. See Figure 4 for description of elements.

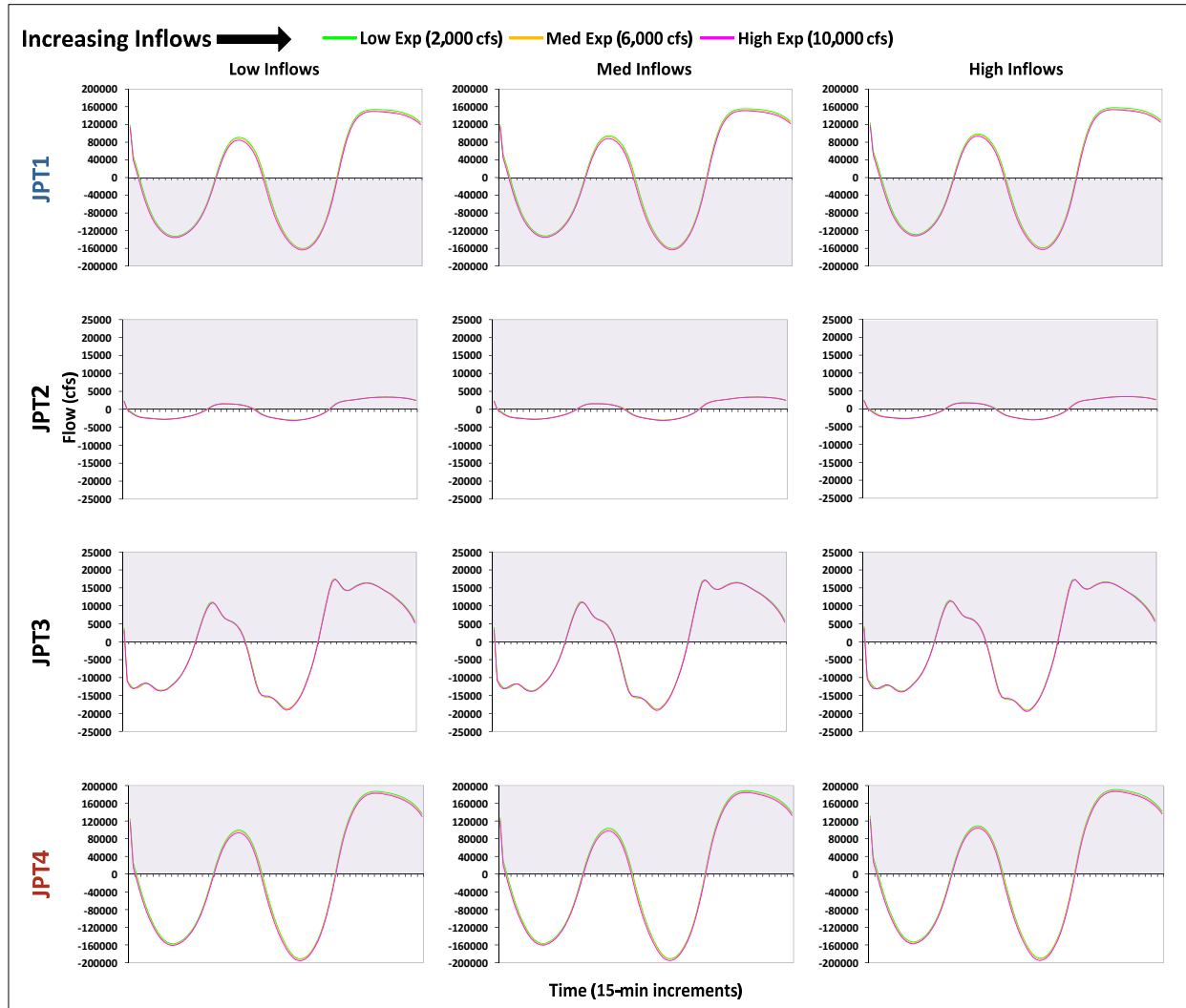


**Figure 31.** JPT: Flow in Jersey Point Junction Channels over 24 Hours. See Figure 5 for description of elements. For channels JPT2 and JPT3, flow displayed in the shaded area is away from the interior Delta; for the other channels, flow displayed in the shaded area is away from the center of the junction.

### ***Proportion and Source of Flow to Interior Delta at FMN, FRV, and JPT Junctions***

**Fisherman's Cut:** The proportion of flow which entered the interior Delta at FMN varied from 0% to 26.4% over 24 hours (Figure 32), depending on inflow and export conditions. At low exports, increasing inflows from low to high accounted for changes in proportion of flow into the interior Delta (FMN2) ranging from -9.7% (at time 0100) to 5.3% (at time 0115). At high exports, increasing inflows from low to high accounted for changes in proportion of flow ranging from -6.6% (at time 1100) to 22.3% (at time 0100). These large changes resulted from a shift in the proportion of flow pattern—from one time interval to another—as well as changes in proportion of flow. Increasing inflows resulted in smaller changes at other times, accounting for an average change of 0.3% across all export levels. At low inflows, increasing exports from low to high accounted for changes in proportion of flow ranging from -18.3% (at time 0100) to 8.4%

(at time 1100). At high inflows, increasing exports from low to high accounted for changes in proportion of flow to the interior Delta ranging from -7.1% (at time 1115) to 13.7% (at time 0100). Increasing exports resulted in smaller changes at other times, accounting for an average change of -0.4% across all inflow levels. Neither increasing inflows nor increasing exports substantially altered proportion of flow patterns over 24 hours.



**Figure 32.** FMN: Proportion of Flow to Interior Delta at Fisherman’s Cut. *See Figure 17 for description of elements.*

Although water which entered the interior Delta via FMN2 was mixed from upstream and downstream directions under some inflow/export conditions (Figure 32), water entered the interior Delta at FMN almost exclusively from the upstream direction—and during ebb tides. Increasing inflows had little effect on the relative proportion of flow entering the interior Delta from upstream versus from downstream. Increasing exports also had little effect on the relative proportion of flow entering the Delta from upstream versus from downstream.

Overall, inflows and exports caused very little change in proportion of flow and direction of flow entering the interior Delta at the FMN junction – nearly an order of magnitude less average change than at junctions further upriver.

**False River:** The proportion of flow which entered the interior Delta at FRV varied from 0% to 82.4% over 24 hours (Figure 33), depending on inflow and export conditions. At low exports, increasing inflows from low to high accounted for changes in proportion of flow into the interior Delta (FRV1) ranging from -39.4% (at time 0045) to 15.1% (at time 0115). At high exports, increasing inflows from low to high accounted for changes in proportion of flow ranging from -34.2% (at time 0045) to 12.8% (at time 0100). These large changes resulted from a shift in the proportion of flow pattern—from one time interval to another—as well as changes in proportion of flow. Increasing inflows resulted in smaller changes at other times, accounting for an average change of -0.2% across all export levels. At low inflows, increasing exports from low to high accounted for changes in proportion of flow to the interior Delta ranging from -13.8% (at time 0100) to 25.6% (at time 0045). At high inflows, increasing exports from low to high accounted for changes in proportion of flow ranging from -11.5% (at time 0115) to 50.6% (at time 1100). Increasing exports resulted in smaller changes at other times, accounting for an average change of 0.8% across all inflow levels. Neither increasing inflows nor increasing exports substantially altered proportion of flow patterns over 24 hours.

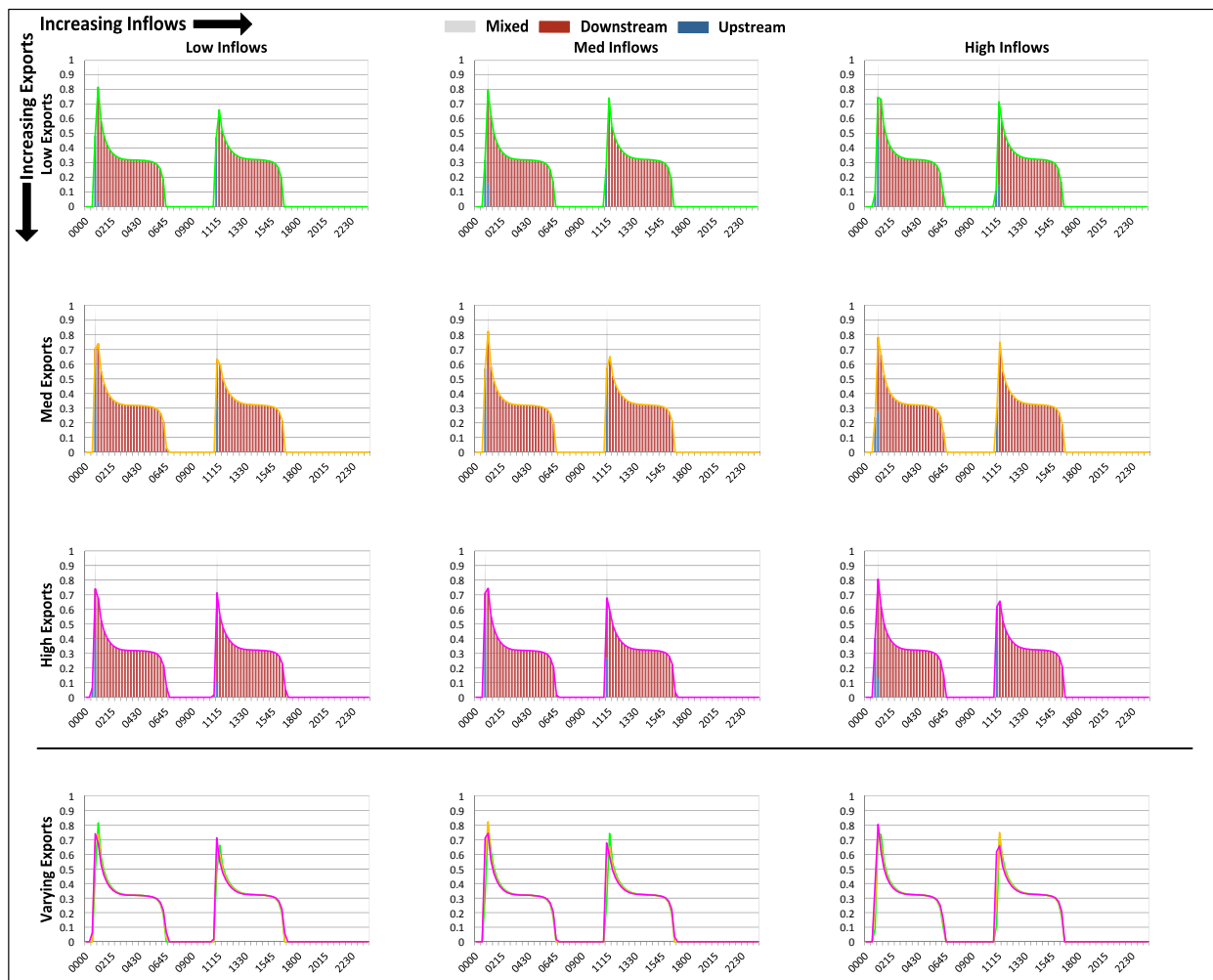


**Figure 33.** FRV: Proportion of Flow to Interior Delta at False River. See Figure 17 for description of elements.

Water entered the interior Delta via FRV1 mostly from the downstream direction, and most of the water entered during high tides; water entered the interior Delta from the upstream direction only very briefly at the beginning of flood tides. As inflows increased, the relative proportion of flow entering the interior Delta from upstream increased only slightly. Increasing exports had little effect on the relative proportion of flow entering the Delta from upstream versus from downstream.

Overall, inflows and exports caused very little change in proportion of flow and direction of flow entering the interior Delta at the FRV junction.

***Jersey Point:*** The proportion of flow which entered the interior Delta at JPT varied from 0% to 53.5% over 24 hours (Figure 34), depending on inflow and export conditions. At low exports, increasing inflows from low to high accounted for changes in proportion of flow into the interior Delta (JPT2 and JPT3) ranging from -17.6% (at time 0030) to 11.7% (at time 0100). At high exports, increasing inflows from low to high accounted for changes in proportion of flow ranging from -8.4% (at time 1030) to 12.4% (at time 0045). These large changes resulted from a shift in the proportion of flow pattern—from one time interval to another—as well as changes in proportion of flow. Increasing inflows resulted in smaller changes at other times, accounting for an average change of 0.1% across all export levels. At low inflows, increasing exports from low to high accounted for changes in proportion of flow to the interior Delta ranging from -15.5% (at time 1100) to 9.6% (at time 1030). At high inflows, increasing exports from low to high accounted for changes in proportion of flow ranging from -9.8% (at time 0100) to 15.9% (at time 1045). Increasing exports resulted in smaller changes at other times, accounting for an average change of -0.2% across all inflow levels. Neither increasing inflows nor increasing exports substantially altered proportion of flow patterns over 24 hours.

Water entered the interior Delta via JPT2 and JPT3 mostly from the downstream direction, and most of the water entered during high tides; water only entered the interior Delta from the upstream direction at the beginning of flood tides. As inflows increased, the relative proportion of flow entering the interior Delta from upstream versus from downstream changed only slightly. Increasing exports had little effect on the relative proportion of flow entering the Delta from upstream versus from downstream.

Overall, inflows and exports caused very little change in proportion of flow and direction of flow entering the interior Delta at the JPT junction.

**REPORT – Investigating the influence of tides, inflows, and exports on sub-daily flow in the Delta**

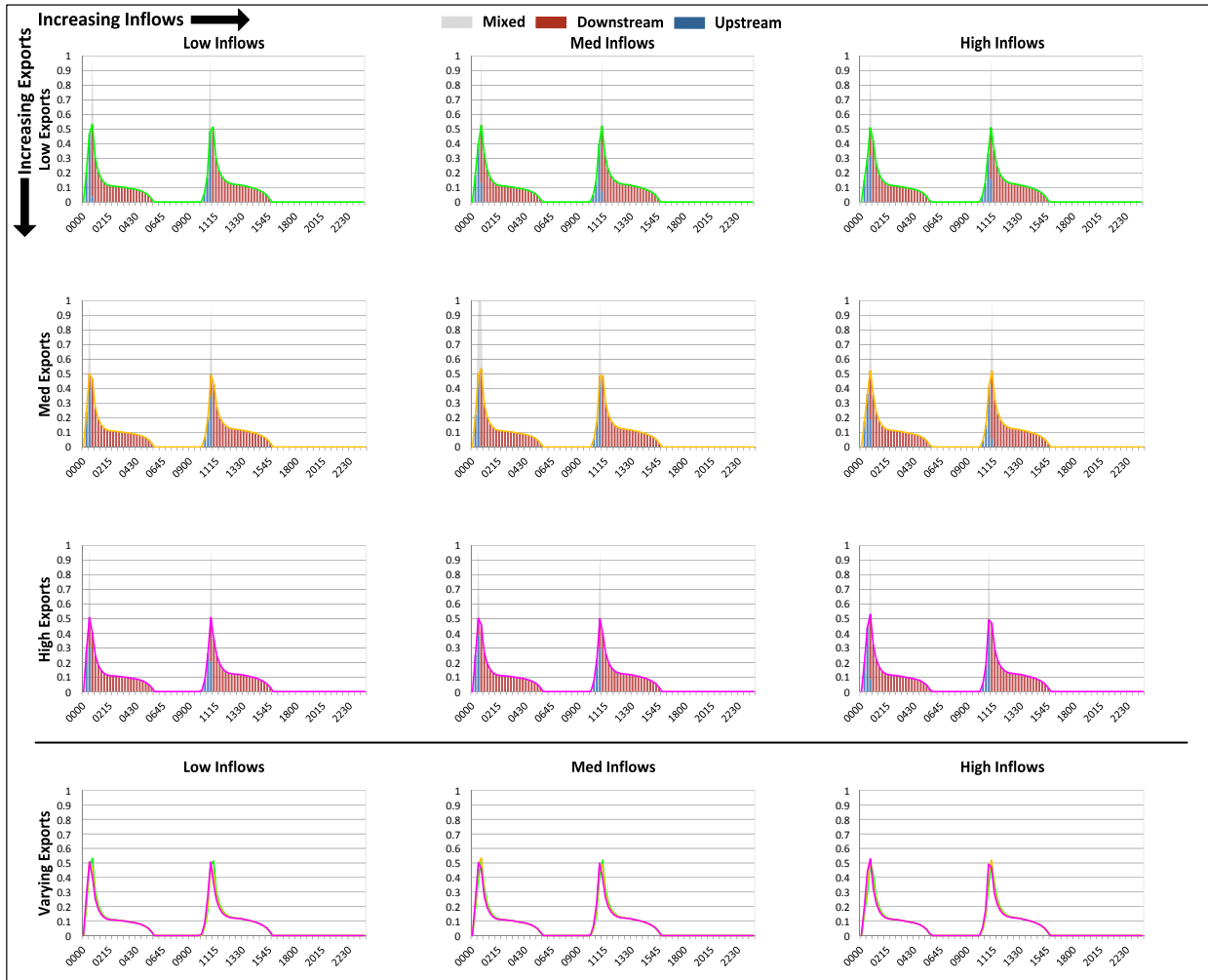


**Figure 34.** JPT: Proportion of Flow to Interior Delta at Jersey Point. See Figure 17 for description of elements.

## **Appendix 2: Details for Total Proportion of Flow to Interior Delta**

For all junctions, total proportions of flow to interior Delta over 24 hours under various inflow/export combinations—including relative proportions from upstream and downstream—are given in Table 3. Changes in proportion of flow to interior Delta over 24 hours with increasing inflows and with increasing exports are given in Table 4 and Table 5, respectively. Figures 35-37 display the data from Table 4 in graphical form (i.e., changes in total and relative proportion to interior Delta over 24 hours with increasing inflows), and Figures 38-40 display the data from Table 5 in graphical form (i.e., changes in total and relative proportion to interior Delta over 24 hours with increasing exports).

**Table 3.** Total Proportion of Flow to Interior Delta over 24 Hours. Data are displayed by junction and export level. Graphs are arranged by inflow level and water source (i.e., upstream or downstream from the junction).

From Upstream+Downstream: Low Inflows			From Upstream: Low Inflows			From Downstream: Low Inflows					
Junction	Exports		Junction	Exports		Junction	Exports				
	Low	Med		Low	Med		Low	Med			
GEO	45.27%	45.90%	46.55%	GEO	23.13%	23.63%	24.05%	GEO	22.14%	22.27%	22.50%
HOR	38.54%	44.20%	48.04%	HOR	22.75%	27.58%	30.86%	HOR	15.79%	16.62%	17.08%
TRN	16.31%	17.26%	18.45%	TRN	2.87%	3.31%	3.55%	TRN	13.45%	13.95%	14.90%
COL	14.97%	16.47%	17.73%	COL	6.21%	7.10%	7.88%	COL	8.75%	9.37%	9.85%
MRV	17.83%	19.03%	20.11%	MRV	0.17%	0.18%	0.52%	MRV	17.66%	18.84%	19.58%
ORV	15.99%	16.79%	17.59%	ORV	3.15%	3.83%	4.09%	ORV	12.84%	12.96%	13.51%
FMN	2.68%	2.44%	2.46%	FMN	2.27%	2.30%	2.40%	FMN	0.40%	0.14%	0.06%
FRV	17.75%	17.92%	18.00%	FRV	1.03%	0.99%	0.61%	FRV	16.72%	16.93%	17.39%
JPT	7.23%	7.08%	6.97%	JPT	1.48%	1.32%	1.20%	JPT	5.75%	5.76%	5.77%

From Upstream+Downstream: Med Inflows			From Upstream: Med Inflows			From Downstream: Med Inflows					
Junction	Exports		Junction	Exports		Junction	Exports				
	Low	Med		Low	Med		Low	Med			
GEO	43.75%	44.20%	44.61%	GEO	37.25%	37.59%	37.94%	GEO	6.51%	6.62%	6.69%
HOR	46.89%	50.13%	52.10%	HOR	42.69%	45.39%	47.20%	HOR	4.20%	4.74%	5.00%
TRN	16.61%	17.71%	18.89%	TRN	2.93%	3.20%	3.73%	TRN	13.68%	14.51%	15.16%
COL	15.12%	16.58%	17.93%	COL	6.28%	7.13%	7.97%	COL	8.84%	9.45%	9.96%
MRV	17.41%	19.41%	20.36%	MRV	0.28%	0.18%	0.55%	MRV	17.13%	19.22%	19.81%
ORV	15.94%	16.97%	17.84%	ORV	3.07%	3.73%	4.26%	ORV	12.87%	13.24%	13.58%
FMN	2.88%	2.64%	2.49%	FMN	2.77%	2.32%	2.37%	FMN	0.11%	0.31%	0.12%
FRV	17.59%	17.98%	18.01%	FRV	0.77%	1.18%	0.88%	FRV	16.81%	16.80%	17.13%
JPT	7.14%	7.24%	7.06%	JPT	1.43%	1.44%	1.29%	JPT	5.71%	5.80%	5.77%

From Upstream+Downstream: High Inflows			From Upstream: High Inflows			From Downstream: High Inflows					
Junction	Exports		Junction	Exports		Junction	Exports				
	Low	Med		Low	Med		Low	Med			
GEO	32.44%	32.72%	32.99%	GEO	32.44%	32.72%	32.99%	GEO	0.00%	0.00%	0.00%
HOR	53.16%	55.25%	56.96%	HOR	53.16%	55.25%	56.96%	HOR	0.00%	0.00%	0.00%
TRN	17.40%	18.38%	19.50%	TRN	3.48%	3.68%	4.03%	TRN	13.92%	14.70%	15.47%
COL	15.78%	17.00%	18.14%	COL	6.71%	7.47%	8.19%	COL	9.07%	9.52%	9.96%
MRV	17.40%	18.94%	20.71%	MRV	0.33%	0.31%	0.43%	MRV	17.07%	17.59%	19.24%
ORV	16.07%	16.91%	17.99%	ORV	3.58%	3.80%	4.26%	ORV	12.49%	13.11%	13.72%
FMN	2.81%	2.93%	2.86%	FMN	2.72%	2.78%	2.54%	FMN	0.09%	0.15%	0.20%
FRV	17.39%	17.65%	17.94%	FRV	0.86%	0.86%	1.09%	FRV	16.53%	16.80%	16.85%
JPT	7.18%	7.21%	7.23%	JPT	1.48%	1.45%	1.45%	JPT	5.70%	5.76%	5.79%

**Table 4.** Change in Total Proportion of Flow to Interior Delta over 24 Hours with Increasing Inflows. Values are for change in total proportion relative to low inflows. Data are displayed by junction and export level. Graphs are arranged by inflow level and water source (i.e., upstream or downstream from the junction).

From Upstream+Downstream: Med Inflows			From Upstream: Med Inflows			From Downstream: Med Inflows					
Junction	Exports		Junction	Exports		Junction	Exports				
	Low	Med		Low	Med		Low	Med			
GEO	-1.52%	-1.70%	-1.94%	GEO	14.12%	13.95%	13.89%	GEO	-15.63%	-15.65%	-15.81%
HOR	8.35%	5.94%	4.07%	HOR	19.94%	17.81%	16.34%	HOR	-11.59%	-11.87%	-12.08%
TRN	0.30%	0.44%	0.44%	TRN	0.06%	-0.11%	0.18%	TRN	0.23%	0.56%	0.25%
COL	0.15%	0.11%	0.20%	COL	0.07%	0.03%	0.10%	COL	0.08%	0.08%	0.10%
MRV	-0.42%	0.38%	0.25%	MRV	0.11%	0.00%	0.02%	MRV	-0.52%	0.38%	0.23%
ORV	-0.05%	0.18%	0.25%	ORV	-0.08%	-0.10%	0.17%	ORV	0.03%	0.28%	0.07%
FMN	0.20%	0.19%	0.03%	FMN	0.49%	0.02%	-0.03%	FMN	-0.29%	0.17%	0.06%
FRV	-0.17%	0.06%	0.01%	FRV	-0.26%	0.19%	0.27%	FRV	0.09%	-0.13%	-0.25%
JPT	-0.10%	0.16%	0.08%	JPT	-0.05%	0.12%	0.09%	JPT	-0.04%	0.04%	0.00%

From Upstream+Downstream: High Inflows			From Upstream: High Inflows			From Downstream: High Inflows					
Junction	Exports		Junction	Exports		Junction	Exports				
	Low	Med		Low	Med		Low	Med			
GEO	-12.83%	-13.18%	-13.56%	GEO	9.31%	9.09%	8.94%	GEO	-22.14%	-22.27%	-22.50%
HOR	14.62%	11.05%	8.92%	HOR	30.41%	27.66%	26.10%	HOR	-15.79%	-16.62%	-17.08%
TRN	1.09%	1.12%	1.04%	TRN	0.61%	0.36%	0.48%	TRN	0.48%	0.75%	0.56%
COL	0.81%	0.53%	0.41%	COL	0.49%	0.38%	0.31%	COL	0.32%	0.15%	0.10%
MRV	-0.43%	-0.08%	0.61%	MRV	0.16%	0.13%	-0.10%	MRV	-0.59%	-1.25%	-0.34%
ORV	0.08%	0.12%	0.39%	ORV	0.44%	-0.03%	0.18%	ORV	-0.35%	0.14%	0.22%
FMN	0.13%	0.49%	0.40%	FMN	0.45%	0.48%	0.14%	FMN	-0.31%	0.01%	0.14%
FRV	-0.36%	-0.26%	-0.06%	FRV	-0.17%	-0.14%	0.48%	FRV	-0.19%	-0.13%	-0.54%
JPT	-0.06%	0.14%	0.26%	JPT	0.00%	0.13%	0.25%	JPT	-0.05%	0.01%	0.02%

**Table 5.** Change in Total Proportion of Flow to Interior Delta over 24 Hours with Increasing Exports. Values are for change in percentage of total proportion relative to low exports. Data are displayed by junction and export level. Graphs are arranged by inflow level and water source (i.e., upstream or downstream from the junction).

From Upstream+Downstream: Low Inflows			From Upstream: Low Inflows			From Downstream: Low Inflows		
Junction	Exports		Junction	Exports		Junction	Exports	
	Med	High		Med	High		Med	High
GEO	0.63%	1.28%	GEO	0.50%	0.92%	GEO	0.13%	0.36%
HOR	5.65%	9.49%	HOR	4.83%	8.11%	HOR	0.82%	1.28%
TRN	0.95%	2.14%	TRN	0.45%	0.68%	TRN	0.50%	1.46%
COL	1.50%	2.76%	COL	0.89%	1.66%	COL	0.62%	1.10%
MRV	1.20%	2.28%	MRV	0.01%	0.35%	MRV	1.18%	1.92%
ORV	0.80%	1.60%	ORV	0.68%	0.94%	ORV	0.12%	0.66%
FMN	-0.24%	-0.22%	FMN	0.02%	0.13%	FMN	-0.26%	-0.34%
FRV	0.17%	0.25%	FRV	-0.04%	-0.42%	FRV	0.21%	0.67%
JPT	-0.15%	-0.26%	JPT	-0.15%	-0.28%	JPT	0.00%	0.02%

From Upstream+Downstream: Med Inflows			From Upstream: Med Inflows			From Downstream: Med Inflows		
Junction	Exports		Junction	Exports		Junction	Exports	
	Med	High		Med	High		Med	High
GEO	0.45%	0.86%	GEO	0.34%	0.69%	GEO	0.11%	0.19%
HOR	3.24%	5.21%	HOR	2.70%	4.51%	HOR	0.54%	0.80%
TRN	1.10%	2.28%	TRN	0.27%	0.80%	TRN	0.82%	1.48%
COL	1.46%	2.81%	COL	0.84%	1.69%	COL	0.62%	1.12%
MRV	1.99%	2.94%	MRV	-0.10%	0.27%	MRV	2.09%	2.68%
ORV	1.03%	1.90%	ORV	0.66%	1.19%	ORV	0.37%	0.71%
FMN	-0.25%	-0.39%	FMN	-0.45%	-0.40%	FMN	0.20%	0.01%
FRV	0.39%	0.43%	FRV	0.40%	0.10%	FRV	-0.01%	0.32%
JPT	0.10%	-0.08%	JPT	0.02%	-0.14%	JPT	0.09%	0.06%

From Upstream+Downstream: High Inflows			From Upstream: High Inflows			From Downstream: High Inflows		
Junction	Exports		Junction	Exports		Junction	Exports	
	Med	High		Med	High		Med	High
GEO	0.28%	0.55%	GEO	0.28%	0.55%	GEO	0.00%	0.00%
HOR	2.09%	3.80%	HOR	2.09%	3.80%	HOR	0.00%	0.00%
TRN	0.98%	2.09%	TRN	0.20%	0.55%	TRN	0.78%	1.54%
COL	1.22%	2.36%	COL	0.77%	1.48%	COL	0.45%	0.88%
MRV	1.54%	3.31%	MRV	-0.02%	0.10%	MRV	0.52%	2.17%
ORV	0.84%	1.91%	ORV	0.22%	0.68%	ORV	0.62%	1.23%
FMN	0.12%	0.05%	FMN	0.06%	-0.18%	FMN	0.06%	0.12%
FRV	0.26%	0.55%	FRV	-0.01%	0.23%	FRV	0.27%	0.32%
JPT	0.04%	0.06%	JPT	-0.02%	-0.03%	JPT	0.06%	0.09%



**Figure 35.** Change in Total Proportion of Flow to Interior Delta over 24 Hours with Increasing Inflows at GEO and HOR. Values are for change in total proportion relative to low inflows. Data are displayed by junction and export level. Graphs are arranged by increasing inflows, and by water source (i.e., upstream or downstream from the junction).

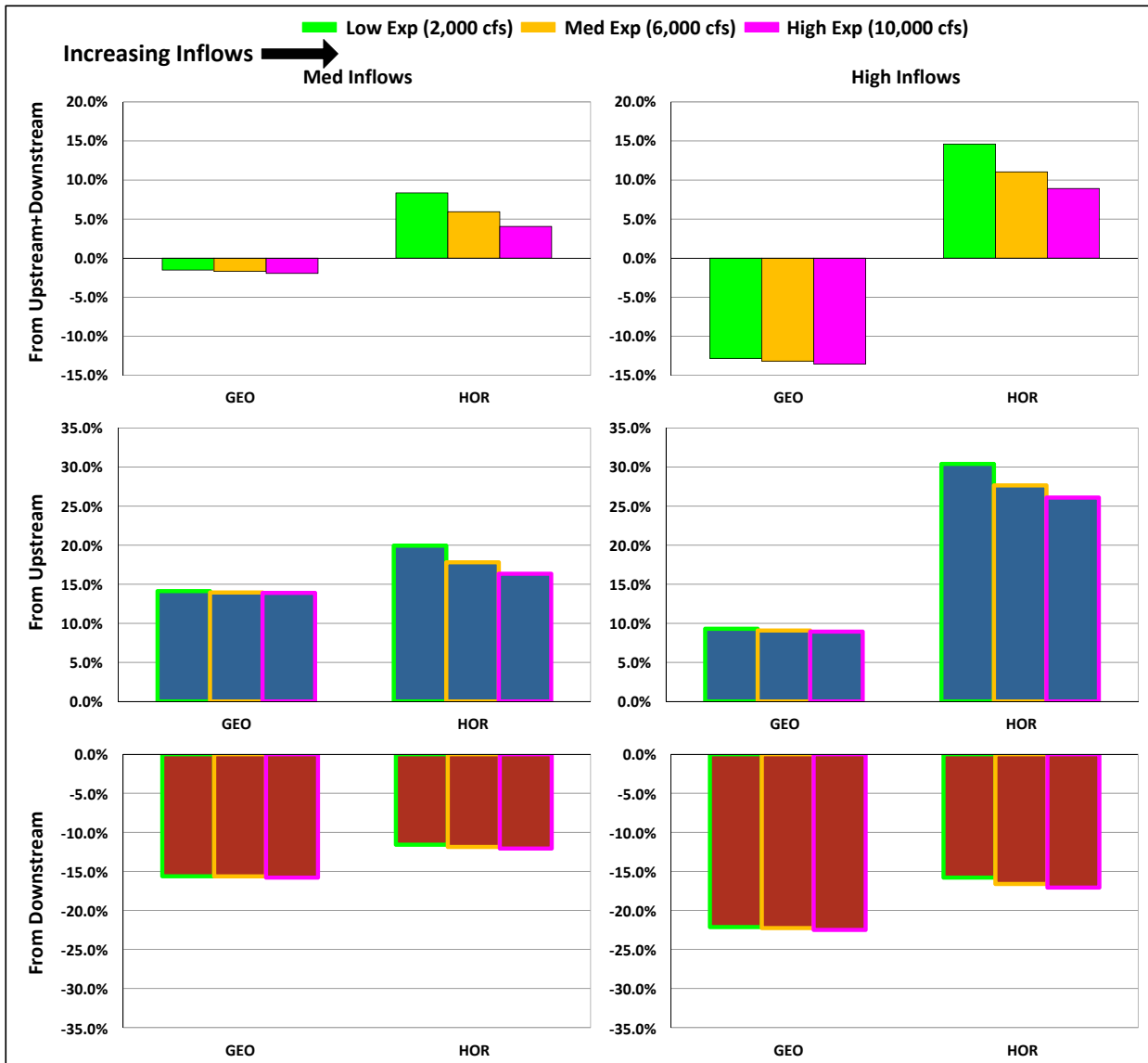


**Figure 36.** Change in Total Proportion of Flow to Interior Delta over 24 Hours with Increasing Inflows at TRN, COL, and MRV. Values are for change in total proportion relative to low inflows. Data are displayed by junction and export level. Graphs are arranged by increasing inflows, and by water source (i.e., upstream or downstream from the junction).

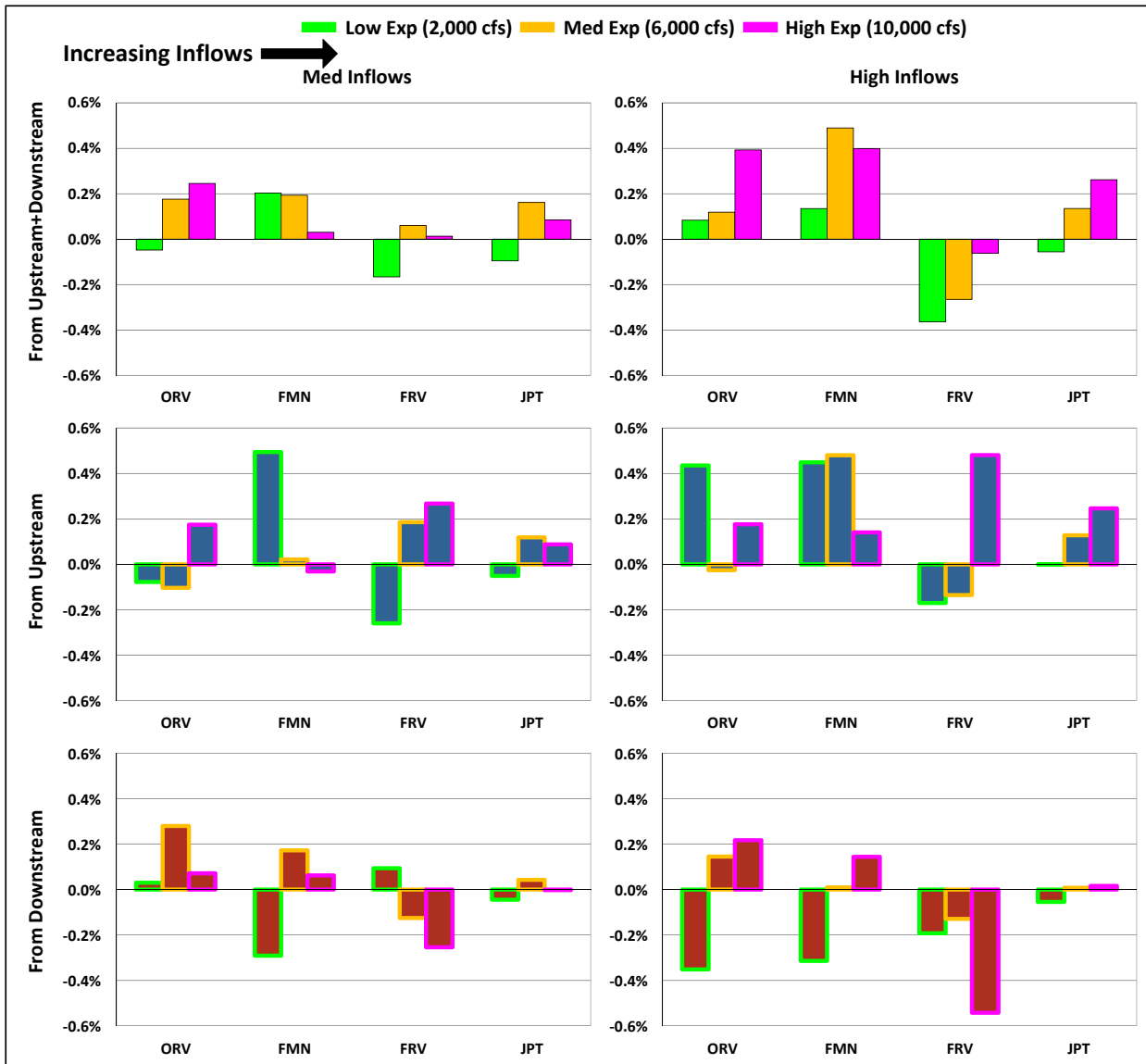


**Figure 37.** Change in Total Proportion of Flow to Interior Delta over 24 Hours with Increasing Inflows at ORV, FMN, FRV, and JPT. Values are for change in total proportion relative to low inflows. Data are displayed by junction and export level. Graphs are arranged by increasing inflows, and by water source (i.e., upstream or downstream from the junction).

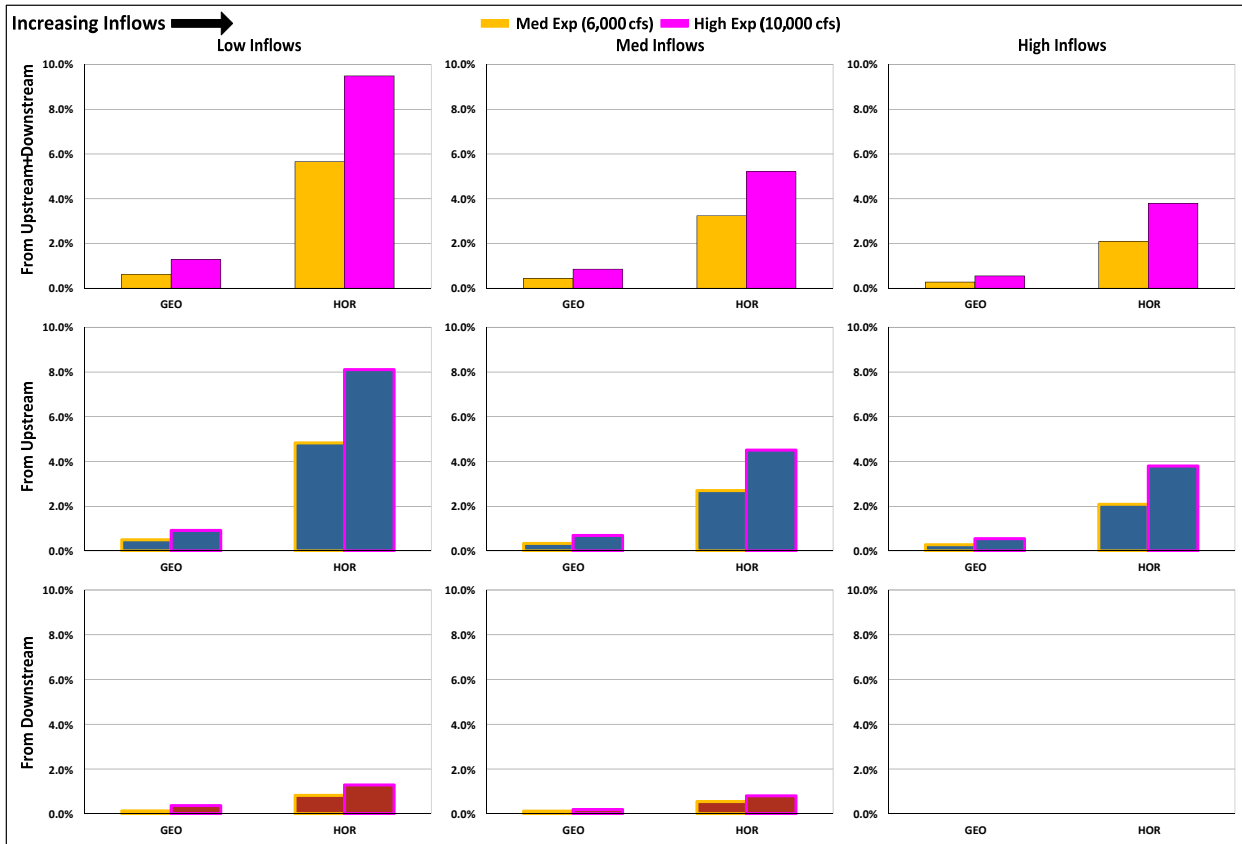


**Figure 38.** Change in Total Proportion of Flow to Interior Delta over 24 Hours with Increasing Exports at GEO and HOR. Values are for change in total proportion relative to low exports. Data are displayed by junction and export level. Graphs are arranged by increasing inflows, and by water source (i.e., upstream or downstream from the junction).



**Figure 39.** Change in Total Proportion of Flow to Interior Delta over 24 Hours with Increasing Exports at TRN, COL, and MRV. Values are for change in total proportion relative to low exports. Data are displayed by junction and export level. Graphs are arranged by increasing inflows, and by water source (i.e., upstream or downstream from the junction).

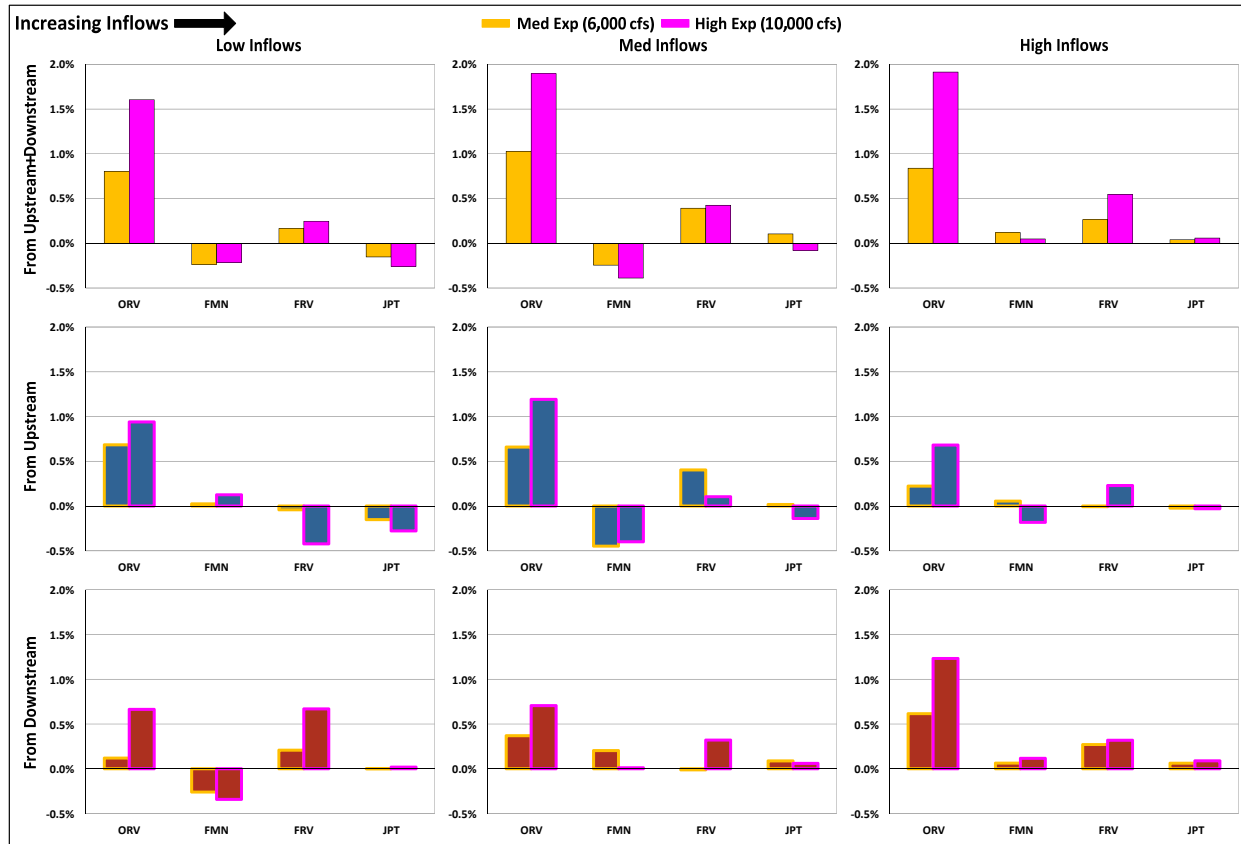


**Figure 40.** Change in Total Proportion of Flow to Interior Delta over 24 Hours with Increasing Exports at ORV, FMN, FRV, and JPT. Values are for change in total proportion relative to low exports. Data are displayed by junction and export level. Graphs are arranged by increasing inflows, and by water source (i.e., upstream or downstream from the junction).